CENTRO DE INVESTIGACIONES EN OPTICA, A.C.

"THEORETICAL STUDY OF MULTIPARTITE QUANTUM CORRELATIONS IN A NON-LINEAR SYSTEM"

Tesis que para obtener el grado de Maestro en Ciencias (Óptica)

Presenta: Héctor Jesús Rodríguez Nava

Director de Tesis: Dra. Laura Elena Casandra Rosales Zárate

Versión Definitiva. Incluye cambios sugeridos por revisores.

León · Guanajuato · México
Septiembre de 2023

Abstract

In recent years, Quantum Mechanics has gained notoriety for challenging our most basic intuition and prior knowledge of the Natural world. Some of the topics that have sparked plenty of interest among the scientific community, as well as the general public, are the so called quantum non-local correlations, from which the better known is *quantum entanglement*. These intriguing phenomena relate physical entities that are spatially separated and make them behave as a single system in a seemingly instantaneous fashion. Furthermore, quantum non-local correlations are not only relevant in a philosophical sense, they also constitute a fundamental resource for future technologies with applications far beyond our current perspective.

Nevertheless, multipartite quantum correlations have only been recently investigated and still there is plenty of research needed to properly understand them. In this work we strive to contribute to this generation of knowledge by studying the Hamiltonian of a non-linear system in a resonance condition that is believed to correlate four modes of light. Our contribution is focused on attempting to certify multipartite quantum correlations using a specific methodology. More specifically, our analysis is made using mathematical tools known as *phase-space methods*, in particular one of these, which is called the positive-P representation. We compare our results by performing a similar analysis using the Heisenberg evolution equations. Afterwards, we use these results to test for two quantum non-local correlations, namely, *entanglement* and *steering* and we do so by employing mathematical criteria called *witnesses*. We found the presence of both of these quantum correlations in a regime characterized by the quotient between two quantities, called the *coupling parameters*.

Acknowledgements

A mi mamá y a mi papá, por su apoyo incondicional y por el gran esfuerzo que siempre han hecho por mi educación.

A mi asesora, la Dra. Laura Rosales, por compartirme de sus conocimientos y por la enorme paciencia que siempre mostró para conmigo. Fue más de la que merecía pero justo la que necesitaba.

Al CIO, por brindarme el entorno y las herramientas necesarias para continuar con mi formación académica.

Contents

Chapter 1

Introduction

1.1 Quantum non-locality

Some of the most emblematic mysteries of modern physics are the phenomena known as non-local quantum correlations. Originally described by Einstein, Podolsky and Rosen on their 1935 article [1], were at first considered as absurd consequences derived from the mathematical structure of quantum mechanics, and used to argue that the latter was an incomplete theory. Years later, several experiments [2–9] showed that these phenomena do occur in Nature and that it is necessary to understand them in order to construct a more realistic model of the Universe.

Non-local quantum correlations have no classical analogy and have defied the comprehension and intuition of generations of physicists. These correlations imply that some specific type of quantum systems can be physically separated in subsystems and still can only be described as, or behave as one. Even though these phenomena is generally referred to under the generic term of *entanglement*, we will later discuss that this is just one type of non-local correlation out of many, and its differences with the rest of them will be pointed out. In particular, we are interested in two of these correlations, called *entanglement* and *steering*.

In quantum mechanics some physical states are described mathematically by a state vector. When this vector cannot be written as the product of the state vector of each of its parts (which are called subsystems) then the whole system is said to be *entangled*. In some entangled physical states a measurement on one of the subsystems can produce effects on some other subsystem, even if these two subsystems are physically separated from one another. Such effect is called *steering*.

In their seminal paper, Einstein, Podolsky and Rosen proposed that the non-local correlations could have been generated by some unknown factors, nowadays called *hidden variables* [1]. In 1964, Bell devised a definition for locality that took into account these hypothetical hidden variables. Based on this definition, he developed a requirement for theories with hidden variables, which is the satisfaction of what is now known as a Bell inequality. If this requirement was not met by the predictions of a theory, then such theory was incompatible with hidden variables. Observations from experiments [4, 5, 10], consistent with predictions from quantum mechanics showed that for some states, Bell's requirement was not met, and therefore, quantum mechanics was incompatible with a hidden variable theory, or in other words, these experiments showed that quantum mechanics was non-local. Thus, with the emergence of the Bell inequalities, a test for non-local quantum correlations came into existence.

Non-local quantum correlations have sparked plenty of interest over recent years because of the profound philosophical implications that they have on physical reality, but also for the potential that they provide for quantum technologies [11, 12]. We will now mention some of the possible applications that have motivated research in quantum non-local correlations. More specifically, in the area of quantum cryptography, which is primarily concerned with developing secure communications, entangled photon pairs have been used to send messages from a satellite to a ground station up to 1200 km away [13] and for distributing a secret key to be used for encrypting messages [14]. Quantum teleportation is another technology that so far has been able to transfer quantum states between photons using non-local correlations [15–17]. Also, algorithms for quantum computing have been proved [18] to take advantage of multipartite entanglement (i.e. entanglement between more than two subsystems) in order to provide the very much expected exponential speed up over classical computing.

1.2   Differences between non-local quantum correlations

As has been noted, the term entanglement has been used to describe all types of quantum non-local correlations. Nowadays, we are aware that there are different types of non-local correlations apart from entanglement. We will now discuss their conceptual differences.

Entanglement and steering

An entangled system is a quantum state that cannot be described mathematically as the product of the quantum states of its subsystems [19]. On the other hand, steerable systems are the ones in which measurements performed in one of the subsystems alter the state of other subsystems even if they are physically separated from each others. Originally in their paper, Einstein, Podolsky and Rosen thought of a quantum system that was formed by two particles. These particles were then distributed between two observers: *Alice* and *Bob*. Originally their reasoning was explained using position and momentum for the two particles, however it can also be explained using spin-$1/2$ particles [20], which is the case that we will use for the following explanation. It is worth noting that there are some other degrees of freedom besides these that can be quantum correlated.

The following is a simplified description of the setup of Einstein, Podolsky and Rosen but using spin as the correlated variable. First, Alice receives her particle and chooses a specific observable to measure. We will call this observable X. It could be spin in the $\hat{X}$ direction, for example. From that measurement Alice will obtain a certain value $x \in \{-1, 1\}$. Afterwards, Bob can perform a measurement on his own and, if he chooses the same observable X, he will obtain a perfectly anticorrelated result. What we mean by anticorrelated, is that he gets the opposite result, in other words, if Alice measures 1, then Bob measures -1. If, by contrast, Alice had chosen to measure spin in the $\hat{Z}$ direction, Bob's measurement of that observable would yield the perfectly anticorrelated value from the one obtained by Alice. We can conclude that Alice, by choosing on her own the observable to measure, is directing Bob's state to an eigenstate of either $\hat{\sigma_x}$ or $\hat{\sigma_z}$ [21, 22]. This ability of her to influence Bob's state from a distance was called *steering* by Schrödinger [23, 24] and still is to this day.

Steering is on itself a non-local quantum correlation and it is important to point out its differences from entanglement since all steerable states are entangled but not all entangled states present steering [21]. Furthermore, some states can present one-way steering, in which Alice can influence Bob but Bob cannot influence Alice, or two-way steering in which both observers can influence the other. Is in this sense that steering is not necessarily a symmetric correlation, while entanglement is, given the fact that the two subsystems are equally entangled to each other.

Bell non-locality

As we have discussed earlier, Bell developed a mathematical requirement for all hidden-variable theories that, if not met by a particular theory, showed that predictions by that theory could not be explained by hidden variables. This requirement was devised as a linear inequality for the measured values of quantum subsystems that are believed to be correlated. Mathematical expressions of such form are called *Bell's inequalities* [25].

If a quantum state violates a Bell inequality it is said to have *Bell non-locality*, which is itself a strong non-local quantum correlation. If a quantum state has Bell non-locality it is also entangled and shows two-way steering [26, 27]. However, it is important to note that some quantum states may present entanglement or steering without violating a Bell inequality [28]. That is one of the reasons there is need for some other tools to test for the presence of entanglement and steering, besides Bell inequalities.

1.3 Multipartite quantum correlations

We have briefly discussed the concepts of quantum correlations and have mentioned that they have potential applications for the development of new technologies. In order to accomplish this, it is needed to build complex systems that involve quantum non-local correlations within multiple parties [29]. For example, in order to build a quantum computer, plenty of qubits will be needed to perform computations, and, to achieve the long awaited quantum speed up, it is necessary that these qubits are entangled [18], or more generally, quantum correlated with each other. That is one of the reasons that multipartite quantum correlations are needed to be studied and better understood. There are more challenges to be faced in this research area, for instance, there is a basically unique way of quantifying bipartite pure state entanglement [30], but the multipartite case treats each situation differently depending on how those entangled states are meant to be used. Furthermore, it has been argued [31] that in the multipartite regime these phenomena will be much richer and will allow researchers to answer questions such as *"What is the natural unit of entanglement?"* or *"When is a state maximally entangled?"* in a less ambiguous way. Summarizing, plenty of research for quantum non-local correlations in the multipartite regime is still needed and that is our main motivation for this work.

Additionally, there are practical applications for systems that exhibit multipartite non-local correlations. For instance, Acín et al. [32], have shown that, in order to prove security for a cryptography protocol, it is necessary that the states produced by it violate a Bell inequality. Later, the authors developed a protocol with this purpose and proved its security against several attacks. On a different work, Giovannetti et

al. [33] have demonstrated that by employing a multipartite entangled state, they can reduce the error on the estimation of a phase shift on a two-level qubit. This phase shift is generated by the dynamics of the system and instead of preparing the state N times and performing a measurement for each of these, they entangle N qubits and perform a collective measurement once. The enhancement on the error is proportional to $\sqrt{N}$, for N entangled qubits.

As has been noted, another type of application for quantum correlations is *quantum teleportation*, in which an unknown quantum state can be transferred between particles at a distance. Until recently, all experiments performed on quantum teleportation were restricted to a two-dimensional sub-space, however, quantum systems might have more than one degree of freedom and these parameters may be defined for high dimensions, such as orbital angular momentum [34], for example. By considering this high dimensional facet, in 2019, Luo et. al. [35] proposed an experimental scheme for teleporting an arbitrarily high dimensional photonic quantum state. The authors also implemented it successfully for a three-dimensional space, thus demonstrating the teleportation of a *qutrit*. For this purpose, the authors used a three-dimensional Bell state, which is a multipartite quantum-correlated system. Furthermore, Hu et. al. [36] also were able to teleport a three-dimensional system using auxiliary pairs of photons that were entangled with each other.

Quantum cryptography can also benefit from multipartite correlations, as has been shown by authors such as Cerf et al. [37] whose work extends quantum cryptography protocols to spaces of d-arbitrary dimensions. In their paper, they also derived a security proof for quantum cryptography using *qudits* that guarantees that a secret key rate can always be produced by these methods. Further research on quantum communications using *d-level* systems has been done, and its benefits and future challenges have been identified, as reported by Cozzolino et al. [38]. Among the benefits discussed by the authors we can find a larger capacity for information transmission and a higher noise resilience. More specifically on this last topic, Cozzolino et al. claim that to guarantee secure communications using quantum systems, a quotient called QBER (Quantum Bit Error Rate), that is the ratio of an error rate to the overall received rate, has to be below a certain threshold. For two-dimensional systems, this number is around 11%, while for systems with $d = 4$ and $d = 8$ levels, the threshold is 18.93% and 24.70%. The errors used to calculate the QBER may have been generated either by environmental noise or by eavesdropping attacks, thus adding dimensions to the communication system enhances its robustness against noise in general.

Generation of multipartite quantum correlations

One specific way to generate photons that share a quantum correlation is by using nonlinear optics. These phenomena is exhibited by media that responds to higher powers of an incident electric field. In the next chapter, we will discuss more thoroughly these processes, but for now we can mention some earlier works that have used them to generate entanglement and steering. For instance, in 2004, Olsen [39] demonstrated that second harmonic generation (SHG) is one nonlinear process that generates both entanglement and steering. In this process, two photons of frequency ω_1 are coupled in a medium with second order susceptibility. By a parametric process (one that involves no molecular transitions) inside the medium, one photon of frequency $\omega_2 = 2\omega_1$ is generated. The author showed that this newly generated photon

presents entanglement and steering with the photons from the fundamental frequency ω_1. Olsen also expanded his work using two processes for third harmonic generation (THG) [40] to generate entangled modes of light. Similar to SHG, in THG, three photons (of frequency ω_1) interact with a medium that generates one photon of frequency $\omega_3 = 3\omega_1$. This process is called *direct third harmonic generation.* Additionally, the author considered a different way of THG that starts with a SHG system that is followed by a sum-frequency generation. After producing the already discussed photon of frequency ω_2 by SHG, another parametric process combines the energy of this photon with one of the undepleted pump of frequency ω_1 to produce $\omega_3 = \omega_2 + \omega_1$. This experimental scheme is called *cascaded third-harmonic generation.* Both systems were shown to produce entanglement and steering [40]. Using a different nonlinear process, Rojas et. al. [41] found that multipartite entanglement between three photons was generated by a process called *triple-photon-generation* (TPG). One of the processes considered takes a photon of frequency ω_p and converts it into a triplet of photons of frequencies $\omega_1, \omega_2, \omega_3$, such that $\omega_p = \omega_1 + \omega_2 + \omega_3$. If just ω_p is pumped into the medium, in other words: used to excite the medium, then the process is called spontaneous, if one or two of the output frequencies are also pumped in, then it is called partially seeded, and if all of the output frequencies are pumped in, is called fully seeded. Authors [41] showed that while the spontaneous case does not produce quantum correlations, the fully seeded case is an efficient way to generate genuine tripartite entanglement.

In this work we will examine a nonlinear physical system that that is doubly pumped by Gaussian modes and that produces a triplet of photons [42]. The triplet of photons is then converted to four modes of light under a specific geometric condition that depends on the relative angle of incidence of the pumps [43]. The resonance condition is generated by walk off effects due to the birrefringence of the medium. This physical system is believed [43] to produce four partite entanglement as well as steering in two continuous variables called the *field quadratures.* In order to certify the presence of this quantum correlation we use the positive-P representation by Drummond and Gardiner [44], as well as the application of entanglement and steering witnesses.

1.4 Layout of the work

The work is divided in the following way: after this brief introduction a chapter is devoted to the theoretical background and concepts developed or used during the work, for example, more formal definitions of the quantum correlations that were studied, the variables that were quantum correlated, the type of quantum states that describe the modes of light that were used in the physical system, etc. Afterwards, the methodology of our research is discussed and comparisons between the two methodologies are made. This is followed by the presentation of our results, namely, the solutions to the differential equations obtained by both methods, the observables that are quantum correlated as well as the witnesses that certify the presence of these quantum correlations. Lastly, we discuss the conclusions and possible incremental research that could be performed for later works.

Chapter 2

Theoretical framework

In this chapter we will discuss the necessary background for the development of our work. Important physical concepts such as entanglement and steering will be mathematically defined, as well as some theoretical tools and methods that are used in our analysis, such as the quantum correlation witnesses and phase space methods. Also, some physical quantities called *quadratures* will be presented, since these are the ones that we are trying to show that are quantum correlated in our system.

2.1 Non-local quantum correlations

2.1.1 Entanglement

In quantum mechanics, a physical system is in a pure state if it can be described by a *state vector* $|\Psi\rangle$ of unit length in a complex Hilbert space $\mathcal{H}$. Some physical systems are formed by two or more subsystems[1], which in turn can be described by two or more state vectors, for example: $|a\rangle$ that belongs to $\mathcal{H}_1$ and $|b\rangle$ that belongs to $\mathcal{H}_2$.

The state vector of the whole system can be in a product form of the vector of its subsystems, such as:

$$|\Psi\rangle = |a\rangle \otimes |b\rangle, \tag{2.1}$$

where $\otimes$ represents the tensor product. State vectors that can be represented in this product form are called *separable* and are *not entangled* [19].

Quantum mechanics also allows for state vectors to be in a superposition (or linear combination) such as:

$$|\psi\rangle = \alpha |A\rangle + \beta |B\rangle, \tag{2.2}$$

where α and β are complex numbers called *probability amplitudes* that satisfy the equation $|\alpha|^2 + |\beta|^2 = 1$. However, for some of these superpositions, it is not possible to write them in product form of the state vectors of its subsystems, for example:

$$|\Phi\rangle = \alpha |a_1\rangle \otimes |b_1\rangle + \beta |a_2\rangle \otimes |b_2\rangle. \tag{2.3}$$

States such as 2.3, that cannot be written as a product of the vector states of their subsystems, are *entangled* [45].

A more general type of state, called mixed state, is described by a density operator $\hat{\rho}$, which is a convex sum of projector operators onto a particular set of pure states

---

[1]Throughout this work the terms *subsystem* and *party* are used interchangeably.

$|\psi_k\rangle$. Mathematically, this is represented by:

$$\hat{\rho} = \sum_{k=1}^{N} p_k |\psi_k\rangle \langle\psi_k| . \tag{2.4}$$

Analogously, for a mixed state, if its density operator can be written as:

$$\hat{\rho} = \sum_{i} p_i |a_i\rangle \langle a_i| \otimes |b_i\rangle \langle b_i| , \tag{2.5}$$

then it is separable. However, it is not trivial to find a decomposition such as 2.1 or 2.5 for a given state [12], even if it exists, and therefore, a more simple way of testing entanglement is needed.

Multipartite entanglement

Generalizing the concept of entanglement to systems that have more than two parties can be done through the following definition [31]. A system has multipartite entanglement if its density operator cannot be written as:

$$\hat{\rho} = \sum_{i} p_i \hat{\rho}_{1,i} \otimes \hat{\rho}_{2,i} \cdots \otimes \hat{\rho}_{n,i}, \tag{2.6}$$

where $\hat{\rho}_{n,i}$ belongs to the Hilbert space $\mathcal{H}_n$ and denotes the density matrix for the n-th subsystem on the state i.

Unlike the bipartite case, there is a distinction between types of multipartite entanglement. In particular, we are referring to the terms of *full* multipartite entanglement and *genuine* multipartite entanglement that sometimes are used indistinctly in the literature, while in fact, they represent different concepts [46, 47]. These terms are used to represent the intuition that this quantum correlation is distributed among all the parties in the system, and not only between *some* of them.

This distinction with the bipartite case becomes necessary for the instance in which, within a system, certain subsystems may be exclusively correlated with each other but not with the rest of the parties. It is important to distinguish this difference while using entanglement certification techniques (which will be discussed below, in subsection 2.9) because it is possible to mistakenly assure that we have multipartite entanglement while in fact, only bipartite entanglement is present. For example, we could have a tripartite system in which subsystems 1 and 2 are entangled with each other, but not with subsystem 3. This state could be represented by the density matrix:

$$\hat{\rho} = \sum_{k} w_k \hat{\rho}_{k,12} \otimes \hat{\rho}_{k,3}. \tag{2.7}$$

Even though the state described in eq. 2.7 presents entanglement between the first two parties, it is *biseparable* because it can be factorized in the bipartition $12 - 3$, therefore it exhibits no multipartite entanglement, just bipartite entanglement.

We will now proceed to explain in more detail the difference between the two definitions: full multipartite entanglement is present when a state cannot be written as a biseparable state, such as the one in eq. 2.7, or a fully separable state [46, 47], for instance eq. 2.6. On the other hand, genuine multipartite entanglement occurs when

the system cannot be written as a biseparable state or fully separable state, nor as a convex sum of biseparable or fully separable states.

We now present an example in which this distinction is clearly shown. One of the biseparable states for the tripartite case corresponds to the density matrix of eq. 2.7, while the other two possible combinations of the three modes are:

$$\hat{\rho} = \sum_k w_k \hat{\rho}_{k,13} \otimes \hat{\rho}_{k,2}, \tag{2.8}$$

$$\hat{\rho} = \sum_k w_k \hat{\rho}_{k,23} \otimes \hat{\rho}_{k,1}. \tag{2.9}$$

Furthermore, the fully separable tripartite state is:

$$\hat{\rho} = \sum_k w_k \hat{\rho}_{k,1} \otimes \hat{\rho}_{k,2} \otimes \hat{\rho}_{k,3}. \tag{2.10}$$

If a quantum system cannot be described by any of the eqs. 2.7 - 2.10, then it exhibits *full multipartite entanglement*.

Subsequently, for a quantum system to exhibit *genuine multipartite entanglement*, it cannot be written as eqs. 2.7 - 2.10, nor it can be a convex sum of biseparable or fully separable states. Mathematically this condition is written as [47]:

$$\hat{\rho}_{NG} = P_1 \sum_i w_i \hat{\rho}_{1,2}^i \hat{\rho}_3^i + P_2 \sum_j w_j \hat{\rho}_{1,3}^j \hat{\rho}_2^j + P_3 \sum_k w_k \hat{\rho}_{2,3}^k \hat{\rho}_1^k, \tag{2.11}$$

where $\sum_{m=1}^3 P_m = 1$, $\sum_n w_n = 1$ and the sign for the outer product, $\otimes$, has been omitted for briefness. If a tripartite quantum state cannot be written in any convex combination of the general form 2.11, then it possesses *genuine multipartite entanglement*.

An important comment on this matter is that even though in general these two definitions are different, for pure states they are equivalent. In other words, if a pure state is fully inseparable, it is also genuinely entangled and presents Bell nonlocality [46, 47]. It is in this sense that some of the earliest experiments that showed the presence of entanglement dealt with proving violations of Bell's inequalities. Examples of these are the Freedman-Clauser experiment [2] as well as the important works by Aspect et al. [4, 5]. The experiment performed by Wu and Shaknov [48] is also very relevant since it is the earliest experiment that showed the presence of entanglement in a physical system. In this work, Wu and Shaknov showed that in a pair of photons that is produced by the annihilation of an electron and a positron, each photon has orthogonal polarization with the other.

We will now mention some possible applications for entanglement. One of these applications is called *dense coding* [49]. What is meant by coding in this context is the usage of a physical system to represent information that we wish to communicate. In particular, we are going to be dealing with transmission of bits of information such as *yes/no* answers. In classical systems, a bit of information could be represented, for example, by the presence of an electrical current or by different voltage levels. On quantum information, however, these two different values are represented by two orthogonal basis states which are called qubits and will be denoted by $|0\rangle$ and $|1\rangle$.

Unlike the classical case, orthogonal basis states can be in a superposition of these two state vectors. An example of this, that uses two qubits, is the Bell basis, which is formed by the four Bell states:

$$\left|\Psi^+\right\rangle = \frac{1}{\sqrt{2}}\left(\left|0\right\rangle\left|1\right\rangle + \left|1\right\rangle\left|0\right\rangle\right),$$

$$\left|\Psi^-\right\rangle = \frac{1}{\sqrt{2}}\left(\left|0\right\rangle\left|1\right\rangle - \left|1\right\rangle\left|0\right\rangle\right),$$

$$\left|\Phi^+\right\rangle = \frac{1}{\sqrt{2}}\left(\left|0\right\rangle\left|0\right\rangle + \left|1\right\rangle\left|1\right\rangle\right),$$

$$\left|\Phi^-\right\rangle = \frac{1}{\sqrt{2}}\left(\left|0\right\rangle\left|0\right\rangle - \left|1\right\rangle\left|1\right\rangle\right). \tag{2.12}$$

An interesting property from this basis is the fact that starting from any of the four Bell states, only manipulation of one of the two qubits is necessary to change to any of the three remaining basis states. This property was used by Bennett and Wiesner [50] to propose an encoding scheme, called dense coding, in which two bits of information can be coded by manipulating only one qubit.

A different application for entanglement is *quantum teleportation*. In this scheme [51], a person, usually called Alice, wants to send a particular quantum state $\left|\phi\right\rangle$ to another person, usually called Bob. Alice does not know what is the state and is not able to send the physical system itself, so she makes it interact with another system in a known state. This new system is called an *ancilla*. After the interaction, the original system is no longer in the state $\left|\phi\right\rangle$, but the information from said state is transmitted to the ancilla system which is now sent to Bob. By considering the actions performed by Alice, Bob can apply some unitary operations to the ancilla system in order to recover the original state $\left|\phi\right\rangle$. For this protocol, is necessary that Alice and Bob share an entangled state beforehand. In particular, they share the $\left|\Psi^-\right\rangle$ state that was defined in eq. 2.12. This is done by sending to each person one of the qubits of the Bell state. Subsequently, Alice will perform a joint measurement on the Bell basis of her system in state $\left|\phi\right\rangle$ with her entangled qubit from state $\left|\Psi^-\right\rangle$ and she will inform the result from her measurement to Bob through a classical channel. Depending on the result that Alice gets, Bob can perform a unitary operation on his qubit from the shared entangled system $\left|\Psi^-\right\rangle$ and recover the original state $\left|\phi\right\rangle$. In this state teleportation, the original state vanishes but it is possible to reconstruct it elsewhere thanks to the entanglement of the Bell state Ψ^-

2.1.2 Steering

Steering is a formalization of the EPR argument [52, 53]. When steering is present, by performing local measurements on one of the subsystems, it is possible to affect the rest of the parties and *steer* them into orthogonal eigenstates of the observable that was measured. Steering is an asymmetric quantum non-local correlation, that means that one of the subsystems may steer the other, but not necessarily the other way around. It is possible, however, to have systems in which there is two-way steering, but that is not the general case.

In a similar fashion to entanglement, steering present in systems with multiple parties can be considered genuine multipartite steering under specific conditions. Namely,

genuine multipartite steering is present when all of the different subsystems (or bipartitions) can steer each other [21, 54].

Steering was formalized by Wiseman, Jones and Doherty in 2007 [22, 55] as the capability of remotely generating ensembles that could not be obtained by a local hidden state (LHS) [56]. That is a state shared by Alice and Bob, $\hat{\rho}_\lambda$, that yields to Bob measurement results given by a probability distribution of the form

$$\int d\lambda \mu(\lambda) p(a|x, \lambda), \tag{2.13}$$

where λ is a hidden variable, unknown to Bob, that produces the result a to Alice when she performs measurements on the observable x, and which is determined by the distribution $\mu(\lambda)$. The authors [22] define a state as not-steerable if it does not produce measurements consistent with distribution 2.13. Notice that the equation depends on the conditional probabilities of measurements performed by Alice. It is in that sense that the definition is asymmetric, for it may change if we consider the probabilities of measurements done by Bob.

Steering was suggested originally by Einstein, Podolsky and Rosen in their seminal paper of 1935 [1] as a consequence of the mathematical formalism of quantum mechanics, even though the term was not proposed by them but by Schrödinger [23, 57]. Several years later, the phenomenon was confirmed experimentally [57, 58]. We will proceed to mention some of the experiments that demonstrated that this was indeed, a physical phenomenon.

In 1992, Ou et al. [58] employed an optical parametric oscillator (OPO) to generate this quantum correlation among signal and idler beams of light. To determine that the two emitted beams were correlated, they measured the quadratures X_i, P_i (these quantities serve as analogous of position and momentum for a mode of light and will be further discussed in this work in section 2.2) of one of the beams (the idler) using homodyne detection. Afterwards they inferred the values for the same observable on the other beam, X_s, P_s, and calculated the variance of the difference between the two of them $\Delta_{\inf}^2 X = \langle (X_s - g_i X_i)^2 \rangle$, where g_i is a real coefficient used for normalization. This normalization is such that, given a value for X_i, one can determine X_s within a very small error if the following relation is satisfied: $\Delta_{\inf}^2 X < 1$. Afterwards, for specific values X_s, P_s the following result arises: $\Delta_{\inf}^2 X \Delta_{\inf}^2 P < 1$ while X and P being non-commutative have to satisfy the Heisenberg relationship: $\Delta^2 X \Delta^2 P \geq 1$. The apparent contradiction is solved, according to the authors, because $\Delta_{\inf}^2 X$ is a conditional distribution between X_s and X_i (with the same argument applying to quadrature P). In other words, the quadratures X_i, for the idler beam, and X_s for the signal, are quantum correlated with each other.

On another instance, Händchen et al. [57] produced one-way steering on Gaussian states (Gaussian states and their importance for our work are discussed in section 2.4). Their experimental setup utilized squeezed states generated by type-I parametric down-conversion as the source. They superimposed this mode of light with a vacuum on a balanced beamsplitter and called one of the outputs state A. The other output was put through a half wave plate and then through a variable beamsplitter where it was superimposed with a second vacuum mode. The contribution of each of these modes could be modified by the authors at will. The output is called state B. Lastly,

the authors performed measurements on states A and B using homodyne detection.

The criteria considered by the authors to certify one way steering is the following (Subsection 2.10, included in this chapter, is devoted to this important topic):

$$V_{B|A}(X_B)V_{B|A}(P_B) \geq 1,$$
$$V_{A|B}(X_A)V_{A|B}(P_A) \geq 1, \tag{2.14}$$

where $V_{B|A}(X_A)$ denotes the conditional variance of the quadrature X_B given a result by a measurement on state A, etc. The violation of the first of these inequalities certifies steering from state A to state B and the violation of the second inequality is the converse case. This specific criterion was defined by Reid [52] and will be revisited in section 2.10.1, since it is also used in this work. The results obtained by the authors were dependent on the contribution of the second vacuum mode (the one used to generate state B) and the regime where they found one-way steering is located between 40% and 70% of the variable beamsplitter for the vacuum mode. Below this threshold they found two-way steering, and above it, they found no steering whatsoever.

Important research has been done on the possible applications of steering, which is arguably one of the most puzzling and interesting phenomena of physics, and therefore, could be used in devices that just a hundred years ago would be thought of as mere fantasy. We will now mention some of these important applications [59–61].

Quantum Key Distribution (QKD) is an area of applied quantum physics where the objective is to send a string of information, which we call *key*, securely to another person, using a quantum system. The reason is that, it was shown by Shannon [62] that if this key distribution is performed securely, and the key itself meets some specific requirements, then it can be used in cryptography protocols such as the *one-time pad*. This protocol is secure against statistical analysis of the encrypted message [62], which would in turn make it applicable for secure communications.

In practice, QKD protocols consider the case in which two people, *Alice* and *Bob*, send each other these bits of information using quantum systems, such as polarized photons, nevertheless, the assumption is made that both Alice and Bob trust their measurement devices. It has been shown that this assumption is not very realistic since these systems can be hacked by a variety of methods [59, 60], thus, it has been proposed by Branciard et al. [61] to use experimental setups that depend on steering, that allow us to trust only one of the measurement devices involved without compromising security. This experimental scheme is more realistic since one of the devices could be owned by a trusted institution, such as a bank for example, while the other may be compromised without risking information leaks.

Later on we will discuss the existence of several criteria that can be used to certify steering. One of the most simple [21, 63] consists of formulating criteria for the statistical correlations between the measurements performed by Alice and by Bob, similar to the one defined by Reid [52] and used by Händchen et al. [57] in the previous subsection.

2.2   Field quadratures

The physical system that we will be studying uses light sources and a specific type of medium to produce four modes of light that, we believe, present genuine multipartite entanglement and steering. The quantum correlations between these modes occur in the quantities called *field quadratures*, or simply *quadratures*. These quantities behave as analogous to position and momentum for modes of light. We will devote this subsection to defining them and listing their properties.

From the classical point of view, light is an electromagnetic wave and, as such, it has a strong relationship with the *harmonic oscillator*. It has been shown [64] that the similarities between the two systems are what allow us to define two analogous quantities to position and momentum for a state of light.

Let us first consider the *classical harmonic oscillator* for a mass m and frequency ω. Its equations of motion are the following:

$$p = m\frac{dx}{dt}, \tag{2.15}$$

$$m\frac{d^2x}{dt^2} = \frac{dp}{dt} = -m\omega^2 x. \tag{2.16}$$

We will also take into account the expression for the total energy of the harmonic oscillator, namely:

$$E = \frac{p^2}{2m} + \frac{1}{2}m\omega^2 x^2. \tag{2.17}$$

On the other hand, we will examine an electromagnetic wave linearly polarized that is contained in a cavity of dimension L. It is moving in the z direction and its electric field oscillates along the x-axis. Solutions for the electric and magnetic fields, respectively, are:

$$E_x(z,t) = E_0 \sin kz \sin \omega t, \tag{2.18}$$

$$B_y(z,t) = B_0 \cos kz \cos \omega t. \tag{2.19}$$

The total energy can be calculated by performing an integral on the energy density, which is:

$$U = \frac{1}{2}\left(\epsilon_0 E^2 + \frac{1}{\mu_0}B^2\right). \tag{2.20}$$

That integral across the length of the cavity yields:

$$E = \frac{V}{4}\left(\epsilon_0 E_0^2 \sin^2(\omega t) + \frac{B_0^2}{\mu_0}\cos^2(\omega t)\right). \tag{2.21}$$

By inspecting and comparing equations 2.17 and 2.21 we can define generalized coordinates $q(t)$ and $p(t)$ as follows:

$$q(t) = \sqrt{m}\left(\frac{\epsilon_0 V}{2\omega^2}\right)^{\frac{1}{2}} E_0 \sin(\omega t), \tag{2.22}$$

$$p(t) = \frac{1}{\sqrt{m}}\left(\frac{V}{2\mu_0}\right)^{\frac{1}{2}} B_0 \cos(\omega t), \tag{2.23}$$

which are analogous to position and momentum for the harmonic oscillator.

Furthermore, these coordinates satisfy the equations of motion for the harmonic oscillator, that is:

$$p = \frac{dq}{dt}, \tag{2.24}$$

and

$$\frac{dp}{dt} = -\omega^2 q \tag{2.25}$$

except for the factor of the mass m. We can now define the (classical) field quadratures as:

$$X_1(t) = \left(\frac{\omega}{2\hbar}\right)^{\frac{1}{2}} q(t), \tag{2.26}$$

$$X_2(t) = \left(\frac{1}{2\hbar\omega}\right)^{\frac{1}{2}} p(t). \tag{2.27}$$

Having established the classical quadratures, we will now present them from a quantum mechanical point of view. The quantum harmonic oscillator can be expressed in terms of the *ladder operators* [65], which are defined as follows:

$$\hat{a} = \frac{1}{(2m\omega\hbar)^{1/2}}(m\omega\hat{x} + i\hat{p}_x), \tag{2.28}$$

$$\hat{a}^\dagger = \frac{1}{(2m\omega\hbar)^{1/2}}(m\omega\hat{x} - i\hat{p}_x). \tag{2.29}$$

By manipulating these operators we can find *position* and *momentum* as a linear combination of them:

$$\hat{x} = \left(\frac{\hbar}{2m\omega}\right)^{1/2}(\hat{a} + \hat{a}^\dagger), \tag{2.30}$$

$$\hat{p}_x = -i\left(\frac{m\hbar\omega}{2}\right)^{1/2}(\hat{a} - \hat{a}^\dagger). \tag{2.31}$$

One can show by substituting the quantum mechanical operators 2.30 and 2.31 on the eqs. 2.26 and 2.27 for position and momentum, and considering a unitary mass $m = 1$, that the field quadratures can be defined quantum mechanically as[2]:

$$\hat{X} = \frac{1}{2}(\hat{a}^\dagger + \hat{a}), \tag{2.32}$$

$$\hat{P} = \frac{i}{2}(\hat{a}^\dagger - \hat{a}). \tag{2.33}$$

On summary, by an analogy with the quantum harmonic oscillator, we can define two continuous variables that act as position and momentum for a mode of light, since they are defined similarly in terms of the ladder operators for a quantum harmonic oscillator of unitary mass. These variables are the quadratures $\hat{X}$ and $\hat{P}$.

2.3   Coherent states

Coherent states are quantum states of light that have been referred as the most similar to light produced by a laser [68, 69]. All modes of light used throughout this work are modeled as coherent states because we are trying to represent a physical system

---

[2]More generally, the constant in these equations is $c/2$, being $1, 2$, and $\sqrt{2}$, the usual values for c. This difference depends on the selection of the value of $\hbar$ for natural units [66, 67].

in which two laser beams are directed into a specific type of medium. The physical system will be more thoroughly discussed later, in section 3.1.

In analogy to how a classical electromagnetic wave is generated, by a displacement of the value of the electric or the magnetic field followed by the self propagation derived from Maxwell equations, the coherent state is defined by the displacement from the quantum vacuum. This displacement is mathematically represented by the action of the *displacement operator*, $\hat{\mathbf{D}}(\alpha)$, defined as:

$$\hat{\mathbf{D}}(\alpha) = \exp\left(\alpha\hat{\boldsymbol{a}}^\dagger - \alpha^*\hat{\boldsymbol{a}}\right). \tag{2.34}$$

where α is a dimensionless complex quantity associated with the classical complex amplitude, which is in turn related to both magnitude and phase of the light mode. Furthermore, the displacement operator is unitary:

$$\hat{\mathbf{D}}^\dagger\hat{\mathbf{D}} = \hat{\mathbf{D}}\hat{\mathbf{D}}^\dagger = \hat{\mathbf{I}}, \tag{2.35}$$

which means its Hermitian conjugate is its inverse: $\hat{\mathbf{D}}^\dagger = \hat{\mathbf{D}}^{-1}$.

Coherent states are therefore defined as:

$$|\alpha\rangle = \hat{\mathbf{D}}(\alpha)|0\rangle, \tag{2.36}$$

and their dual vector is:

$$\langle\alpha| = \langle 0|\hat{\mathbf{D}}^\dagger(\alpha). \tag{2.37}$$

Coherent states are eigenstates of the annihilation operator:

$$\hat{\boldsymbol{a}}|\alpha\rangle = \alpha|\alpha\rangle, \tag{2.38}$$

and their dual vectors are eigenstates of the creation operator:

$$\langle\alpha|\hat{\boldsymbol{a}}^\dagger = \alpha^*\langle\alpha|. \tag{2.39}$$

The average number of photons in a coherent state can be calculated by the evaluation of the *photon number operator* defined as:

$$\hat{\boldsymbol{n}} = \hat{\boldsymbol{a}}^\dagger\hat{\boldsymbol{a}}, \tag{2.40}$$

which yields:

$$\langle\alpha|\hat{\boldsymbol{n}}|\alpha\rangle = \alpha^*\alpha = |a|^2, \tag{2.41}$$

thus giving physical meaning to the quantity $|\alpha|^2$ where α was the displacement applied to the vacuum state.

Coherent states form an overcomplete basis

$$\int|\alpha\rangle\langle\alpha|\,d^2\alpha = \pi > 1, \tag{2.42}$$

but are not orthogonal:

$$\langle\beta|\alpha\rangle = \exp\left[\frac{1}{2}(\beta^*\alpha - \beta\alpha^*)\right]\exp\left[-\frac{1}{2}|\beta - \alpha|^2\right] \neq 0. \tag{2.43}$$

2.4 Gaussian modes

Gaussian modes are quantum states light of continuous variables that can be represented in terms of Gaussian functions [67, 70]. More specifically, a mode is said to be Gaussian if its Wigner function (which is a phase-space distribution) is a Gaussian function. Moreover Gaussian transformations are those operations that take a Gaussian state and map it to another Gaussian state.

These type of states and transformations are very relevant in practice. For example, there are plenty of nonlinear processes that can be modeled with high accuracy by Gaussian transformations, like squeezing, which is a process that decreases the variance of one continuous variable while increasing the variance of its conjugate variable. Some other Gaussian transformations are phase rotation transformations, the displacement operator, the beam splitter transformation, the one mode squeezing operator, among others [66, 67].

On the other hand, examples of Gaussian states of light are the vacuum state, $|0\rangle$, that is the state with zero photons, the thermal states, the coherent states, $|\alpha\rangle$, which are the most relevant Gaussian states to our work since those are the ones being modeled, and the squeezed states.

2.5 Phase-space methods

As in classical mechanics there is a defined *phase space* in which we can represent a dynamical system in terms of its position and momentum at any given time, an optical phase space can be analogously defined. For this purpose the field quadratures will take the role of position and momentum, each representing an axis on the plane, and the particular state of the system will be represented as a vector.

It is important to note that since position and momentum do not commute, neither do the field quadratures, therefore there is an uncertainty relation between the two of them that can be showed to be [71]:

$$\Delta \hat{X} \Delta \hat{P} \geq \frac{1}{4}. \tag{2.44}$$

As a consequence of this uncertainty the state vector in phase space does not point to a specific point, but to a circle (more generally an area of undefined shape) on the plane. See figure 2.1 for a graphical representation. This area represents a set of allowed values for the quadratures that satisfy the relation 2.44. The change of shape of the area represents the augmentation of precision in one of the quadratures but that implies the decrement on the other one.
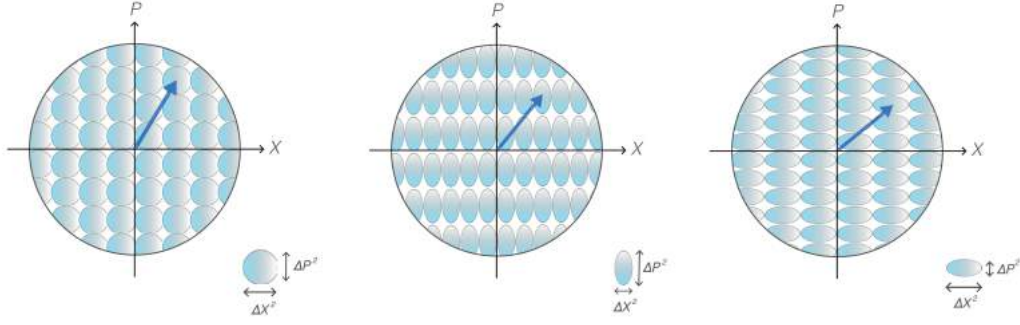
FIGURE 2.1: Graphical representation of the state vector in the phase space. The area of the circles and ellipses is all the same as it represents the uncertainty relation between the two quadratures. It is possible to augment the precision in one of the quadratures by lowering it on the other one. This trade off is represented by the variances of the quadratures, and thus by ellipticities of the ellipses, in the lower right corner of the figures.

Phase space distributions

Having defined a phase space, it is possible to define a distribution function. On a context of statistical mechanics, that is a function that yields the probability of finding a particular state vector within a small area of the phase space. In quantum optics however, there are analogous functions that yield the expectation values for observables of a quantum system [72]. Therefore, we can describe the system in terms of the evolution of these distribution functions, which are called quasiprobability functions.

There are several of these functions and we obtain them by writing the density operator in terms of an overcomplete basis. Important differences between probability functions and quasiprobability functions are that the latter may have negative values and may not be normalized to unity. Phase space distributions have been used in quantum optics to study a variety of phenomena regarding quantum non-local correlations [73, 74].

More specifically, if we consider the density operator for a quantum state in terms of coherent states:

$$\hat{\rho} = \int P(\alpha) \left| \alpha \right\rangle \left\langle \alpha \right| d^2\alpha, \tag{2.45}$$

we encounter the weight function $P(\alpha)$ known as the Glauber-Sudarshan P-function [69, 75]. Like a classical probability distribution function, the P-function is normalized to unity, that is:

$$\int P(\alpha) d^2\alpha = 1, \tag{2.46}$$

since $\hat{\rho}$ is a Hermitian operator, $P(\alpha)$ must be real.

The reason for which we are interested in these distribution functions is because, depending on the ordering of a product of annihilation and/or creation operators with the density matrix, we can choose a phase space distribution to map said product of operators to a function of the phase space [72]. In that way the density operator is mapped to these type of quasiprobability distributions. Furthermore, the evolution equation for the density operator may be mapped to a Fokker-Planck equation [72] in terms of this P-function and then to a set of stochastic differential equations which

can be solved numerically [76, 77].

Moreover, the P-function can help us to characterize a system in the following sense: if said system is classical, then the P-function will only take positive values as a real probability density function [71]. If the system is nonclassical, then the Glauber-Sudarshan P-function takes negative or singular values [44].

2.6 Positive-P representation

As it has been mentioned before, the Glauber-Sudarshan function can take negative or very singular values if the photon statistics are nonclassical [69, 71, 72]. In order to solve quantum optical problems of this nature in a more simple way, Drummond and Gardiner formulated [44] a generalisation of the P representation by using non-diagonal coherent state projectors in the density operator expansion.

In the cited paper, Drummond and Gardiner [44] prove that for a given density operator $\hat{\rho}$, if a Glauber-Sudarshan function exists, then there is also a positive non-diagonal P-function defined as:

$$P(\alpha) = \left(\frac{1}{4\pi^2}\right) \exp\left[-|\alpha - \beta^*|^2/4\right] \langle (\alpha + \beta^*)/2| \,\hat{\rho}\, |(\alpha + \beta^*)/2\rangle \tag{2.47}$$

This representation takes place in a phase space twice the size of the classical one, in which (α, β) can vary independently over the whole complex plane. Similarly to the P-representation, it is possible to obtain a Fokker-Planck equation using this distribution and utilize it to study the dynamics of the system.

In particular, the following correspondences between the products of the creation and annihilation operators, $\hat{a}, \hat{a}^\dagger$, the density matrix, $\hat{\rho}$, and the positive-P function and its parameter α, will be used later in this work:

$$
\begin{aligned}
\hat{a}\hat{\rho} &\to \alpha P, \\
\hat{\rho}\hat{a} &\to (\alpha - \frac{\partial}{\partial \alpha^\dagger})P, \\
\hat{a}^\dagger\hat{\rho} &\to (\alpha^\dagger - \frac{\partial}{\partial \alpha})P, \\
\hat{\rho}\hat{a}^\dagger &\to \alpha^\dagger P.
\end{aligned}
\tag{2.48}
$$

Previous research has shown [78–81] that the Positive-P representation yields successful results in the field of quantum optics. Some examples on this matter include, but are not limited to, the following: Rosales-Zárate et al. [78] performed probabilistic quantum simulations of Bell inequality violations . To map from the traditionally used operator eigenvalues to the phase-space probabilistic method, the positive-P representation was used. Drummond and Raymer [79], presented a theory of propagation for non-classical radiation in a medium near resonance conditions. They also used the positive-P representation and compared their results with Heisenberg equations of motion. Their results allowed them to calculate statistics for the radiation field such as photon antibunching. Also, Vyas and Singh [80] employed the positive-P representation to study the dynamics of the *optical parametric oscillators* (OPOs) and their coherence properties. Additionally, Drummond et al. [81] used the positive-P

representation to simulate quantum states in a linear photonic network. Their results allowed them to compute measurable probabilities and certify the presence of entanglement.

2.7   Fokker-Planck equations

This type of equation was first used by Fokker and Planck to describe the Brownian motion of particles [82]. A deterministic equation of motion for a small particle immersed in a liquid would need to consider the force exerted by every molecule of the fluid on the particle, however, this is not possible due to the enormous amount of molecules, so we treat the macroscopic system stochastically, or in other words, probabilistically. A Fokker-Planck equation arises as a distribution function for macroscopic quantities that are fluctuating, position in the case of Brownian motion.

A general case for N-variables has the following form [82]:

$$\frac{\partial W}{\partial t} = \left[-\sum_{i=1}^{N} \frac{\partial}{\partial x_i} \boldsymbol{A}(x) + \sum_{i,j=1}^{N} \frac{\partial^2}{\partial x_i \partial x_j} \boldsymbol{D_{ij}}(\boldsymbol{x}) \right] W, \tag{2.49}$$

where $\boldsymbol{A}$ is called the drift vector and $\boldsymbol{D}$ is called the diffusion matrix, and where they generally depend on the N variables: $x_1, x_2, \ldots x_N$. A Fokker-Planck equation can be obtained from the mapping between the positive P-function and the density operator.

Furthermore, if the diffusion matrix can be factorized as the product $\boldsymbol{D} = \boldsymbol{B}\boldsymbol{B}^T$, then it is possible to map the Fokker-Planck equation to a set of N stochastic differential equations of the following form:

$$\frac{dx_i}{dt} = A_i(x) + B_{ij}(x)\zeta_j, \tag{2.50}$$

where x_i denote the N variables of the system and ζ_j is a random process with mean zero and finite variance.

2.8   Stochastic differential equations

An stochastic differential equation (SDE) is a differential equation in which there is at least one parameter that is determined by a random process. These type of equations were introduced by Langevin to describe the movement of small particles immersed in fluids [83, 84], just as it was the case for the Fokker-Planck equation. This particle movement can be summarized as starting from an initial position and after a brief time step, receiving a small push that moves the particle in one direction or its opposite (for one dimensional SDEs). The direction for each small push is determined randomly. The particle's final position will consist of the initial position plus the algebraic sum of all the displacements occurred within the time window. We will now present the general structure and properties of an stochastic differential equation.

Lets consider the ordinary differential equation:

$$\frac{dx(t)}{dt} = a(t)x(t), \tag{2.51}$$

where $a(t)$ denotes an stochastic parameter defined as:

$$a(t) = f(t) + h(t)\zeta(t), \tag{2.52}$$

and where $\zeta(t)$ is a white noise process, which is a random process with mean zero and a finite variance. This white noise process generates different trajectories which will be averaged to obtain the solution of our SDE. This mathematical white noise is important because it corresponds to quantum noise originated in the physical system from the uncertainty in the observable from quantum mechanical objects [85]. Then we can write the SDE as:

$$\frac{dx(t)}{dt} = f(t)x(t) + h(t)x(t)\zeta(t). \tag{2.53}$$

Writing it in its differential form, the SDE takes the following representation:

$$dx(t) = f(x)x(t)dt + h(t)x(t)dW(t), \tag{2.54}$$

where $dW(t)$ is notation for the differential form of the brownian motion, also called Wiener process [84].

We could also express eq. 2.53 as follows:

$$\frac{dx(t)}{dt} = a(x, t) + b(x, t)\zeta(t), \tag{2.55}$$

in which we have defined $a(x, t) = f(t)x(t)$ and $b(x, t) = h(t)x(t)$. Expression 2.55 is what is known as the *Langevin equation* [83]. This definition will be useful in subsection 2.8.2 when we define an *Ito Stochastic Differential Equation*.

The solution for the Langevin eq. 2.55 is:

$$x(t) - x(0) = \int_0^t a(x(t'), t')dt' + \int_0^t b(x(t'), t')dW(t')dt', \tag{2.56}$$

if it can be shown that the second integral from the right hand side does exist. Several authors [83, 84, 86] have demonstrated that this in fact can be proven if we consider this integral to be the limit, as $n \to \infty$, of the following approximation:

$$S = \sum_{i=1}^n b(x(\tau_i), \tau_i)\left(W(t_i) - W(t_{i-1})\right), \tag{2.57}$$

in which we have defined τ_i to be an *arbitrary* intermediate point in the interval $[t_{i-1}, t_i]$. The difference between these two instants in time is called a *time step* and is denoted by Δt. These n intervals span the entirety of the time domain $[t_0 = 0, t_n = t]$.

It is important to notice that the selection of the point τ_i does make a difference in the behaviour of the function b, thus making a difference on the final outcome. Two specific choices have been proven to be useful:

- If one chooses $\tau_i = t_{i-1}$, that is, the left end point of the time interval, then we obtain the *Ito integral* [84, 86].

- On the other hand, if we choose $\tau_i = \frac{t_{i-1}+t_i}{2}$, in other words, the midpoint of the time interval, we get the *Stratonovich integral* [84, 86].

Each of these possibilities has its properties and, depending on the problem to be solved, its advantages. Since our purpose is to solve SDEs numerically by different algorithms, the choice of the form of the differential equation will depend on the specific algorithm that will be used.

2.8.1 Numerical methods for solving SDEs

As we have previously discussed, stochastic differential equations produce random trajectories. The noise is different for each trajectory (since it is random), so, even if both displacements start from the same initial, the trajectories will be different in general. This means that a single SDE can produce an infinite number of paths. It is possible, however, to obtain averages after calculating a sufficiently large amount of these trajectories, even if it is a finite number of them. The average of any observable is obtained by averaging over the stochastic trajectories numerically.

Numerical methods are, in general, algorithms that are utilized to approximate values for quantities that not necessarily have an analytical solution, or that have one that is not possible to be computed within a reasonable time. These approximations usually rely on iterative processes and often start with an estimated guess that is refined until convergence is achieved. The time efficiency for numerical method approximation is usually determined by the computational power used [76]. More efficient methods, which are called of higher order of convergence, achieve higher precision with less operations but are often more difficult to implement.

Numerical methods for solving differential equations are often used to solve ordinary or partial differential equations [76]. However, there are modifications to the algorithms that can be implemented for SDEs. They usually consist on the addition of random fluctuations on each iteration, as is the case for the Euler-Maruyama method [76].

2.8.2 Ito and Stratonovich calculus

Depending on the type of integral (or interpretation, as it is called by some authors [76]) used for the stochastic differential equations, different methodology emerges for calculating the solution. Specifically in the context of numerical methods, which are iterative, the computation of the next step in time depends for each equation in the following way [87]:

Let us consider $x_0 = x(t_0)$, $t_1 = t_0 + \Delta t$, $\overline{x} = \frac{x_1 + x_0}{2}$ and lastly $\overline{t} = \frac{t + \Delta t}{2}$, then for calculating the next step in time we do the following:

- Ito calculus is defined by functions of the initial points:

$$x_1 = x_0 + (a(x_0, t_0) + b(x_0, t_0)\zeta)\,\Delta t. \tag{2.58}$$

- Stratonovich calculus uses points in the middle of the time step:

$$x_1 = x_0 + \left(a\left(\overline{x}, \overline{t}\right) + b\left(\overline{x}, \overline{t}\right)\zeta\right)\Delta t. \tag{2.59}$$

As has been mentioned in the previous section, the integral is defined as the limit in which the number of small time intervals $n \to \infty$, or equivalently: $\Delta t \to 0$.

2.8.3 Algorithms for numerical calculation

We will now discuss the numerical algorithms used in this work, but we will first introduce some useful notation. We define the following quantity:

$$\mathcal{D}(x, t) = a(x, t) + b(x, t)\zeta, \tag{2.60}$$

so that we can write the Langevin equation 2.55 as:

$$\frac{dx}{dt} = \mathcal{D}(x, t). \tag{2.61}$$

The following are the numerical methods that were used to solve the SDEs as they are discussed by Drummond and Kiesewetter [87].

- **Euler-Maruyama**: This is a traditional method that is only convergent to first order and usually has large errors. It approximates the derivative as a finite difference and refines the value of the function iteratively. It is designed to be used with an Ito SDE. We start from t_0 and with the definition $t_{n+1} = t_n + \Delta t$ we calculate:

$$\begin{aligned} \Delta x_n &= \mathcal{D}(x_n, t_n)\Delta t, \\ x_{n+1} &= x_n + \Delta x_n. \end{aligned} \tag{2.62}$$

- **Midpoint**: This numerical method is convergent to second order and is also based on the Euler-Maruyama method [87] but calculates the value of the slope for the midpoint between the time steps, $\overline{x}$. It is designed to be used with a Stratonovich SDE. We start by defining an intermediate time for the respective interval $\overline{t}_n = t + \Delta t/2$ and we calculate the following:

$$\begin{aligned} \overline{x}_n &= x_n + \mathcal{D}(x_n, \overline{t})\frac{\Delta t}{2}, \\ x_{n+1} &= (2\overline{x} - x_n). \end{aligned} \tag{2.63}$$

- **Runge-Kutta of 4th order**: This is an algorithm based on Euler's method that considers four values for the slope of the function within the same time interval to provide a more precise solution. It has to be used with a Stratonovich SDE. The relevant quantities for this algorithm:

$$\begin{aligned} \mathbf{d}^{(1)} &= \mathcal{D}(x_n, t_n)\frac{\Delta t}{2}, \\ \mathbf{d}^{(2)} &= \mathcal{D}(x_n + \mathbf{d}^{(1)}, \overline{t})\frac{\Delta t}{2}, \\ \mathbf{d}^{(3)} &= \mathcal{D}(x_n + \mathbf{d}^{(2)}, \overline{t})\frac{\Delta t}{2}, \\ \mathbf{d}^{(4)} &= \mathcal{D}(x_n + 2\mathbf{d}^{(3)}, \overline{t}_{n+1})\frac{\Delta t}{2}, \\ x_{n+1} &= \left(x_n + (\mathbf{d}^{(1)} + 2(\mathbf{d}^{(2)} + \mathbf{d}^{(3)}))/3\right) + \mathbf{d}^{(4)}/3. \end{aligned} \tag{2.64}$$

- **Central difference:** This algorithm calculates an approximation of the derivative of the function by averaging the values at the start and at the end of the time step, as well as adding a random fluctuation. Like the majority of the algorithms discussed so far, it requires a Stratonovich SDE. The relevant quantities for this algorithm are the following:

$$\begin{aligned}
\overline{x}_n &= x_n + \mathcal{D}(x_n, t)\Delta t, \\
x_{n+1} &= \left(x_n + \overline{x}\right)/2.
\end{aligned} \tag{2.65}$$

The algorithms presented so far were the ones we used in our work, however there are plenty of algorithms for solving SDEs that we did not mention, for example [76]: lower orders of the Runge-Kutta method, a variation for the midpoint algorithm which is called *adaptive midpoint* and the implicit Ito-Euler algorithm that requires an implicit Ito SDE, among others. The reason for choosing these algorithms is that they minimize the computational time for our calculations and they all yield the same results.

2.9   Entanglement witnesses

As has been noted, there are several distinct non-local quantum correlations. One of the first ways to test for non-local correlations was by using Bell's inequality [2, 4, 5]. Furthermore, it has been shown that for pure states, all entangled systems exhibit steering as well as Bell non-locality [26, 88]. For mixed states, however, the situation is more complex, as demonstrating the presence of a quantum correlation does not guarantee the presence of the other stronger correlations. Therefore methods to test for entanglement and steering independently are needed.

Nowadays if one wants to test if a quantum correlation is present there are several criteria available. For example, in bipartite systems, entanglement can be found using the Peres-Horodecki criterion [89, 90] which states that if a system is separable then its density operator partial transpose will have no negative eigenvalues, while in the case of an entangled system, it will have at least one negative eigenvalue. This criterion, however, depends on the prior knowledge of the density operator, but this is not the case in practice. For these situations a different type of criteria called *witnesses* were developed. These quantities are operators defined in terms of observables that are sensitive to these non-local effects. If the expectation value of these quantities exceed a certain threshold, it indicates that the system has presence of said correlation.

Witnesses are useful since they can be used in a wider variety of physical systems compared to the Bell inequalities, and test weaker correlations as entanglement and steering on their own, as well as depending on directly measureable observables.

Non-local quantum correlations have been mostly studied on bipartite systems, and standard criteria has been developed to test for entanglement, steering and Bell non-locality. On the other hand, multipartite systems are still being characterized and there is a vast amount of witnesses used to test for these multipartite correlations. Below we mention some witnesses that are useful for our work. We start by defining what is a bipartition: for a system with n-parties, a bipartition is the formation of two non-empty sets that together contain all the n-subsystems. Both sets cannot contain

the same elements, but different bipartitions can be defined and studied for the same system. For a schematic diagram of what is a bipartition see figure 2.2.
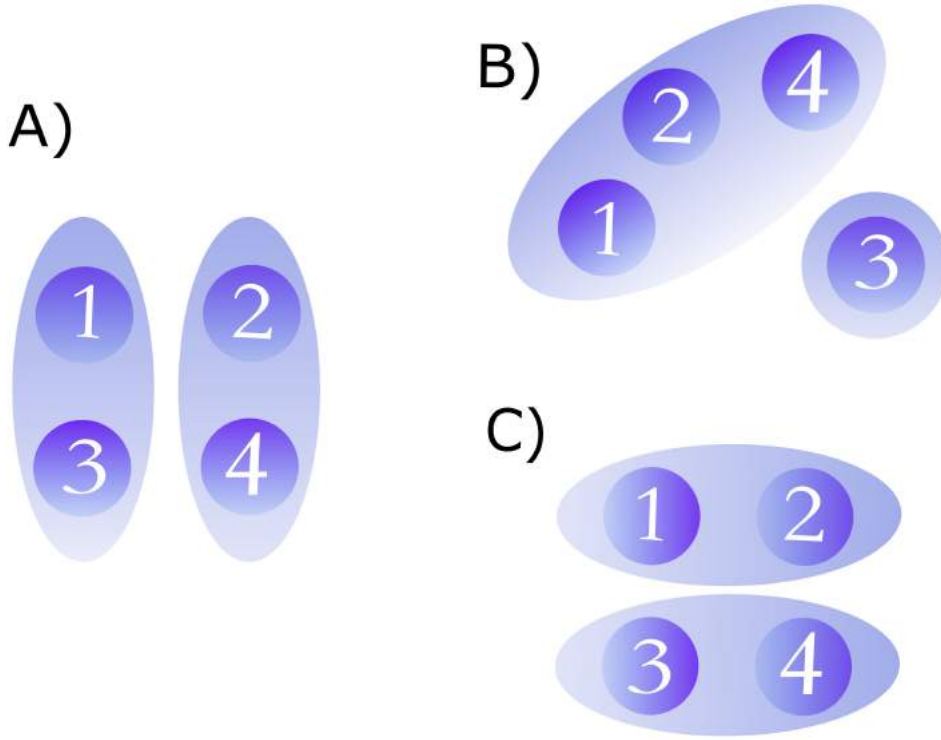

FIGURE 2.2: Schematic representation of three different bipartitions for a set of 4 elements. There are in total, seven different bipartitions for four elements.

2.9.1 Duan-Giedke-Cirac-Zoller (DGCZ) criterion

As it was mentioned previously, there are plenty of witnesses that serve as criterion for separability in quantum systems. This entanglement criterion in particular is used for continuous variable bipartite systems and is based on the calculation of variances of specially defined operators. Duan, Giedke, Cirac and Zoller (DGCZ) [91] demonstrated that the sum of the total variance of linear combinations of continuous variables for separable states is bounded below a certain threshold.

The authors start by using the quadrature definition:

$$
\begin{aligned}
\hat{X}_j &= (\hat{a}_j^\dagger + \hat{a}_j), \\
\hat{P}_j &= i(\hat{a}_j^\dagger - \hat{a}_j),
\end{aligned}
\tag{2.66}
$$

and define the following operators in terms of the quadratures:

$$
\begin{aligned}
\hat{U} &= \hat{X}_i - \hat{X}_j, \\
\hat{V} &= \hat{P}_i - \hat{P}_j,
\end{aligned}
\tag{2.67}
$$

and showed that it is a sufficient criterion to certify entanglement if the following condition is violated:

$$
D_{i,j} = \langle \Delta^2 U \rangle + \langle \Delta^2 V \rangle \geq 4.
\tag{2.68}
$$

This criterion is a sufficient but not necessary condition for entanglement to be present, which in turn means that a system may exhibit entanglement without violating the condition.

2.9.2 General separability criterion

Giovannetti et al. derived a generalization of these criteria [92] that is based on the commutation relations satisfied by the observables used. This general criterion is specific for bipartite systems.

The authors start by considering a bipartite separable state that can be written as:

$$\hat{\rho}_{sep} = \sum_k w_k \hat{\rho}_{k,1} \otimes \hat{\rho}_{k,2}, \tag{2.69}$$

where $\hat{\rho}_{k,1}, \hat{\rho}_{k,2}$ are normalized density matrices and w_k are coefficients of a normalized convex combination.

Giovannetti et al. proceed to select two different arbitrary observables for each subsystem. These observables will be called $\hat{r}_j, \hat{s}_j$, where $j = 1, 2$. Here, the subindices represent each party of the bipartition. Afterwards, the authors use these observables to define the operators:

$$\hat{C}_j = i \left[\hat{r}_j, \hat{s}_j \right]. \tag{2.70}$$

The following quantities are then introduced:

$$\begin{aligned} \hat{u} &= a_1 \hat{r}_1 + a_2 \hat{r}_2, \\ \hat{v} &= b_1 \hat{s}_1 + b_2 \hat{s}_2, \end{aligned} \tag{2.71}$$

where a_1, a_2, b_1, b_2 are arbitrary, real coefficients.

Subsequently, Giovannetti et al. prove that every separable bipartite state satisfies the following inequality:

$$\langle \Delta^2 \hat{u} \rangle \langle \Delta^2 \hat{v} \rangle \geq \overline{\mathcal{O}}^2, \tag{2.72}$$

where $\overline{\mathcal{O}}$ is defined as:

$$\overline{\mathcal{O}} = \frac{1}{2} \left(|a_1 b_1| \overline{\mathcal{O}}_1 + |a_2 b_2| \overline{\mathcal{O}}_2 \right), \tag{2.73}$$

which in turn depends on:

$$\overline{\mathcal{O}}_j = \sum_k w_k |\langle \hat{C}_j \rangle_k|. \tag{2.74}$$

Lastly, $\langle \hat{C}_j \rangle_k$ is the expectation value of $\hat{C}_j$ for the state k in eq. 2.69.

Summarizing, if a bipartite quantum system violates the inequality 2.72, then it is entangled. The threshold depends on the chosen observables $\hat{r}_j, \hat{s}_j$ and on the definitions 2.71. This result is very relevant to the study of bipartite quantum correlations because it provides us with a general recipe to test for entanglement. Here, by general, we refer to the fact that we can define a witness and calculate its corresponding threshold for any arbitrary pair of observables just by considering their commutation relations. Some of the following entanglement criteria used within this work are of the general form of eq. 2.72.

2.9.3   van Loock-Furusawa criterion.

In the same spirit as the prior criterion, authors van Loock and Furusawa [93] developed a method to test for entanglement in multipartite systems. Their operator definition for an N-partite system is the following:

$$
\begin{aligned}
\hat{u} &= g_1 \hat{X}_1 + \cdots + g_N \hat{X}_N, \\
\hat{v} &= h_1 \hat{P}_1 + \cdots + h_N \hat{P}_N,
\end{aligned}
\tag{2.75}
$$

where g_i, h_i are arbitrary real numbers. Authors have shown that if the system is separable in a bipartition of modes r and s, it will satisfy the following condition:

$$
(\Delta u)^2 + (\Delta v)^2 \geq 2 \left(\left| \sum_{k_r}^n h_{k_r} g_{k_r} \right| + \left| \sum_{k_s}^n h_{k_s} g_{k_s} \right| \right).
\tag{2.76}
$$

In order to prove full N-partite entanglement it is needed to show that no possible bipartition of the N-modes of the system is separable, therefore the single following inequality is sufficient to demonstrate N-partite entanglement:

$$
(\Delta u)^2 + (\Delta v)^2 \geq 2 \min\{S_B\},
\tag{2.77}
$$

where S_B is the set of numbers $\left(\left| \sum_{k_r}^n h_{k_r} g_{k_r} \right| + \left| \sum_{k_s}^n h_{k_s} g_{k_s} \right| \right)$, evaluated for each possible bipartition of modes r and s.

In particular, Teh and Reid [47], considered the 4-partite case and defined the operators from equations 2.75 as:

$$
\begin{aligned}
\hat{U} &= \hat{X}_1 - \frac{1}{\sqrt{3}} \left(\hat{X}_2 + \hat{X}_3 + \hat{X}_4 \right), \\
\hat{V} &= \hat{P}_1 + \frac{1}{\sqrt{3}} \left(\hat{P}_2 + \hat{P}_3 + \hat{P}_4 \right).
\end{aligned}
\tag{2.78}
$$

Considering the 4 modes, we can consider the following 7 bipartitions: $1-234$, $2-134$, $3-124$, $4-123$, $12-34$, $13-24$, $14-23$. Afterwards, the quantities: $\left| \sum_{k_r}^n h_{k_r} g_{k_r} \right| + \left| \sum_{k_s}^n h_{k_s} g_{k_s} \right|$, which constitute the set S_B, for each of the mentioned bipartitions, are calculated as:

- Bipartition $1-234$: $|h_1 g_1| + |h_2 g_2 + h_3 g_3 + h_4 g_4| = |1| + \left| -\frac{1}{3} - \frac{1}{3} - \frac{1}{3} \right| = 2$.

- Bipartition $2-134$: $|h_2 g_2| + |h_1 g_1 + h_3 g_3 + h_4 g_4| = \left| -\frac{1}{3} \right| + \left| 1 - \frac{1}{3} - \frac{1}{3} \right| = \frac{2}{3}$.

- Bipartition $3-124$: $|h_3 g_3| + |h_1 g_1 + h_2 g_2 + h_4 g_4| = \left| -\frac{1}{3} \right| + \left| 1 - \frac{1}{3} - \frac{1}{3} \right| = \frac{2}{3}$.

- Bipartition $4-123$: $|h_4 g_4| + |h_1 g_1 + h_2 g_2 + h_3 g_3| = \left| -\frac{1}{3} \right| + \left| 1 - \frac{1}{3} - \frac{1}{3} \right| = \frac{2}{3}$.

- Bipartition $12-34$: $|h_1 g_1 + h_2 g_2| + |h_3 g_3 + h_4 g_4| = \left| 1 - \frac{1}{3} \right| + \left| -\frac{1}{3} - \frac{1}{3} \right| = \frac{4}{3}$.

- Bipartition $13-24$: $|h_1 g_1 + h_3 g_3| + |h_2 g_2 + h_4 g_4| = \left| 1 - \frac{1}{3} \right| + \left| -\frac{1}{3} - \frac{1}{3} \right| = \frac{4}{3}$.

- Bipartition $14-23$: $|h_1 g_1 + h_4 g_4| + |h_2 g_2 + h_3 g_3| = \left| 1 - \frac{1}{3} \right| + \left| -\frac{1}{3} - \frac{1}{3} \right| = \frac{4}{3}$.

These calculations yield three different results, which in turn can be used to obtain three different thresholds for bipartition entanglement using expression 2.76. Furthermore, the lowest value of the set is $\frac{4}{3}$, thus the threshold for the N-partite entanglement using only the inequality from eq. 2.77 is two times this value, that is $\frac{8}{3}$.

2.9.4   Teh-Reid criteria for genuine N-partite entanglement.

The criterion developed by van Loock and Furusawa is useful to certify full N-partite entanglement. However, it has been pointed out that this is different to genuine multipartite entanglement because the latter also prohibits convex sums of biseparable states. Authors Teh and Reid have shown [47] that by defining a quantity $I_k = (\Delta u)^2 + (\Delta v)^2$, where u and v are linear combinations of the system observables $\hat{X}_j$, $\hat{P}_j$, for a certain bipartition labeled k, violation of the inequality $I_k \geq 4$ will certify entanglement for that bipartition. Furthermore if the sum of I_k for all possible bipartitions in the system violates the following inequality:

$$\sum_k I_k \geq 4, \tag{2.79}$$

then the system is *genuinely entangled*. More so, the authors prove that if there is a single quantity, which we will call I, that negates separability for all bipartitions on its own, then it can also certify *genuine multipartite entanglement* if the following requirement is not met:

$$I \geq 4. \tag{2.80}$$

It is important to note that the threshold value equal to 4 in expressions 2.79 and 2.80 is a function of the commutator of the observables $\hat{X}_j, \hat{P}_j$ and the linear coefficients used in u and v, thus this limit may change depending on how these operators are defined. The particular case outlined here applies to the definitions in eq. 2.66.

The importance of this result is not only that increments what can be known with certain criteria, but the fact that this result is more general. More specifically, the van Loock-Furusawa criterion described in eq. 2.77 can be seen as a special case of inequality 2.80, but it is certainly not the only one.

As an example, Teh and Reid [47] consider the 4-partite case, and using the following inequalities (which were also defined by van Loock and Furusawa [93]):

$$\begin{aligned}
B_I &= \left[\Delta^2(X_1 - X_2)\right] + \left[\Delta^2(P_1 + P_2 + g_3 P_3 + g_4 P_4)\right] \geq 4, \\
B_{II} &= \left[\Delta^2(X_2 - X_3)\right] + \left[\Delta^2(g_1 P_1 + P_2 + P_3 + g_4 P_4)\right] \geq 4, \\
B_{III} &= \left[\Delta^2(X_1 - X_3)\right] + \left[\Delta^2(P_1 + g_2 P_2 + P_3 + g_4 P_4)\right] \geq 4, \\
B_{IV} &= \left[\Delta^2(X_3 - X_4)\right] + \left[\Delta^2(g_1 P_1 + g_2 P_2 + P_3 + P_4)\right] \geq 4, \\
B_V &= \left[\Delta^2(X_2 - X_4)\right] + \left[\Delta^2(g_1 P_1 + P_2 + g_3 P_3 + P_4)\right] \geq 4, \\
B_{VI} &= \left[\Delta^2(X_1 - X_4)\right] + \left[\Delta^2(P_1 + g_2 P_2 + g_3 P_3 + P_4)\right] \geq 4,
\end{aligned}$$

demonstrate that the violation of the single inequality:

$$\sum_{j=1}^{6} B \geq 12, \tag{2.81}$$

certifies genuine 4-partite entanglement. Summarizing, Teh and Reid have shown [47] that the criterion of eq. 2.77 is part of a family of entanglement witnesses that not only certify full multipartite entanglement but also genuine multipartite entanglement. Criteria of this family can always be defined for N-partite systems.

2.10 Steering witnesses

Similarly to the entanglement witnesses that have been discussed so far, there are also witnesses that can be used to detect steering. The most important difference between these two types of witnesses is that, since entanglement is a symmetric correlation, the entanglement witnesses yield the same results for any given pair of subsystems, regardless of the order in which the modes are operated. On the other hand, steering is an asymmetric correlation, therefore the steering witness can produce different results for the same pair of subsystems depending on whether we are testing if subsystem A steers subsystem B, or if B steers A. Similarly to the entanglement case, steering in multipartite systems is also distinguished between *full N-partite steering* and *genuine N-partite steering*.

2.10.1 Bipartite steering

A criterion proposed by Reid and Drummond [94] used to test for steering between two parties of a system is:

$$\mathrm{EPR}_{i|j} = V_{\mathrm{inf}}(\hat{X}_i)V_{\mathrm{inf}}(\hat{P}_i) < 1. \tag{2.82}$$

Here, $V_{inf}(\hat{A})$ is the inferred variance for an arbitrary operator $\hat{A}$. These quantities are defined as follows:

$$
\begin{aligned}
V_{\mathrm{inf}}(\hat{X}_i) &= \Delta^2(\hat{X}_i) - \frac{\left[\Delta^2(\hat{X}_i, \hat{X}_j)\right]^2}{\Delta^2(\hat{X}_j)}, \\
V_{\mathrm{inf}}(\hat{P}_i) &= \Delta^2(\hat{P}_i) - \frac{\left[\Delta^2(\hat{P}_i, \hat{P}_j)\right]^2}{\Delta^2(\hat{P}_j)},
\end{aligned}
\tag{2.83}
$$

where $\Delta^2(\hat{A}, \hat{B}) = \frac{1}{2}\langle \hat{A}\hat{B} + \hat{B}\hat{A}\rangle - \langle \hat{A}\rangle\langle \hat{B}\rangle$ is the covariance of the operators $\hat{A}$ and $\hat{B}$. If the inequality 2.82 is satisfied, steering from subsystem i onto subsystem j is certified.

2.10.2 Full N-partite steering criterion

A different criterion used by Teh et al. [95] to detect steering is:

$$S_{A|B} = \Delta\left(\hat{X}_A - \hat{X}_B\right)\Delta\left(\hat{P}_A - \hat{P}_B\right) < 1. \tag{2.84}$$

If this inequality is violated, then steering of subsystem B by subsystem A is certified. Furthermore, a more general form for this criterion is:

$$S_{A|B} = \Delta\left(\hat{X}_A - \hat{O}_B^1\right)\Delta\left(\hat{P}_A - \hat{O}_B^2\right) < 1. \tag{2.85}$$

where $\hat{O}_B^1$ and $\hat{O}_B^2$ are observables for subsystem B, which might be in turn, conformed by more than one subsystem, thus allowing us to use the criterion to test for N-partite steering. In order to certify full N-partite steering, this correlation has to be found for any possible bipartition of the N modes in its two-way version.

2.10.3   Genuine multipartite steering criterion.

A criterion used to certify genuine multipartite steering was developed by Teh et al. [95]. If we define the following operators:

$$
\begin{aligned}
u &= h_1 x_1 + h_2 x_2 + h_3 x_3 + h_4 x_4, \\
v &= g_1 p_1 + g_2 p_2 + g_3 p_3 + g_4 p_4,
\end{aligned}
\tag{2.86}
$$

then, we can consider the following bipartitions: 1-234, 2-134, 3-124, 4-123 as well as: 12-34, 13-24, 14-23. For the first bipartition, the violation of the following inequality:

$$
\Delta u \Delta v \geq |g_1 h_1|,
\tag{2.87}
$$

where Δu, denotes the standard deviation for operator u and Δv is the corresponding quantity for v; implies the steering of system 1 by subsystems 2, 3 and 4. Similarly, violation of:

$$
\Delta u \Delta v \geq |g_2 h_2 + g_3 h_3 + g_4 h_4|,
\tag{2.88}
$$

implies the steering of partition 234 by subsystem 1. Thus, the violation of the following inequality implies two-way steering [95]:

$$
\Delta u \Delta v \geq \min \left\{ |g_1 h_1|, |g_2 h_2 + g_3 h_3 + g_4 h_4| \right\}.
\tag{2.89}
$$

If a different bipartition is considered, such as 13-24, then the inequality would be:

$$
\Delta u \Delta v \geq \min \left\{ |g_1 h_1 + g_3 h_3|, |g_2 h_2 + g_4 h_4| \right\}.
\tag{2.90}
$$

In order to certify genuine multipartite steering across the system, the two-way steering has to be present for every possible bipartition by an inequality such as the former [95]. Furthermore, if we consider the minimal number from these bipartition inequalities, we certify genuine multipartite steering by using just one inequality.

For the 4 partite case, there are 7 bipartitions, and using results obtained previously from subsection 2.9.3, in which u and v are defined identically, we can obtain the thresholds for two-way steering:

- Bipartition $1 - 234$: $\min\{|h_1 g_1|, |h_2 g_2 + h_3 g_3 + h_4 g_4|\} = 1$.

- Bipartition $2 - 134$: $\min\left\{|h_2 g_2|, |h_1 g_1 + h_3 g_3 + h_4 g_4|\right\} = \frac{1}{3}$.

- Bipartition $3 - 124$: $\min\left\{|h_3 g_3|, |h_1 g_1 + h_2 g_2 + h_4 g_4|\right\} = \frac{1}{3}$.

- Bipartition $4 - 123$: $\min\left\{|h_4 g_4|, |h_1 g_1 + h_2 g_2 + h_3 g_3|\right\} = \frac{1}{3}$.

- Bipartition $12 - 34$: $\min\left\{|h_1 g_1 + h_2 g_2|, |h_3 g_3 + h_4 g_4|\right\} = \frac{2}{3}$.

- Bipartition $13 - 24$: $\min\left\{|h_1 g_1 + h_3 g_3|, |h_2 g_2 + h_4 g_4|\right\} = \frac{2}{3}$.

- Bipartition $14 - 23$: $\min\left\{|h_1 g_1 + h_4 g_4|, |h_2 g_2 + h_3 g_3|\right\} = \frac{2}{3}$.

If we obtain values for $\Delta u \Delta v$ that are below the minimum value of these thresholds, then genuine 4-partite steering is certified.

2.11   Monogamy relations

In the context of quantum correlations, monogamy relations refer to the way that entanglement or steering are distributed among the multiple parties of a system. In particular, monogamy relations quantify the amount of each of these correlation among each of the parties of the system. A system is monogamous if quantum correlations are restricted quantitatively between different subsystems. For example, in a tripartite quantum system if two parties, A and B, are maximally correlated, then they cannot share any correlation with party C [96]. This restriction on the ability of the parties to be correlated with each other is exclusive to the quantum phenomena, since classical correlations do not have these constraints.

Our interest in monogamy relations emerges because it is important to understand how the quantum correlations are distributed among the different parties in a quantitative way. It was our intention to include monogamy relations in our study to make it more thorough, however, as far as we are concerned, there are no proposals for monogamy relations for the 4-partite case for continuous variable systems using witnesses. Nevertheless, we include this topic in our work because we believe it can provide for an interesting continuation of our analysis. In this section of the work we will start by discussing the first monogamy relation established, which is in a work by Coffman, Kundu and Wootters [97] and which is defined for tripartite systems. Later on, we will discuss the generalized case for N subsystems.

In order to quantify the amount of entanglement distributed among the parties of a quantum system, it is necessary to quantify the entanglement itself, that is why Coffman, Kundu and Wootters (CKW) [97] start by defining the *tangle* for that purpose. They consider their system to be conformed by two two-level qubits, such as spin-$\frac{1}{2}$ particles, but claim that their methodology could also be used for larger systems.

For a pair of qubits called A and B, on a pure state, described by the density matrix $\hat{\rho}_{AB}$, the authors define the *spin-flipped* density matrix as:

$$\overline{\rho}_{AB} = (\sigma_y \otimes \sigma_y)\, \rho^*_{AB}\, (\sigma_y \otimes \sigma_y)\,, \tag{2.91}$$

where the asterisk represents the complex conjugate and σ_y is the standard Pauli spin matrix:

$$\sigma_y = \begin{pmatrix} 0 & -i \\ i & 0 \end{pmatrix}. \tag{2.92}$$

Afterwards, the authors calculate the product $\rho_{AB}\overline{\rho}_{AB}$ that has only real, non-negative eigenvalues $\lambda_1, \ldots, \lambda_4$, though it is not Hermitian. Then, the *tangle* of the density matrix ρ_{AB} is defined as:

$$\tau_{AB} = (\max\left[\lambda_1 - \lambda_2 - \lambda_3 - \lambda_4, 0\right])^2. \tag{2.93}$$

Coffman, Kundu and Wootters argue that $\tau = 0$ corresponds to an unentangled state, while $\tau = 1$ is the result obtained from a maximally entangled state.

The relationship between this, seemingly arbitrary quantity, and the entanglement of a physical system is discussed on a previous work by Wootters [98]. In it, the author defines a different quantity called the *concurrence*, which is the square root of the tangle. That is:

$$\mathcal{C}_{AB} = (\max\{\lambda_1 - \lambda_2 - \lambda_3 - \lambda_4, 0\}) \tag{2.94}$$

Even though the concurrence itself is very used in the literature [99–101], in the more recent article CKW argue that the mathematical manipulation simplifies greatly by introducing the new term.

The importance of this measurement for multipartite entanglement resides on the fact that an N-partite system can be analyzed through bipartitions of the parties. Subsequently, for a given bipartition, we can study the level of entanglement between the two parties within it, and use that value to determine if these two share a quantum correlation with the rest of the system. Moreover, the bipartitions for the whole system do not need to be restricted to just two subsystems. The two parties of the bipartition may be conformed by more than one physical subsystem, in other words, for a tripartite system composed by subsystems A, B and C, the bipartition $A - BC$ is perfectly valid.

So far the measurement for entanglement has been provided, and with it the monogamy relation can be defined. For a pure-state tripartite quantum system between two parties the monogamy relation is defined as:

$$\tau_{AB} + \tau_{AC} \leq \tau_{A(BC)}, \tag{2.95}$$

which can be interpreted as follows: the amount of entanglement that A has with BC, bounds the total amount of entanglement, that is, entanglement of A with B and C, individually. Additionally to this bound, the amount of entanglement that A has with B is not available to C [97].

The monogamy definition of inequality 2.95 applies specifically to pure states but a generalization to mixed states is also available [97]. If instead of being in a pure state our tripartite quantum system is described by the density operator ρ, then, we first have to consider all possible pure-state decompositions. In other words, all sets $\{\psi_j, \omega_j\}$, such that our density operator can be written as:

$$\hat{\rho} = \sum_j \omega_j \ket{\psi_j} \bra{\psi_j}.$$

Once this is done, it is possible to calculate the average tangle for each of these decompositions [97]:

$$\langle \tau_{A(BC)} \rangle = \sum_j \omega_j \tau_{A(BC)}(\psi_j). \tag{2.96}$$

Once all of these quantities are calculated, the minimum of the set of the tangles calculated, $\min\{\tau_{A(BC)}\}$, will take the place of the right hand side of inequality 2.95. Mathematically, this is expressed as:

$$\tau_{AB} + \tau_{AC} \leq \min\{\tau_{A(BC)}\}. \tag{2.97}$$

Moreover, this important result by CKW was generalized years later by Osborne and Verstraete [102] to include not only tripartite quantum systems, but an arbitrary number N of subsystems.

General monogamy relations

In this work, not only we are interested in entanglement, but also in other quantum correlations. In that sense, it is important to mention that, just as monogamy was defined for the tangle, an arbitrary quantum correlation measure can yield a corresponding monogamy relation [96]. For a given bipartite quantum correlation measure, $\mathcal{Q}$, the monogamy relation is expressed as [96]:

$$\mathcal{Q}(\rho_{AB}) + \mathcal{Q}(\rho_{AC}) \leq \mathcal{Q}(\rho_{A(BC)}). \tag{2.98}$$

If a system does not satisfy relation 2.98, then it is non-monogamous for measure $\mathcal{Q}$. We believe it is important to clarify that the tangle or the concurrence are not the only entanglement measures. Alternatives for this purpose include: negativity [89], Tsallis entropy [103] or *contangle* (which is the analogous of tangle for continuous variables) [104], among others. Therefore, the monogamy relation for entanglement on equations 2.95 and 2.98, is not the only one.

Monogamy without quantification

Monogamy relations can be established without the need for a quantifier of the quantum correlation. For instance, Rosales-Zárate et al. [105] defined a monogamy relation that uses the previously discussed DGCZ criterion to certify entanglement. Unlike the monogamy relations discussed so far, this *entanglement certifier* does not quantify entanglement yet it can be used for a monogamy relation.

Let us re-write the DGCZ criterion to introduce notation necessary for the monogamy relation. Tan and DGCZ [91, 106] define the following quantity:

$$D_{ij} = \Delta^2 \left(\frac{X_i - X_j}{2} \right) + \Delta^2 \left(\frac{P_i - P_j}{2} \right), \tag{2.99}$$

where, Δ^2 denotes the variance and X, P denote the quadratures of the mode of light. Then, if the following inequality is violated:

$$D_{ij} \geq 1, \tag{2.100}$$

entanglement is certified between modes i and j. Subsequently, Rosales-Zárate et al. proved [105] that for a tripartite quantum system conformed by modes A, B, and C, and using the mentioned entanglement criterion, the following monogamy relation exists:

$$D_{BA} + D_{BC} \geq \max\{1, S_{B|AC}\}, \tag{2.101}$$

where $S_{B|AC}$ is a steering certifier defined by Wiseman et al. [22, 55] that finds said correlation on B by system AC when $S_{B|AC} < 1$.

Furthermore, the authors also derived a monogamy relation for another entanglement criterion, namely the Ent_{ij} certifier introduced by Giovanneti, Mancini, Vitali and Tombesi (GMVT) [92]. For this certifier, GMVT defined the quantities:

$$\text{Ent}_{ij} = \frac{\Delta \left(X_i - g_{ij}^x X_j \right) \Delta \left(P_i - g_{ij}^p P_j \right)}{1 + g_x g_p}, \tag{2.102}$$

where g_{ij}^x and g_{ij}^p are real constants chosen specifically to minimize the value of Ent_{ij}. GMVT showed that if the condition $\mathrm{Ent}_{ij} < 1$ holds, then it is also true that modes i and j are entangled with each other.

Rosales-Zárate et al. found an optimal value for the real constants g_{ij}^x and g_{ij}^p, which happens to be:

$$g_{ij}^x = g_{ij}^p = g_{ij}^{(\mathrm{sym})}, \tag{2.103}$$

where $g_{ij}^{(\mathrm{sym})}$ depends on the covariances of the quadratures and is fixed for each pair of modes ij. The monogamy relation for a tripartite system is [105]:

$$\mathrm{Ent}_{BA}\mathrm{Ent}_{BC} \geq \frac{\max\{1, S_{B|(AC)}^2\}}{\left(1 + g_{BA}^{sym}\right)\left(1 + g_{BC}^{sym}.\right)} \tag{2.104}$$

Monogamy for steering

As it has been mentioned previously, it is possible to define monogamy relations for all measureable quantum correlations, including steering. For that purpose we need a steering parameter, in other words, a measure that quantifies the amount of steering present in a system. Since we are interested in continuous variable (CV) systems we will use the witness defined by Reid [107] as:

$$E_{B|A} = \left(\Delta_{\inf}X_{B|A}\right)\left(\Delta_{\inf}P_{B|A}\right), \tag{2.105}$$

where $\Delta_{\inf}X_{B|A}$ denotes the standard deviation of the conditional distribution for the measurement X_B given a measurement at A, and where X_j and P_j denote the position and momentum quadratures respectively.

Using this steering parameter we can certify the presence of the correlation in the system if the following inequality is satisfied:

$$E_{B|A} < 1. \tag{2.106}$$

It is important to notice that the quantity $E_{B|A}$ is, in general, different from $E_{A|B}$, even for the same pair of subsystems A and B. What this means conceptually is that the ability of subsystem A to modify or steer subsystem B does not automatically imply that B is able to steer A. Even though it is possible, it has to be tested independently since steering is an asymmetric quantum correlation. Entanglement, on the other hand, is a symmetric correlation because if A is entangled with B, then B is also entangled with A.

Similarly to our previous discussion about entanglement, we can proceed to state the monogamy relation for steering presented by Reid [107]: for a Gaussian CV system of three parties, A, B and C, if $E_{B|A} < 1$ is satisfied, then the following inequality is also true:

$$E_{B|A}E_{B|C} \geq 1. \tag{2.107}$$

In other words, if A steers B, then C cannot steer B as well. In that sense, we can say that all steerable systems that satisfy the mentioned conditions present monogamy. We can summarize this important result as follows: One subsystem cannot be steered independently by two or more *distinct* subsystems. There is, however, a way in which

steering can be distributed among several parties.

For a given set of N elements we can generate a bipartition by defining two subsets in which all of the elements are included. For a tripartite system, such as the one discussed by Reid, these bipartitions can be written as: $\{A, BC\}, \{B, AC\}, \{C, AB\}$. For the last of these bipartitions, for example, we can treat both parties AB as a single entity, thus it is possible that bipartite steering onto subsystem C is distributed among the two subsystems A and B with one restriction. Reid showed [107] that for these bipartitions recently discussed, if there is steering of party C by the group AB, that is: $E_{C|AB} < 1$, then, the following inequality is also true:

$$E_{C|A} + E_{C|B} \geq 2E_{C|AB}, \tag{2.108}$$

which mathematically signifies the fact that the individual steering on C by A or on C by B is bounded by the steering of the group AB onto C.

2.12 Non-linear optics

Non-linear optics is the area of physics that studies interactions of electromagnetic radiation with media that responds to higher powers of the incident electric field.

More specifically, media in general exhibits a phenomenon known as *polarisation* in which electrically charged constituents are relocated within the media in presence of an external electromagnetic field. This polarisation is proportional to the strength of the electric field by a parameter called susceptibility, usually denoted by the greek letter χ. This relationship can be summarized by the following equation:

$$\boldsymbol{P}(r,t) = \epsilon_0 \chi \boldsymbol{E}(r,t). \tag{2.109}$$

However, eq. 2.109 is a simplification, given the fact that the susceptibility can be treated as a constant for most media, but it is not in general. In non-linear optics, susceptibility is better described as a tensor and the phenomena arising from its interaction with higher orders of the electrical field are studied. Polarisation, therefore becomes better described as:

$$P(r,t) = \epsilon_0 \chi E(r,t) + \chi^{(2)} E^2(r,t) + \chi^{(3)} E^3(r,t) + \ldots \tag{2.110}$$

where $\chi^{(2)}, \chi^{(3)}, \ldots$, etc. denote susceptibilities of higher order, namely of second and third order respectively, etc. The nonlinear susceptibilities have decreasing magnitudes as their order increases. A typical second order susceptibility may be as small as 8 orders of magnitude lower with respect to the linear parameter χ, while the typical third order, $\chi^{(3)}$, is 16 orders of magnitude smaller [108].

The linear susceptibility is responsible for the refractive index, absorption, dispersion, and birefringence [108]. On the other hand, some examples of non-linear phenomena of second order are Second Harmonic Generation (SHG), in which two photons of angular frequency ω_0 are converted into one photon of frequency $2\omega_0$, frequency mixing and parametric generation. For third order nonlinearities some examples are Third Harmonic Generation (THG) and stimulated Raman scattering, among others [108].

In practice, plenty of non-linear optical processes have been studied in crystals [108]. For example, phenomena that relies on second order susceptibility requires an anisotropic medium. That property can be found in crystals such as calcite ($CaCO_3$), Potassium Titanyl Phosphate (KTP) or Barium Borate (BBO). The latter is of special relevance since our work consists of modeling a non-linear process that has been implemented in a BBO crystal [42].

2.12.1   Spontaneous Parametric Down Conversion (SPDC)

Spontaneous parametric down conversion is a non-linear process of second order in which a photon is converted spontaneously into two photons of lower energies [109]. It is a process that has been widely studied lately as it is used in many applications for the development of quantum technologies [110–113]. SPDC is a very inefficient process that converts only a small proportion of incident photons, therefore high power pump sources are needed to generate it [109].

There are two special conditions relevant to the process of SPDC. These are called *phase matching conditions*:

$$\hbar\omega_0 = \hbar(\omega_1 + \omega_2), \tag{2.111}$$

$$\vec{k}_0 = \vec{k}_1 + \vec{k}_2, \tag{2.112}$$

and signify conservation of energy and conservation of momentum respectively. Eq. 2.111 correlates the angular frequency ω_0 of the pump photon to the frequencies of the two photons generated by SPDC: ω_1 and ω_2. On the other hand, eq. 2.112 correlates the wave vector of the three photons involved in the process. A special case for these phase matching conditions consists of the generation of twin photons that have the same energy, that is, half of the energy of the original photon:

$$\omega_1 = \omega_2 = \frac{\omega_0}{2}. \tag{2.113}$$

This specific case is also referred to as degenerate SPDC, and is the time reversible phenomenon with respect to SHG. Non-degenerate SPDC occurs when each of the two photons generated have different wavelengths and its time reversible phenomenon is sum-frequency generation (SFG).

SPDC can be further classified into type-I or type-II. These categories refer to the polarization of the down-converted photons. In type-I SPDC, the two photons generated have the same polarization , while the type-II SPDC produces two photons with different polarization from each other [114]. For the degenerate emission, type-I SPDC photons emerge on a cone that is centered along the propagation direction of the pump beam. In this type of SPDC, entangled photons are generated in diametrically opposed points of this cone. See figure 2.3 for a diagram of the emission cone and the emission points of entangled photons. In type-II SPDC the photons are produced and emitted in two cones [115], one ordinarily polarized, while the other is extraordinarily polarized. The two cones intersect in one line that is collinear to the pump beam direction of propagation and is on those two points of intersection that the entangled photons are emitted.

This experimental scheme involving type-II phase matching is very relevant for quantum optics since it has been shown [114] that in the section where the cones
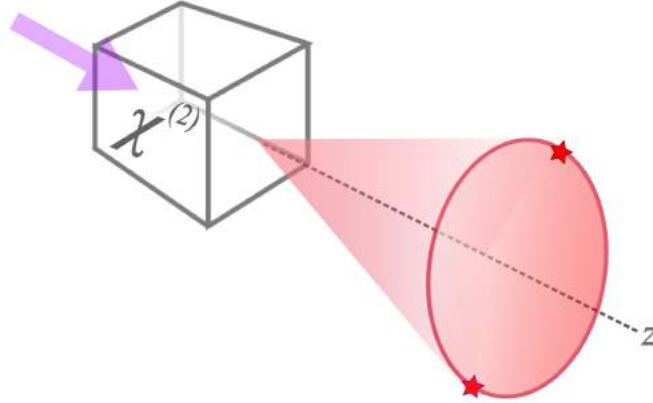
FIGURE 2.3: Diagram of emission by SPDC of type-I. The purple arrow represents the pump beam and the emission is generated in one cone. Two entangled photons are generated in points that are diametrically opposed in this cone.

overlap, light can be described by the quantum entangled state:

$$|\psi\rangle = \frac{1}{\sqrt{2}} \left(|H,V\rangle + e^{i\alpha} |V,H\rangle \right), \tag{2.114}$$

where the relative phase α originates from the crystal birefringence. By adding a phase shifter or by rotating the non-linear crystal itself, the phase α can be set as desired, for example to the values 0 or π. Furthermore, by adding a half wave plate in one of the paths the polarization can be switched from vertical to horizontal, thus allowing us to produce any of the four EPR-Bell states:

$$\begin{aligned} \left|\psi^{\pm}\right\rangle &= \frac{1}{\sqrt{2}} \left(|H,V\rangle \pm |V,H\rangle \right), \\ \left|\phi^{\pm}\right\rangle &= \frac{1}{\sqrt{2}} \left(|H,H\rangle \pm |V,V\rangle \right). \end{aligned} \tag{2.115}$$

which are the maximally entangled quantum states for two parties. This is mentioned as an example of the importance of SPDC in the study of quantum correlations in quantum optics.

Quantum correlations generated by SPDC

Spontaneous parametric down conversion has been identified as a reliable source for entangled modes of light. Quantum correlated states have been generated using type-II noncollinear SPDC in crystals, as reported by Kwiat et al. [114]. In this work, the authors generate pairs of photons that are entangled in their polarization. Furthermore, SPDC is able to generate entanglement in other degrees of freedom, for instance, in *orbital angular momentum* as was demonstrated by Vaziri et al. [116]. In their experimental scheme, the authors utilize a nonlinear crystal cut for type-I phase matching and generate a pair of entangled photons. Afterwards they send each of

these photons through displaced holograms that transfer them to different superpositions of eigenstates of orbital angular momentum. Detecting one of the photons in a specific eigenstate guarantees that the other photon will be found in another element of the base. The claim that the photons were correlated with each other was confirmed by the violation of a Bell inequality. Recently, SPDC was also used by Agusti et al. [117] to produce genuine tripartite entanglement utilizing criteria to certify it specifically designed for the multipartite case.

Chapter 3

Entanglement and steering in a nonlinear process

In this chapter we introduce the physical system which is studied in this work as well as the conditions necessary for the generation of multipartite quantum correlations. A specific medium will be irradiated with two sources of light, which will be called *pump beams*. By means of a parametric processes, four photons will be produced. The main objective of our work is to certify that these four photons are quantum correlated to each other on their quadratures $\hat{X}$ and $\hat{P}$. We are interested in this specific system because we want to study multipartite quantum correlations for systems larger than the tripartite case. The system has been analyzed before but using a different methodology that did not yield the dynamical behaviour of the modes of light nor did it study the presence of steering [43].

3.1 Description of the physical system

The physical system in which the four modes of light are generated is a bulk anisotropic crystal that is being pumped by two Gaussian beams that propagate in a non-collinear way. An schematic diagram of the system is provided in figure 3.1. In this crystal, two non-linear processes of type-I SPDC occur. In each of these, three photons are involved: the pump, the signal and the idler. It has been reported [118] that under specific conditions, two triplets of photons are converted into four coupled modes.

The medium in which the physical process occurs is a standard $\chi^{(2)}$ bulk crystal. This type of medium is necessary because it exhibits birrefringence, which is needed for the parametric process. The experimental scheme has been implemented successfully using a BBO (Beta-Barium-Borate) crystal [118], but there are other options that might be used, as long as they exhibit birrefringence [119, 120]. In the physical implementation reported by Gatti et al. [42], the two pumps have a wavelength of $\lambda_p = 352$ nm while signal and idler have the corresponding $\lambda_s = \lambda_i = 704$ nm. Inside of the medium, by changing the direction of propagation of the pump, a geometrical condition is fulfilled, in which uncoupled triplets of photons, which can be seen schematically represented in figure 3.2, are converted into four entangled modes [121]. To achieve this condition of resonance a rotation along the incidence plane of the crystal has to be performed. There is a specific angle of rotation needed for each angle of propagation between the two pumps. For a schematic representation of this rotation, see figure 3.3. This geometric condition changes the size of the emission cones so that they overlap, and is in this intersection that entangled photons from one cone match the entangled photons from the other cone. See figures 3.4 and 3.5 for a schematic representation of the emission cones. In these diagrams, the modes of light are linked

with each other through some quantities g_1 and g_2. These are called *coupling parameters* and are proportional to the complex amplitude of the pump beams. A schematic representation of the four entangled modes can be seen in figure 3.6.
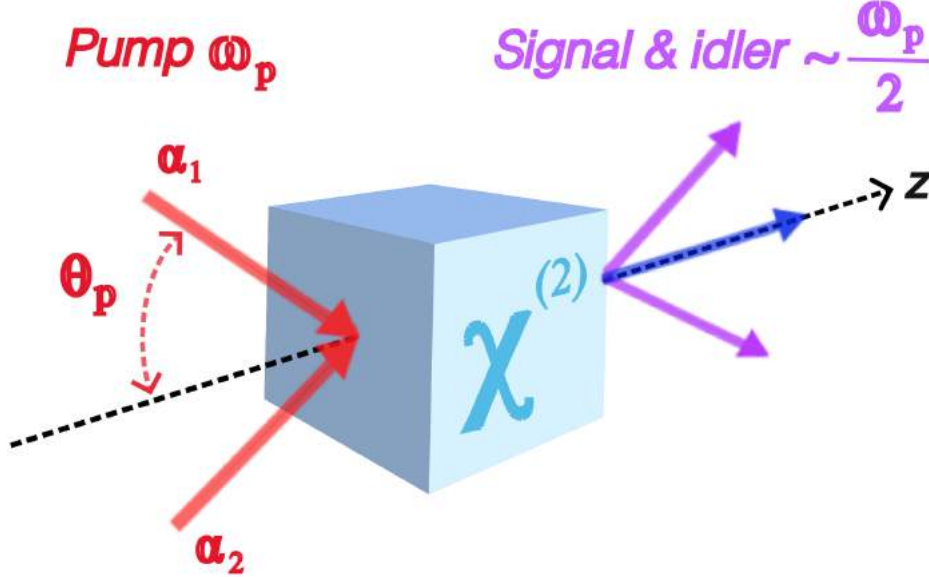

FIGURE 3.1: Diagram of a physical system in which the SPDC process occurs. Under certain conditions of resonance, this type of system produces four modes of light.

In the experimental scheme [42] the active material is a BBO crystal in which two processes of type-I non collinear parametric down conversion occur [42], one for each of the two incident beams. This is the scheme that will be modeled in our work. The two pump modes are directed at different angles with respect to the optical axis and experience different refraction indices. This happens because media with $\chi^{(2)}$ is anisotropic [108], thus a different refraction index is experienced by light that travels in different directions. The tilt angle between the pumps is related to the resonance condition that is needed to produce 4-mode entanglement because for a given angle between the two lasers, there is an specific angle, which is called β, to which the crystal has to be rotated in order to achieve this conversion [118]. The rotation occurs along the incidence plane.

FIGURE 3.2: Diagram of the 3-mode coupling generated by the SPDC. The $\hat{a}_0$ represents the mode of light from the undepleted pump, while $\hat{a}_1$ and $\hat{a}_2$ represent the signal and the idler, respectively. In this case $\hat{a}_1$ is coupled exclusively with $\hat{a}_0$ and the same is true for $\hat{a}_2$. Each correlation happens because of coupling parameters g_1 and g_2, respectively.
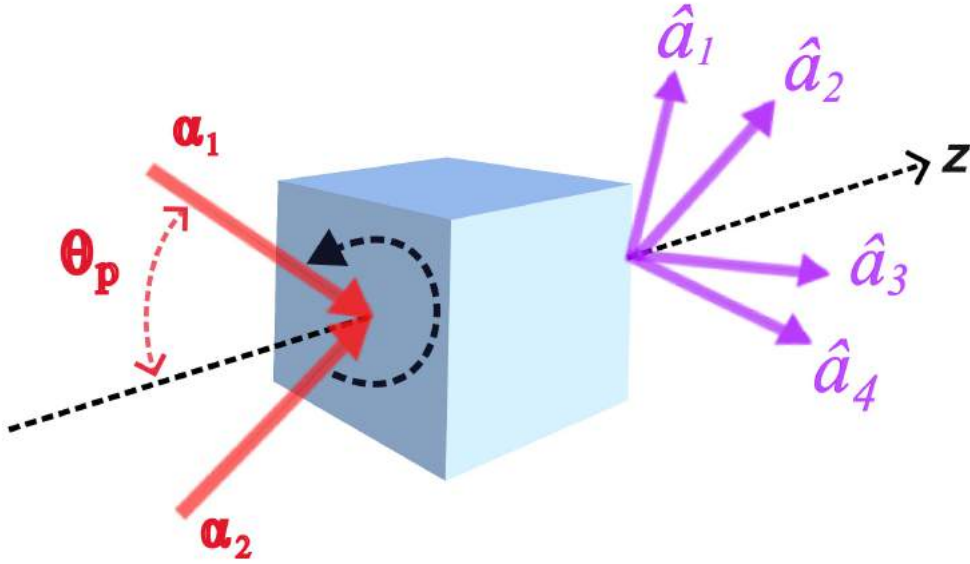
FIGURE 3.3: Schematic diagram of the geometric condition that produces the four modes of light. Depending on the relative angle of propagation θ_p, there is a specific rotation angle (β) along the incidence plane of the crystal that produces the four modes.
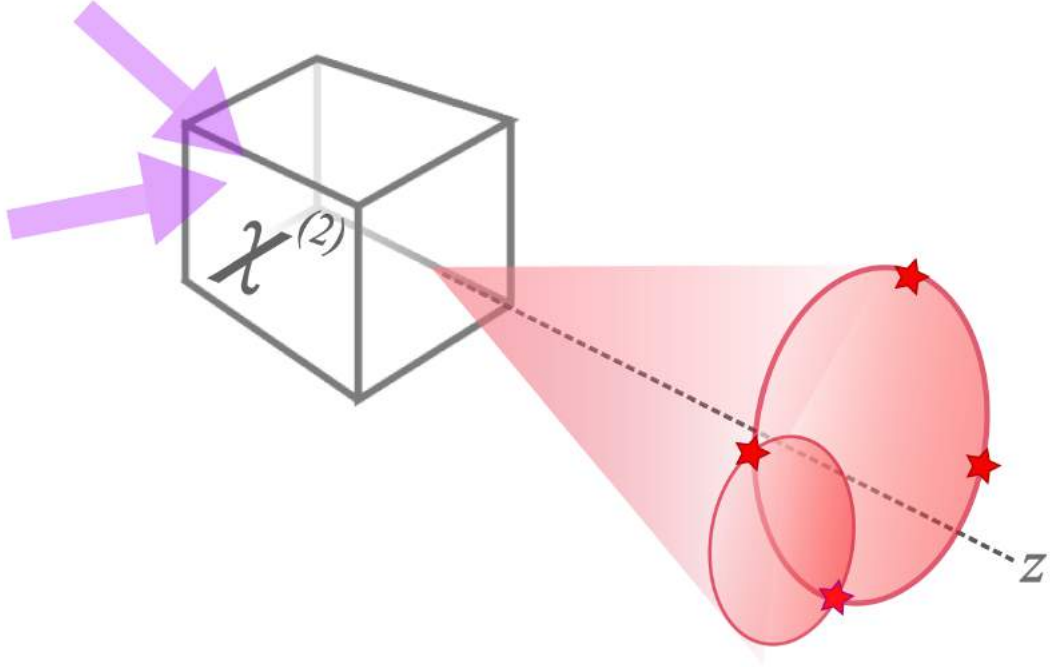
FIGURE 3.4: Schematic representation of the two processes of SPDC type-I occurring inside the BBO crystal. Each emission cone is generated by one of the pump modes and a geometrical condition overlaps them, creating the entanglement.

$$\beta = 0^o \qquad\qquad \beta = 7^o$$
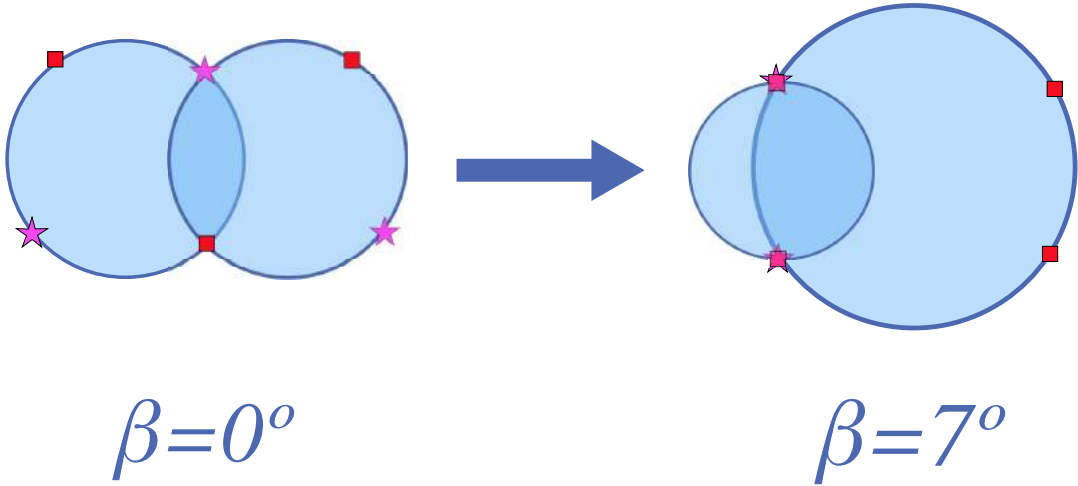
FIGURE 3.5: To the left side of the image we see the two emission cones produced by the processes of SPDC type-I. Diametrically opposed points (which are represented by the stars or by the squares) on each of these cones contain entangled photons. Once the geometrical condition has been achieved by the rotation of the crystal, diametrically opposed points from the two circles are overlapped, thus generating the four entangled photons that we are studying.
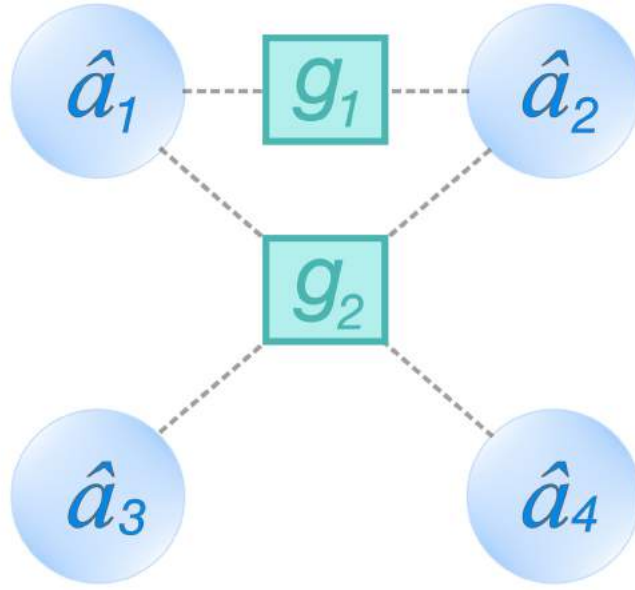
FIGURE 3.6: Schematic diagram of the entanglement for the 4 photons generated in the special resonance condition and its relation with the coupling parameters. Unlike the diagram 3.2, this one shows coupling between modes 1 and 4, 1 and 2 and 2 and 3.

3.2 Fokker-Planck equation for a fourth particle Hamiltonian.

In this section, we will obtain a Fokker-Planck equation to study the dynamics of the system and find out if it presents entanglement and steering. We start by considering the Hamiltonian reported by Gatti [43]:

$$\hat{H} = -i\hbar(g_1\hat{a}_1^\dagger\hat{a}_2^\dagger + g_2\hat{a}_2^\dagger\hat{a}_3^\dagger + g_2\hat{a}_4^\dagger\hat{a}_1^\dagger - g_1\hat{a}_1\hat{a}_2 - g_1\hat{a}_2\hat{a}_3 - g_1\hat{a}_4\hat{a}_1). \qquad (3.1)$$

Next, since we wish to also analyse the dynamics of the system, we consider the time evolution equation for the density matrix:

$$i\hbar\frac{\partial\hat{\rho}}{\partial t} = [\hat{H}, \hat{\rho}], \qquad (3.2)$$

on substituting the Hamiltonian of eq. 3.1 on eq. 3.2, and on performing the commutator, we obtain:

$$
\begin{aligned}
\frac{\partial\hat{\rho}}{\partial t} &= -i\hbar(g_1\hat{a}_1^\dagger\hat{a}_2^\dagger\hat{\rho} - g_1\hat{a}_1\hat{a}_2\hat{\rho} + g_2\hat{a}_2^\dagger\hat{a}_3^\dagger\hat{\rho} + g_2\hat{a}_4^\dagger\hat{a}_1^\dagger\hat{\rho} - g_2\hat{a}_2\hat{a}_3\hat{\rho} - g_2\hat{a}_4\hat{a}_1\hat{\rho} \\
&\quad - g_1\hat{\rho}\hat{a}_1^\dagger\hat{a}_2^\dagger + g_1\hat{\rho}\hat{a}_1\hat{a}_2 - g_2\hat{\rho}\hat{a}_2^\dagger\hat{a}_3^\dagger - g_2\hat{\rho}\hat{a}_4^\dagger\hat{a}_1^\dagger + g_1\hat{\rho}\hat{a}_2\hat{a}_3 + g_2\hat{\rho}\hat{a}_4\hat{a}_1). \qquad (3.3)
\end{aligned}
$$

Using the known correspondences, 2.48, between the density matrix and the positive-P function we acquire the following expression:

$$
\begin{aligned}
\frac{\partial \hat{\rho}}{\partial t} =& -\Bigg[g_1 \left(\alpha_1^\dagger - \frac{\partial}{\partial \alpha_1} \right) \left(\alpha_2^\dagger - \frac{\partial}{\partial \alpha_2} \right) + g_2 \left(\alpha_2^\dagger - \frac{\partial}{\partial \alpha_2} \right) \left(\alpha_3^\dagger - \frac{\partial}{\partial \alpha_3} \right) \\
& + g_2 \left(\alpha_4^\dagger - \frac{\partial}{\partial \alpha_4} \right) \left(\alpha_1^\dagger - \frac{\partial}{\partial \alpha_1} \right) + g_2 \left(\alpha_1 - \frac{\partial}{\partial \alpha_1^\dagger} \right) \left(\alpha_4 - \frac{\partial}{\partial \alpha_4^\dagger} \right) \\
& + g_1 \left(\alpha_2 - \frac{\partial}{\partial \alpha_2^\dagger} \right) \left(\alpha_1 - \frac{\partial}{\partial \alpha_1^\dagger} \right) + g_2 \left(\alpha_3 - \frac{\partial}{\partial \alpha_3^\dagger} \right) \left(\alpha_2 - \frac{\partial}{\partial \alpha_2^\dagger} \right) \\
& - g_1 \alpha_1 \alpha_2 - g_2 \alpha_2 \alpha_3 - g_2 \alpha_4 \alpha_1 - g_1 \alpha_2 \alpha_1 - g_2 \alpha_3 \alpha_2 - g_2 \alpha_1^\dagger \alpha_4^\dagger \Bigg] P. \quad (3.4)
\end{aligned}
$$

After distributing and simplifying we arrive at:

$$
\begin{aligned}
\frac{\partial \hat{\rho}}{\partial t} =& -\Bigg[-g_1 \alpha_1^\dagger \frac{\partial}{\partial \alpha_2} - g_1 \frac{\partial}{\partial \alpha_1} \alpha_2^\dagger - g_2 \alpha_2^\dagger \frac{\partial}{\partial \alpha_3} - g_2 \frac{\partial}{\partial \alpha_2} \alpha_3^\dagger - g_2 \alpha_4^\dagger \frac{\partial}{\partial \alpha_1} - g_2 \frac{\partial}{\partial \alpha_4} \alpha_1^\dagger \\
& - g_1 \alpha_2 \frac{\partial}{\partial \alpha_1^\dagger} - g_1 \frac{\partial}{\partial \alpha_2^\dagger} \alpha_1 - g_2 \alpha_3 \frac{\partial}{\partial \alpha_2^\dagger} - g_2 \frac{\partial}{\partial \alpha_3^\dagger} \alpha_2 - g_2 \alpha_1 \frac{\partial}{\partial \alpha_4} - g_2 \frac{\partial}{\partial \alpha_1^\dagger} \alpha_4 \\
& + g_1 \frac{\partial^2}{\partial \alpha_1 \partial \alpha_2} + g_2 \frac{\partial^2}{\partial \alpha_2 \partial \alpha_3} + g_2 \frac{\partial^2}{\partial \alpha_4 \partial \alpha_1} + g_1 \frac{\partial^2}{\partial \alpha_2^\dagger \partial \alpha_1^\dagger} + g_2 \frac{\partial^2}{\partial \alpha_3^\dagger \partial \alpha_2^\dagger} + g_2 \frac{\partial^2}{\partial \alpha_1^\dagger \partial \alpha_4^\dagger} \Bigg] P,
\end{aligned}
$$
$$(3.5)$$

which is a Fokker-Planck equation of the general form:

$$
\frac{\partial \hat{\rho}}{\partial t} = \left[-\sum \frac{\partial}{\partial x_i} A_i(x) + \frac{1}{2} \sum \frac{\partial^2}{\partial x_i \partial x_j} D_{ij}(x) \right] P(x), \quad (3.6)
$$

where $\boldsymbol{A}(x)$ is called the drift matrix and $\boldsymbol{D}(x)$ is called the diffusion matrix.
If we consider the ordering $\alpha_1, \alpha_2, \alpha_3, \alpha_4, \alpha_1^\dagger, \alpha_2^\dagger, \alpha_3^\dagger, \alpha_4^\dagger$, then the drift matrix A_i is:

$$
\boldsymbol{A} = -(g_1 \alpha_2^\dagger + g_2 \alpha_4^\dagger, g_1 \alpha_2^\dagger + g_2 \alpha_4^\dagger, g_2 \alpha_2^\dagger, g_2 \alpha_1^\dagger, g_1 \alpha_2 + g_2 \alpha_4, g_1 \alpha_1 + g_2 \alpha_3, g_2 \alpha_2, g_2 \alpha_1).
$$
$$(3.7)$$

And the diffusion matrix is:

$$
\boldsymbol{D} = \begin{pmatrix}
0 & g_1 & 0 & g_2 & 0 & 0 & 0 & 0 \\
g_1 & 0 & g_2 & 0 & 0 & 0 & 0 & 0 \\
0 & g_2 & 0 & 0 & 0 & 0 & 0 & 0 \\
g_2 & 0 & 0 & 0 & 0 & 0 & 0 & 0 \\
0 & 0 & 0 & 0 & 0 & g_1 & 0 & g_2 \\
0 & 0 & 0 & 0 & g_1 & 0 & g_2 & 0 \\
0 & 0 & 0 & 0 & 0 & g_2 & 0 & 0 \\
0 & 0 & 0 & 0 & g_2 & 0 & 0 & 0
\end{pmatrix}. \quad (3.8)
$$

As was discussed previously in section 2.7, if the diffusion matrix $\boldsymbol{D}$ can be written as $\boldsymbol{D} = \boldsymbol{B}\boldsymbol{B}^T$, then a set of stochastic differential equations can be obtained from the Fokker-Planck equation. In particular, since this matrix $\boldsymbol{D}$ can indeed be factorized as $\boldsymbol{D} = \boldsymbol{B}\boldsymbol{B}^T$, therefore we are able to map it to a set of stochastic differential equations. We proceed to find the matrix $\boldsymbol{B}$, since this is needed in order to find the set

of stochastic differential equations.

In order to obtain $\boldsymbol{B}$, first, we consider the matrix $\boldsymbol{D}$ to be formed by 4 submatrices with dimensions 4×4, that is:

$$\boldsymbol{D} = \begin{pmatrix} \boldsymbol{d} & \boldsymbol{0} \\ \boldsymbol{0} & \boldsymbol{d} \end{pmatrix}, \tag{3.9}$$

where $\boldsymbol{0}$ denotes a 4×4 null matrix which is filled exclusively with zeros, and where we have defined $\boldsymbol{d}$ as:

$$\boldsymbol{d} = \begin{pmatrix} 0 & g_1 & 0 & g_2 \\ g_1 & 0 & g_2 & 0 \\ 0 & g_2 & 0 & 0 \\ g_2 & 0 & 0 & 0 \end{pmatrix}.$$

Next, we consider $\boldsymbol{B}$ to also be formed by 4 submatrices:

$$\boldsymbol{B} = \begin{pmatrix} \boldsymbol{b}_1 & \boldsymbol{b}_2 \\ \boldsymbol{b}_3 & \boldsymbol{b}_4 \end{pmatrix}. \tag{3.10}$$

On performing the matrix multiplication we obtain: $\boldsymbol{B}\boldsymbol{B}^T$

$$\boldsymbol{B}\boldsymbol{B}^T = \begin{pmatrix} \boldsymbol{b}_1\boldsymbol{b}_1^T + \boldsymbol{b}_2\boldsymbol{b}_2^T & \boldsymbol{b}_1\boldsymbol{b}_3^T + \boldsymbol{b}_2\boldsymbol{b}_4^T \\ \boldsymbol{b}_3\boldsymbol{b}_1^T + \boldsymbol{b}_4\boldsymbol{b}_2^T & \boldsymbol{b}_3\boldsymbol{b}_3^T + \boldsymbol{b}_4\boldsymbol{b}_4^T \end{pmatrix}. \tag{3.11}$$

By equating that matrix 3.11 to matrix 3.9, we can simplify our calculations by proposing that the matrix $\boldsymbol{B}$ is formed by null matrices in its antidiagonal. That is:

$$\boldsymbol{B} = \begin{pmatrix} \boldsymbol{b}_1 & \boldsymbol{0} \\ \boldsymbol{0} & \boldsymbol{b}_4. \end{pmatrix} \tag{3.12}$$

Thus, the product in eq. 3.11 simplifies to:

$$\boldsymbol{B}\boldsymbol{B}^T = \begin{pmatrix} \boldsymbol{b}_1\boldsymbol{b}_1^T & \boldsymbol{0} \\ \boldsymbol{0} & \boldsymbol{b}_4\boldsymbol{b}_4^T \end{pmatrix}. \tag{3.13}$$

Afterwards, by equating $\boldsymbol{D} = \boldsymbol{B}\boldsymbol{B}^T$ using equations 3.9 and 3.13 respectively, we obtain:

$$\begin{pmatrix} \boldsymbol{d} & \boldsymbol{0} \\ \boldsymbol{0} & \boldsymbol{d} \end{pmatrix} = \begin{pmatrix} \boldsymbol{b}_1\boldsymbol{b}_1^T & \boldsymbol{0} \\ \boldsymbol{0} & \boldsymbol{b}_4\boldsymbol{b}_4^T \end{pmatrix}. \tag{3.14}$$

We realize that both terms on the diagonal of matrix $\boldsymbol{B}\boldsymbol{B}^T$ have to be equal. In other words: $\boldsymbol{b}_1\boldsymbol{b}_1^T = \boldsymbol{b}_4\boldsymbol{b}_4^T$. This can be simplified by defining one submatrix $\boldsymbol{b} = \boldsymbol{b}_1 = \boldsymbol{b}_4$ without subindices:

$$\boldsymbol{B}\boldsymbol{B}^T = \begin{pmatrix} \boldsymbol{b}\boldsymbol{b}^T & \boldsymbol{0} \\ \boldsymbol{0} & \boldsymbol{b}\boldsymbol{b}^T \end{pmatrix}. \tag{3.15}$$

After obtaining this result we realize that the matrix $\boldsymbol{B}$ can be obtained by finding a matrix $\boldsymbol{b}$ that satisfies the following equation: $\boldsymbol{b}\boldsymbol{b}^T = \boldsymbol{d}$. For such a purpose we propose a matrix $\boldsymbol{b}$ of the following form:

$$\boldsymbol{b} = \begin{pmatrix} a & b & c & q \\ e & f & g & h \\ r & j & k & l \\ m & n & o & p \end{pmatrix}, \tag{3.16}$$

where variables a through p denote complex numbers. We then perform the matrix multiplication $\boldsymbol{b}\boldsymbol{b}^T = \boldsymbol{d}$ and end up with a system of 16 equations. After proposing that variables $e = g = k = r = n = p = 0$, we simplify to 10 equations for 10 variables. Afterwards, by using *Mathematica 13.0* to solve the system, we find the following solution:

$$\boldsymbol{b} = \begin{pmatrix} -i & -i & 1 & 1 \\ 0 & i\frac{g_1}{2} & 0 & \frac{g_1}{2} \\ 0 & -i\frac{g_2}{g_1} & 0 & \frac{g_2}{g_1} \\ i\frac{g_2}{2} & 0 & \frac{g_2}{2} & 0 \end{pmatrix}. \tag{3.17}$$

That in turn gives us the solution for $\boldsymbol{B}$ as:

$$\boldsymbol{B} = \begin{pmatrix} -i & -i & 1 & 1 & 0 & 0 & 0 & 0 \\ 0 & i\frac{g_1}{2} & 0 & \frac{g_1}{2} & 0 & 0 & 0 & 0 \\ 0 & -i\frac{g_2}{g_1} & 0 & \frac{g_2}{g_1} & 0 & 0 & 0 & 0 \\ i\frac{g_2}{2} & 0 & \frac{g_2}{2} & 0 & 0 & 0 & 0 & 0 \\ 0 & 0 & 0 & 0 & -i & -i & 1 & 1 \\ 0 & 0 & 0 & 0 & 0 & i\frac{g_1}{2} & 0 & \frac{g_1}{2} \\ 0 & 0 & 0 & 0 & 0 & -i\frac{g_2}{g_1} & 0 & \frac{g_2}{g_1} \\ 0 & 0 & 0 & 0 & i\frac{g_2}{2} & 0 & \frac{g_2}{2} & 0 \end{pmatrix}. \tag{3.18}$$

Lastly, we add that this solution for $\boldsymbol{b}$, and thus, for $\boldsymbol{B}$ is not unique, but it serves our purpose as long as it satisfies the equation $\boldsymbol{D} = \boldsymbol{B}\boldsymbol{B}^T$. Now that we have obtained an expression for the matrix $\boldsymbol{B}$ we can use its elements to generate a set of SDE's. This procedure will be explained in the following subsection.

3.3   Stochastic Differential Equations

Once that a Fokker-Planck equation is obtained, it is possible to map it to a set of stochastic differential equations (SDE's) by the following correspondence that was also previously mentioned in section 2.7. Given the Fokker-Planck equation:

$$\frac{\partial P}{\partial t} = \left[-\sum \frac{\partial}{\partial x_i} A_i(x) + \frac{1}{2} \sum \frac{\partial^2}{\partial x_i \partial x_j} D_{ij}(x) \right] P(x),$$

then the stochastic differential equation for each variable is written as:

$$\frac{dx_i}{dt} = A_i(x) + B_{ij}(x)\zeta_j,$$

where ζ_j is a delta-correlated Gaussian noise. That is:

$$\langle \zeta_i(t)\zeta_j(t') \rangle = \delta_{ij}\delta(t - t'). \tag{3.19}$$

In other words, the noise produced by one of these functions at an instant t has no statistical correlation with noise from the same function at a different time [72]. These values also have no statistical correlation with the ones produced by other, similarly defined functions.

For the variables $\alpha_1, \ldots \alpha_4, \alpha_1^\dagger \ldots \alpha_4^\dagger$, we obtain the following SDE's in differential form:

$$
\begin{aligned}
d\alpha_1 &= (-g_1\alpha_2^\dagger - g_2\alpha_4^\dagger)dt + (\zeta_3 + \zeta_4) - i(\zeta_1 + \zeta_2), \\
d\alpha_2 &= (-g_1\alpha_1^\dagger - g_2\alpha_3^\dagger)dt + \frac{g_1}{2}(\zeta_4 + i\zeta_2), \\
d\alpha_3 &= -g_2\alpha_2^\dagger dt + \frac{g_2}{g_1}(\zeta_4 - i\zeta_2), \\
d\alpha_4 &= -g_2\alpha_1^\dagger dt + \frac{g_2}{2}(\zeta_3 + i\zeta_1), \\
d\alpha_1^\dagger &= (-g_2\alpha_4 - g_1\alpha_2)dt + (\zeta_7 + \zeta_8) - i(\zeta_5 + \zeta_6), \\
d\alpha_2^\dagger &= (-g_1\alpha_1 - g_2\alpha_3)dt + \frac{g_1}{2}(\zeta_8 + i\zeta_6), \\
d\alpha_3^\dagger &= -g_2\alpha_2 dt + \frac{g_2}{g_1}(\zeta_8 - i\zeta_6), \\
d\alpha_4^\dagger &= -g_2\alpha_1 dt + \frac{g_2}{2}(\zeta_7 + i\zeta_5).
\end{aligned}
\tag{3.20}
$$

Afterwards, this set of stochastic differential equations is solved numerically using the central difference algorithm. These solutions are particular, since we have established the initial values for the numerical algorithm.

3.4 Heisenberg equations

In contrast to the phase space methods that we have already discussed, we can also study the evolution of the operators using analytical methods instead of numerical ones. We do so by using the Heisenberg equations of time evolution. This procedure is described in this section.

We consider the same Hamiltonian from eq. 3.1, which is :

$$
\hat{H} = -i\hbar(g_1\hat{a}_1^\dagger\hat{a}_2^\dagger + g_2\hat{a}_2^\dagger\hat{a}_3^\dagger + g_2\hat{a}_4^\dagger\hat{a}_1^\dagger - g_1\hat{a}_1\hat{a}_2 - g_1\hat{a}_2\hat{a}_3 - g_1\hat{a}_4\hat{a}_1).
\tag{3.21}
$$

Then, using the Heisenberg equations for the time evolution of an operator, which are defined as [122]:

$$
\frac{1}{i\hbar}\frac{d\hat{A}}{dt} = [\hat{A}, \hat{H}].
\tag{3.22}
$$

On substituting the Hamiltonian in eq. 3.22 and by first considering the annihilation operator of mode 1:

$$
[\hat{a}_1, \hat{H}] = i\hbar([\hat{a}_1, -g_1\hat{a}_1^\dagger\hat{a}_2^\dagger] + [\hat{a}_1, -g_2\hat{a}_4^\dagger\hat{a}_1^\dagger] + [\hat{a}_1, g_1\hat{a}_1\hat{a}_2] + [\hat{a}_1, g_2\hat{a}_4\hat{a}_1]),
\tag{3.23}
$$

$$
\implies [\hat{a}_1, \hat{H}] = -i\hbar(g_1[\hat{a}_1, \hat{a}_1^\dagger\hat{a}_2^\dagger] + g_2[\hat{a}_1, \hat{a}_4^\dagger\hat{a}_1^\dagger]),
\tag{3.24}
$$

where we have considered the following commutation relation:

$$
\left[\hat{a}_i, \hat{a}_j^\dagger\right] = \delta_{i,j}.
\tag{3.25}
$$

Here $\delta_{i,j}$ denotes the Kronecker delta. Then, by using the commutator relation:

$$
[\hat{A}, \hat{B}\hat{C}] = ([\hat{A}, \hat{B}]\hat{C} + \hat{B}[\hat{A}, \hat{C}]),
\tag{3.26}
$$

we end up with the following expression and differential equation:

$$[\hat{a}_1, \hat{H}] = -i\hbar(g_1\hat{a}_2^\dagger + g_2\hat{a}_4^\dagger). \tag{3.27}$$

Thus, we obtain:

$$\frac{d\hat{a}_1}{dt} = -g_1\hat{a}_2^\dagger - g_2\hat{a}_4^\dagger. \tag{3.28}$$

By performing a similar process on the rest of the operators of the Hamiltonian we obtain the following set of coupled differential equations:

$$
\begin{aligned}
\frac{d\hat{a}_1^\dagger}{dt} &= -g_1\hat{a}_2 - g_2\hat{a}_4, \\
\frac{d\hat{a}_2}{dt} &= -g_1\hat{a}_1^\dagger - g_2\hat{a}_3^\dagger, \\
\frac{d\hat{a}_2^\dagger}{dt} &= -g_1\hat{a}_1 - g_2\hat{a}_3, \\
\frac{d\hat{a}_3}{dt} &= -g_2\hat{a}_2^\dagger, \\
\frac{d\hat{a}_3^\dagger}{dt} &= -g_2\hat{a}_2, \\
\frac{d\hat{a}_4}{dt} &= -g_2\hat{a}_1^\dagger, \\
\frac{d\hat{a}_4^\dagger}{dt} &= -g_2\hat{a}_1^\dagger.
\end{aligned}
\tag{3.29}
$$

This system of equations is consistent with the one obtained from the Fokker-Planck equation except for the terms of Gaussian white noise.

Solutions to this system of coupled differential equations can be calculated using software. These analytical expressions have closed form and are written in terms of the operator's initial values, which are their expectation values at $t = 0$. In other words, we have obtained particular solutions to this system of equations. These solutions were not written in this section for the sake of brevity, but their behaviour is shown in Chapter 4. Furthermore, these solutions will be used to calculate quantities such as the expectation value for the quadratures and the number operator.

3.5   Parameter optimization for steering witness S

Some of the witnesses designed to test for the presence of quantum correlations depend on numerical parameters in addition to the observables of the system. These parameters can take arbitrary values, thus, it is possible to optimize them in order to obtain the best value of the witness. This is particularly important for witnesses that have to satisfy a particular inequality to certify the quantum correlation.

In our work, this optimization was performed for the parameter k in the steering witness S defined by Teh and Reid [95]. As was mentioned in section 2.10.2, this witness is defined as:

$$S_{a|b} = \Delta\left(\hat{X}_a - g_x\hat{X}_b\right)\Delta\left(\hat{P}_a + g_p\hat{P}_b\right) < 1, \tag{3.30}$$

but we consider the symmetric case: $k \equiv g_x = g_p$. The reason for which we have chosen this case involving symmetry is because it simplifies the computational complexity of the optimization.

The factors in the definition of S are the standard deviations. That is, the square root of the variance, thus, we start by expanding the operations in the definition of the variance for the quantities of $\hat{X}_a - k\hat{X}_b$ and $\hat{P}_a + k\hat{P}_b$. By doing this, we obtain the following expressions:

$$\Delta^2\left(\hat{X}_a - k\hat{X}_b\right) = \langle X_a X_a \rangle - \langle X_a \rangle^2 + 2k(\langle X_a \rangle \langle X_b \rangle - \langle X_a X_b \rangle) + k^2(\langle X_b X_b \rangle - \langle X_b \rangle^2),$$

$$\Delta^2\left(\hat{P}_a + k\hat{P}_b\right) = \langle P_a P_a \rangle - \langle P_a \rangle^2 + 2k(\langle P_a \rangle \langle P_b \rangle - \langle P_a P_b \rangle) + k^2(\langle P_b P_b \rangle - \langle P_b \rangle^2).$$

After calculating the square root for each of these variances, performing the multiplication between these two factors, and calculating the expectation values for each of the terms, we obtain a function that depends solely on k. We minimized that function by using *Matlab*. It is important to notice that the expectation values in this function are themselves a function of time, thus the optimal value for k changes after each instant.

Once this quantity k has been optimized, we can calculate S for different modes of light in order to find if they present steering. These results are shown in the next chapter, in section 4.7.2.

Chapter 4

Results

We will now present the solutions of the stochastic differential equations obtained by the positive-P representation and the differential equations from the Heisenberg evolution method. These solutions describe the temporal behaviour of the annihilation and creation operators for the four modes of light. These operators are important because they are used to define the quadratures and thus, the witnesses that certify the quantum correlations. Each of these witnesses has an associated criterion, that, if satisfied, certifies the presence of the corresponding quantum correlation. These criteria are usually expressed as inequalities between the witness and a particular threshold.

An initial condition has to be specified in order to solve each of the differential equations, whether they are stochastic or not. In this case it is a number corresponding to the expectation value of the creation and annihilation operators at $t = 0$, that is: $\langle \hat{a}_i(0) \rangle$, or $\langle \hat{a}_i^\dagger(0) \rangle$. These conditions were set arbitrarily, but not randomly, in order to describe a coherent state properly. More specifically, we chose this initial values because they yield an initial number of photons equal to 100. A very small number of photons, such as two or three, is not characteristic of a coherent state.

It is important to remember that the numerical solutions of the stochastic differential equations are an average of a large number of random paths produced by the stochastic noise. This was mentioned in section 2.8.1. For these numerical solutions we specify the number of random paths averaged and we denote it with nsu (number of sub-ensembles). The set of trajectories with different random paths is called an ensemble. An average is calculated for each ensemble and this process is repeated several times. The number of ensembles for each simulation is denoted by the parameter ne. For all of the results presented in this chapter the number of ensembles is 10. Moreover, the random noise in the stochastic process is added after each time step, whose duration can be specified. We denote the duration of the time step, as it was defined in section 2.8, with the parameter dt, for which we use the value of $dt = 0.001$.

Once the solutions to the differential equations have been presented, we use them to calculate different operators. Linear combinations of these operators are what constitute the entanglement and steering witnesses. By varying the coupling parameters g_1 and g_2 we find a regime in which these witnesses violate their respective threshold, thus certifying the presence of non-local quantum correlations. The variation for these coupling parameters is presented employing the quotient between the two, that is: g_2/g_1. Results obtained for these operators, as well as for the witnesses are presented in this chapter.

4.1 Annihilation & creation operators

The solutions we obtained from the two methodologies describe the dynamical behaviour of the annihilation and creation operators for the four modes of light that we believe that are entangled. We showcase the results obtained for the annihilation operators in figure 4.1.
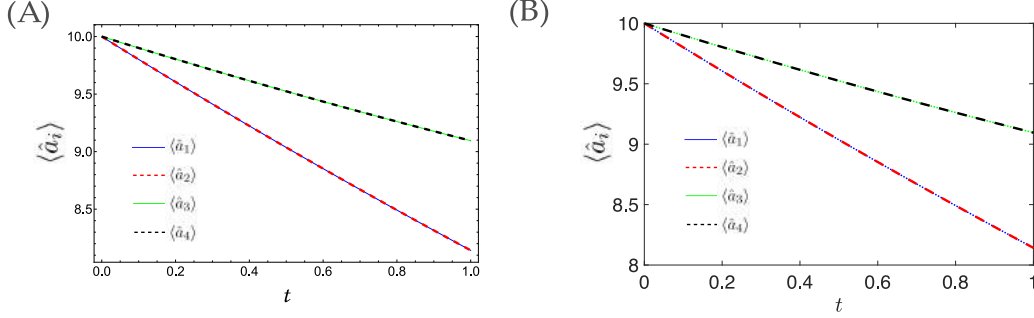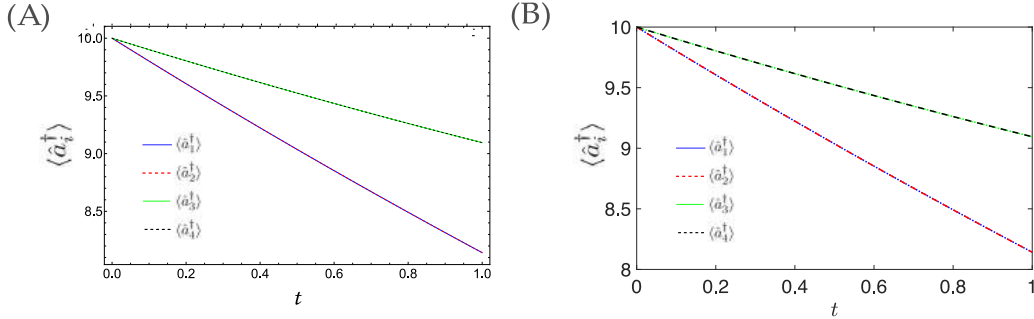

FIGURE 4.1: Expectation values for the annihilation operators of the four modes using coupling parameters $g_2/g_1 = 3$: (A) From the Heisenberg evolution equations. (B) From the positive-P representation with $nsu = 3 \times 10^6$, $dt = 0.001$. Modes 1 and 2 are equal to each other, as well as modes 3 and 4.

As the former operators describe the absorption of one photon, the creation operators describe the emission of one photon, and their behaviour is presented in figure 4.2.

FIGURE 4.2: Expectation values for the creation operators of the four modes using coupling parameters $g_2/g_1 = 3$: (A) From the Heisenberg evolution equations. (B) From the positive-P representation with $nsu = 3 \times 10^6$, $dt = 0.001$. Modes 1 and 2 are equal to each other, as well as modes 3 and 4.

It is worth noting that both methods yield the same results for these operators. The initial values for these quantities were chosen so that the average number of photons was large enough in order to represent a coherent state of light, since this is the representation needed for the Gaussian pumps. From these important results the remaining quantities will be calculated. Moreover, these results show that there are two pairs of shared modes: modes 1 and 2 on one hand, as well as modes 3 and 4 on the other.

4.2   Number operator

Once we have calculated the expressions for the creation and annihilation operators, we can use them to calculate observables such as the number operator, defined as $\hat{n}_i = \hat{a}_i^\dagger \hat{a}_i$. The expectation value for this observable represents the average number of photons in a given mode of light.

The main reason for calculating this observable is to certify that our results are sensible in a physical context. If the number operator calculated yields a negative, or complex, number of photons, this would mean that these solutions do not describe a physical mode of light, but that was not the case for our solutions. The expected number of photons for the four modes of light can be seen in figure 4.3.

(A)

(B)
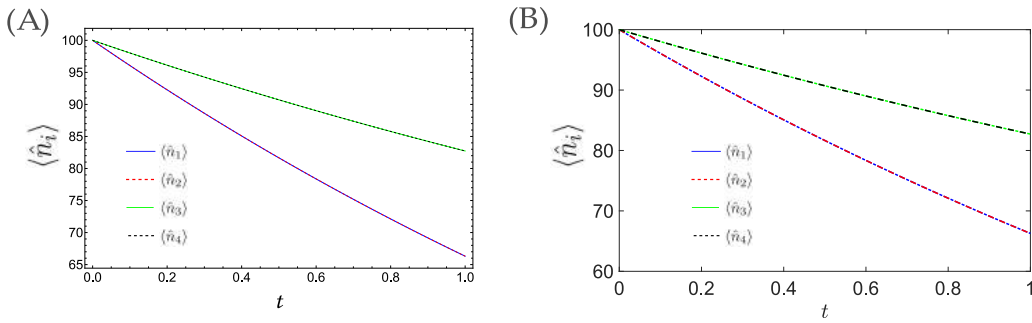
FIGURE 4.3:   Expectation values for the number of photons with $g_2/g_1 = 3$. On (A) we show results from the Heisenberg evolution equations. On (B), results from the positive-P representation using $nsu = 3 \times 10^6$.

Once again, both methods produce results that are consistent with each other. The number of photons decreases as time goes by and reaches lower values at $t = 1$ when the quotient between the coupling parameters g_2/g_1 is higher. On the other hand, for all the values under consideration, we obtained the initial value for the number of photons when $t = 0$, which indicates that our results are correct.

4.3 $\hat{X}$ quadratures

As was mentioned in the theoretical background, the $\hat{X}$ quadrature, which is a continuous variable, serves as analogous to position for modes of light, and is defined as: $\hat{X}_j = \left(\hat{a}_j^\dagger + \hat{a}_j \right)$. These quantities are important since they will be used to define the witnesses that cerify the quantum correlations. Their expectation values are shown in figure 4.4 and show consistency between the Heisenberg evolution equations and the phase space method.
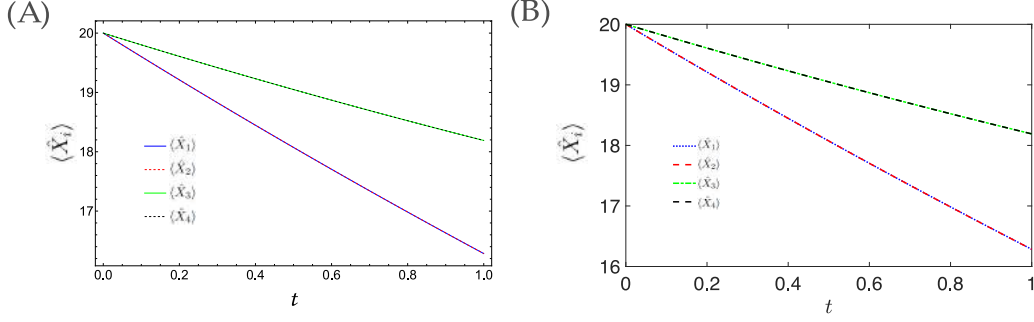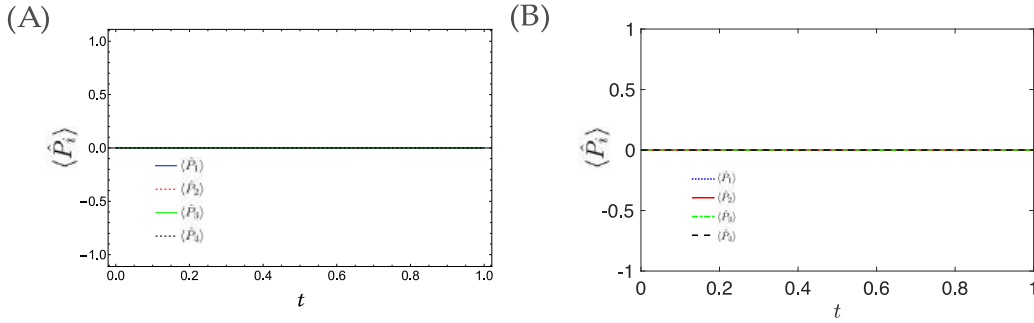
FIGURE 4.4: Expectation values for the $\hat{X}$ operators denoted by $X_i = \langle \hat{X}_i(t) \rangle$. (A) shows results from the Heisenberg evolution equations. (B) corresponds to the positive-P representation using parameters $g_2/g_1 = 3$, $nsu = 3 \times 10^6$.

Results obtained for these quantities, as well as those for $\hat{P}$ quadratures, could be verified using homodyne or heterodyne detection.

4.4 $\hat{P}$ quadratures

The $\hat{P}$ quadratures are the analogous to the momentum for the modes of light and their definition is: $\hat{P}_j = i \left(\hat{a}_j^\dagger - \hat{a}_j \right)$, where i denotes the imaginary unit. The solutions we obtained for the creation and annihilation operators were equal when referred to the same mode, thus the quantites $\langle \hat{P}_i \rangle$ were always equal to zero (except for statistical fluctuations due to white noise in the phase space methodology). Results for these quantities can be seen in figure 4.5.

FIGURE 4.5: Expectation values for the $\hat{P}$ operators denoted by $P_i = \langle \hat{P}_i(t) \rangle$. (A) shows results from the Heisenberg evolution equations. (B) corresponds to the positive-P representation using parameters $g_2/g_1 = 3$, $nsu = 3 \times 10^6$.

4.5 Quadrature products

In order to certify entanglement and steering we use the entanglement witnesses presented in the previous sections. These witnesses are linear combinations of operators that depend on the quadratures. Furthermore, because of the definition of the variance as $\langle \Delta^2 \hat{U} \rangle = \langle \hat{U}^2 \rangle - \langle \hat{U} \rangle^2$, we have to perform products among the quadratures. For example, if we consider an operator defined as $\hat{U} = \hat{X}_i - \hat{X}_j$, then $\Delta^2 \hat{U} = \langle (\hat{X}_i - \hat{X}_j)^2 \rangle - \langle \hat{X}_i - \hat{X}_j \rangle^2$. This is, in turn:

$$\Delta^2 \hat{U} = \langle \hat{X}_i \hat{X}_i \rangle - \langle \hat{X}_i \hat{X}_j \rangle - \langle \hat{X}_j \hat{X}_i \rangle + \langle \hat{X}_j \hat{X}_j \rangle - \langle \hat{X}_i \rangle^2 + 2\langle \hat{X}_i \rangle \langle \hat{X}_j \rangle - \langle \hat{X}_j \rangle^2. \quad (4.1)$$

As we can see from the right hand side of eq. 4.1, to calculate these variances it is needed to compute the quadrature products first. Their expectation values are shown in figures 4.6 and 4.7. These preliminary results were useful for debugging the programs with the numerical algorithms used to solve the SDE's by comparing the results from the two methods. The final results also show consistency between the two methodologies. From this point forward, only results from the phase space methodology will be presented since they show consistency with the Heisenberg equations and they constitute the main methodology of this work.

Quadrature products involving $\hat{X}_i$

We now present the results for the quadrature products involving $\hat{X}$ quadratures. Similarly to the annihilation and creation operators, modes 1 and 2 behave equally as well as modes 3 and 4. For these products, as well as for the rest of our results, calculations were made using $g_2/g_1 = 1$, $g_2/g_1 = 3$ and $g_2/g_1 = 3.5$, but the important differences from changing the value of this parameter are only seen for the witnesses, thus, we only include results for $g_2/g_1 = 1$ in this section.
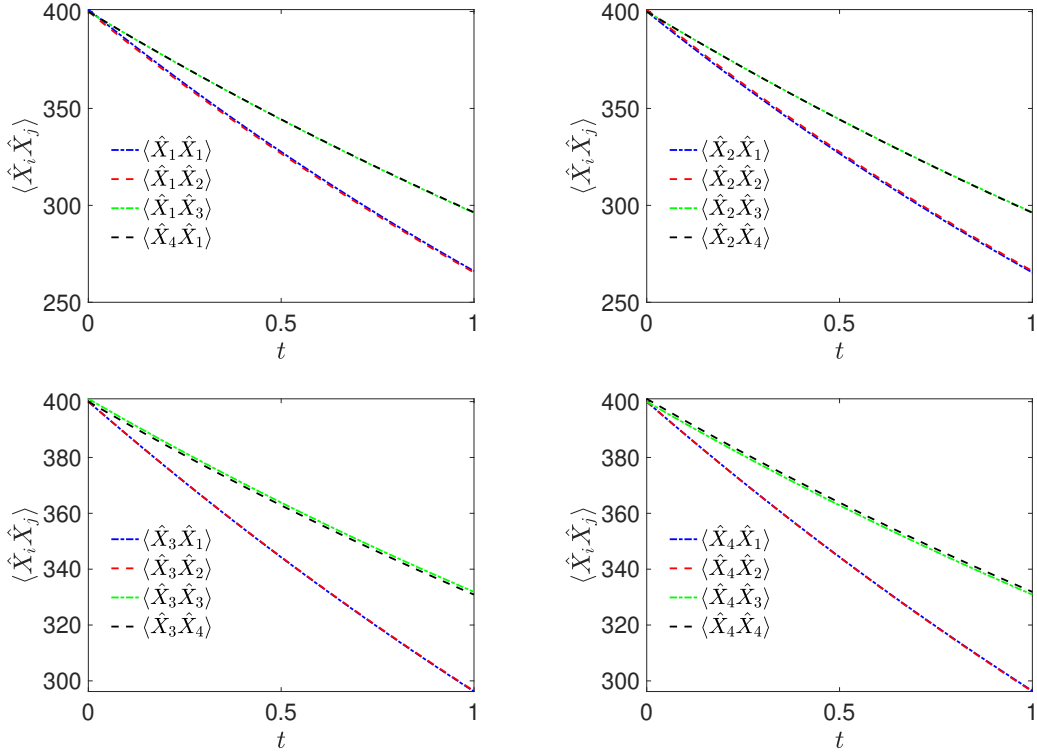
FIGURE 4.6: Expectation values of the quadrature products $X_i X_j$, for $i, j = 1, 2, 3, 4$ using the parameters $g_2/g_1 = 1$, $nsu = 10^7$ for the positive-P representation.

Quadrature products involving $\hat{P}_i$

As the former results, these products are also used to calculate variances for the entanglement witnesses. Their expectation values are shown in figure 4.7.
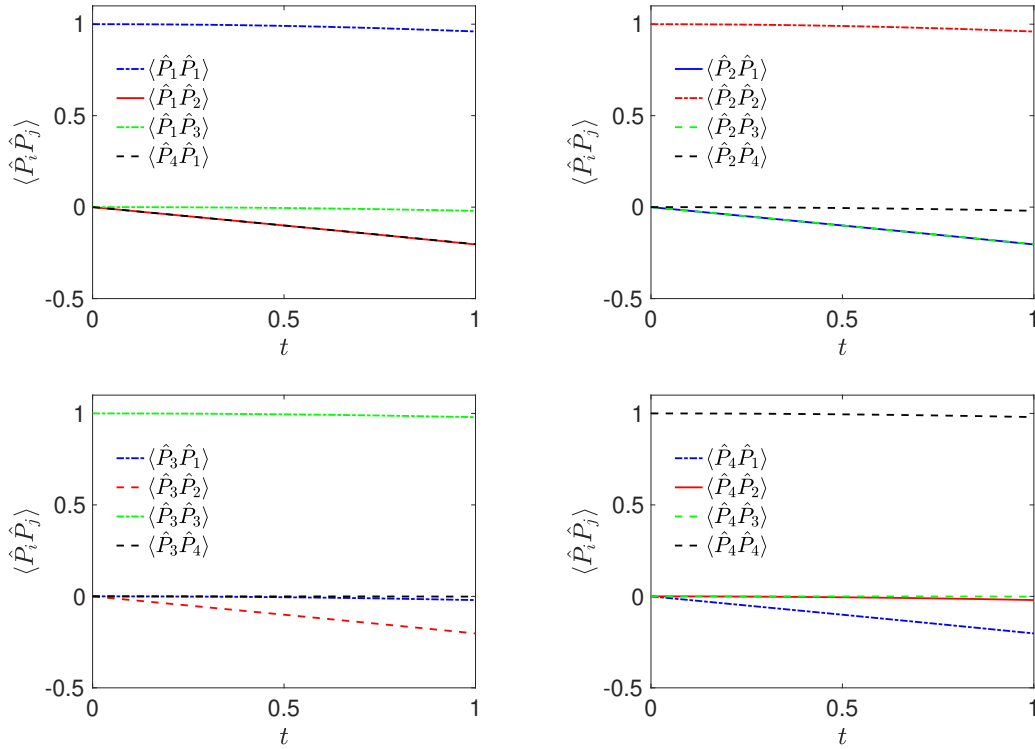
FIGURE 4.7: Expectation values of the quadrature products P_iP_j, for $i, j = 1, 2, 3, 4$ using the parameters $g_2/g_1 = 1$, $nsu = 10^7$ for the positive-P representation.

Results shown in figure 4.7 are, in general, different to zero, unlike the expectation values $\langle \hat{P}_i \rangle$. The reason for this is because $\hat{P}$ is defined as a difference, while the quadrature products have this subtraction of terms as well as some others crossed terms from the multiplication. It is also notorious that products from the same mode are always equal to one. This fact arises from the commutation relation for the creation and annihilation operators: $[\hat{a}_i, \hat{a}_j] = \delta_{i,j}$, where $\delta_{i,j}$ is the Kronecker delta. Explicitly, when we are performing multiplication for quadratures of the same mode we encounter products of annihilation and creation operator for the same mode that yield this value of 1.

4.6 Entanglement witnesses

Now that we have calculated the expectation values for some operators and some observables, we can use these results to test for quantum correlations in the system. We start by considering the case for entanglement and therefore present the results in this section. The first three criteria that we present consider the bipartite case for two of the four possible modes involved in the process. We will examine with these bipartite witnesses all of the possible pairings for two out of the four modes to show they are all quantum correlated to each other. The last criterion of this section considers the 4-partite case directly.

4.6.1   DGCZ entanglement criterion

As it was previously mentioned in subsection 2.9.1, the following operators for a given pair of modes of light were defined as:

$$\begin{aligned} \hat{U}_{ij} &= \hat{X}_i - \hat{X}_j, \\ \hat{V}_{ij} &= \hat{P}_i + \hat{P}_j. \end{aligned} \tag{4.2}$$

The entanglement witness D_{ij} is defined as follows, and entanglement is certified if the inequality is violated:

$$D_{ij} = \Delta^2 U_{ij} + \Delta^2 V_{ij} \geq 4. \tag{4.3}$$

The results obtained for these witnesses are shown in figures 4.8, 4.9, and 4.10.
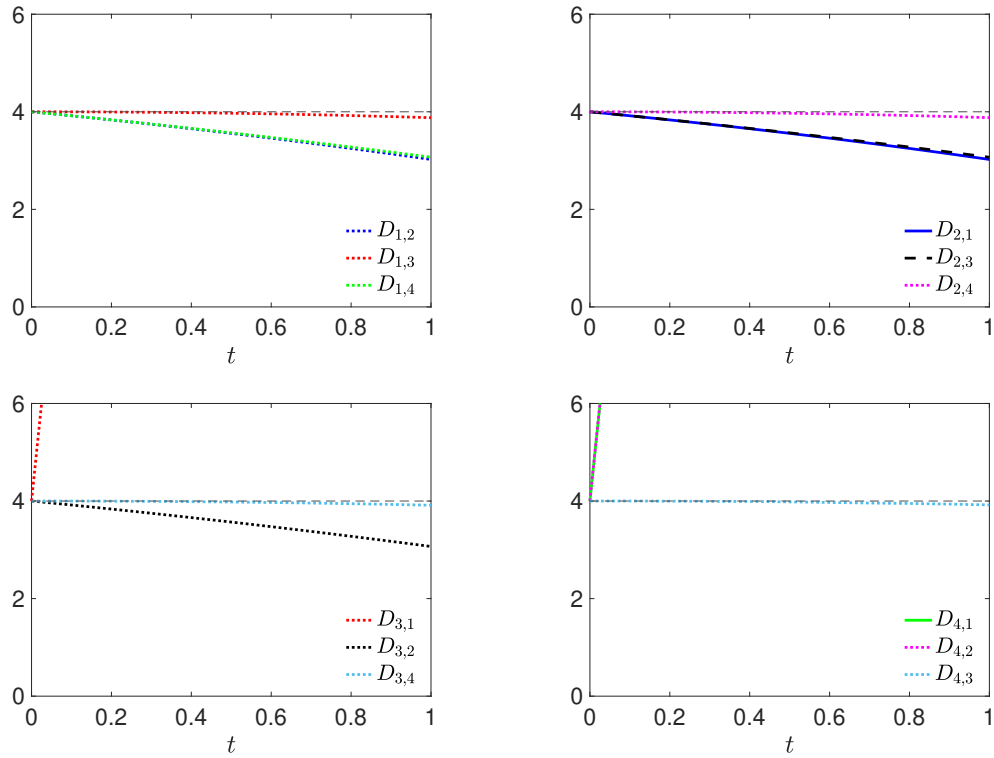
FIGURE 4.8: Entanglement witness D_{ij}, for different mode pairings using the following parameters: $g_2/g_1 = 1$, $nsu = 10^7$.
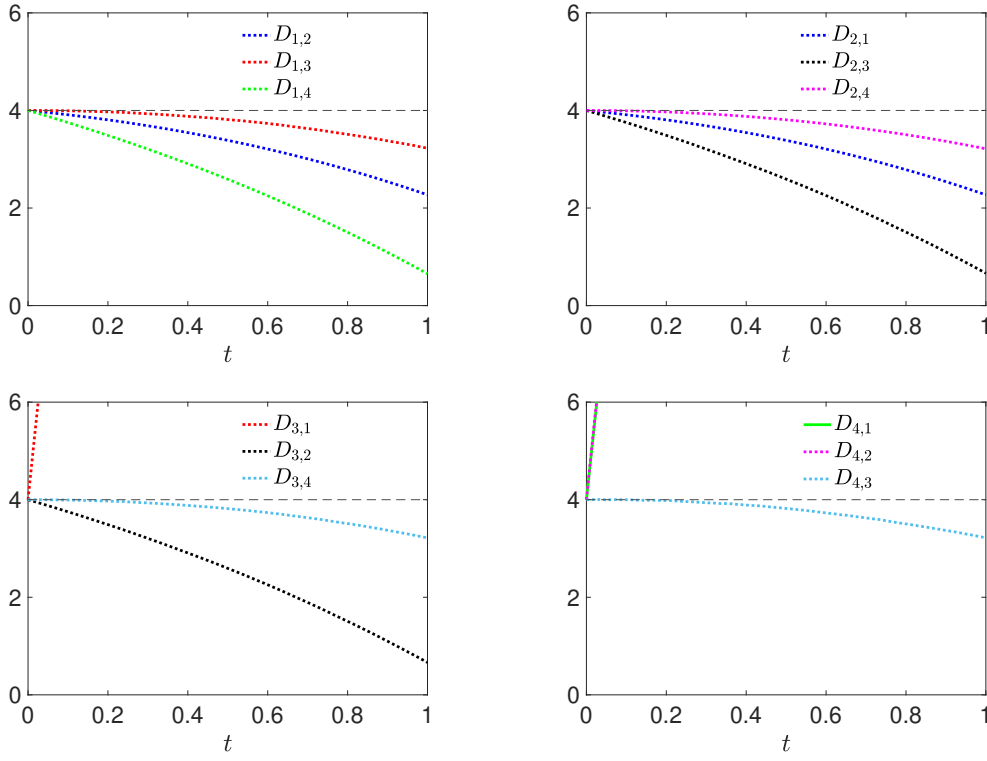
FIGURE 4.9: Entanglement witness D_{ij}, for different mode pairings using the following parameters: $g_2/g_1 = 3$, $nsu = 10^7$.
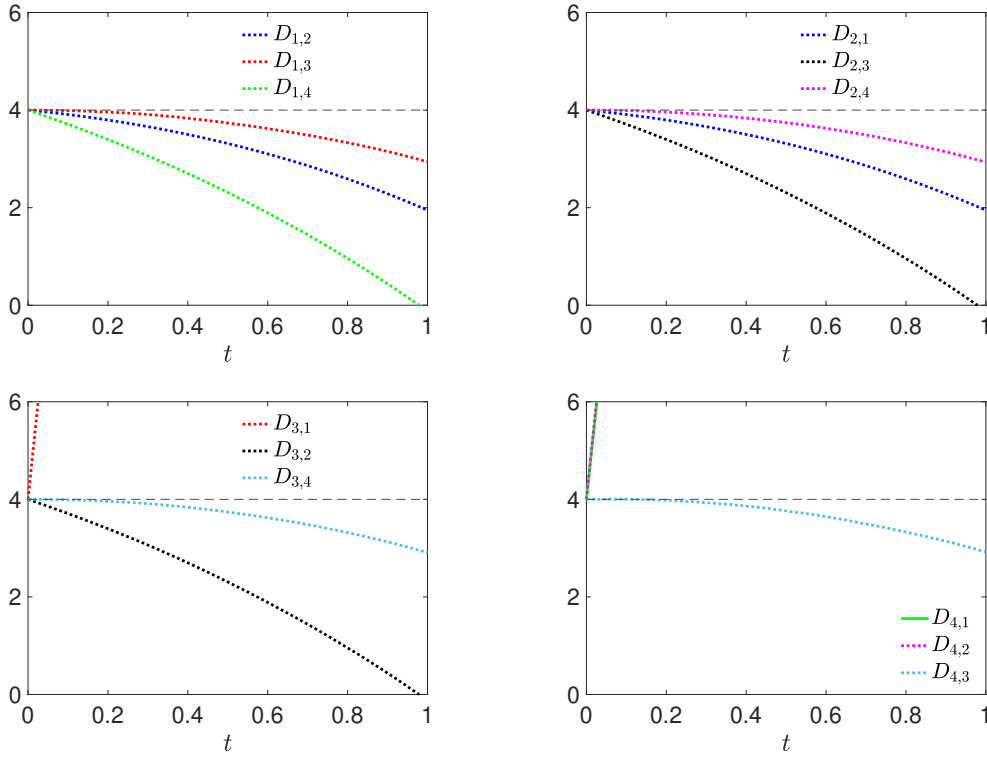
FIGURE 4.10: Entanglement witness D_{ij}, for different mode pairings using the following parameters: $g_2/g_1 = 3.5$, $nsu = 10^7$.

The results shown in the top right graph of each figure indicate that for any given pair of modes that includes mode 1, entanglement is certified. Similarly, this is confirmed for mode 2. However, for mode 3, only two out of three possible pairings violate the threshold, being the pairing with mode 1 the one that does not violate it. Since entanglement is a symmetric quantum correlation, and this witness is a sufficient but not necessary condition, we can also certify entanglement between modes 1 and 3 by using the top left subfigure. The same argument holds for pairings with mode 4, which only violate the threshold once in the bottom right subfigure for D_{43} for every quotient of the coupling parameters. As the quotient g_2/g_1 increases, the witnesses D_{ij} that go below the threshold do so in a faster way.

4.6.2 $\mathbf{ENT^{\pm}}$

In the second chapter we mentioned that Giovannetti et al. [92] defined an entanglement criterion that is based on two real parameters called g_x and g_p. The expression is shown in eq. 2.102. If those two parameters are chosen to be $g_x = -1$ and $g_p = 1$, then the expression is called ENT^+. If these values are switched, we obtain ENT^-. We can write these two expressions briefly as follows:

$$\text{ENT}_{ij}^{\pm} = \sqrt{\Delta^2(\hat{X}_i \mp \hat{X}_j)\Delta^2(\hat{P}_i \pm \hat{P}_j)} \tag{4.4}$$

This entanglement witness is used in the following criterion: if the following inequality is satisfied, then entanglement is certified:

$$\text{ENT}^{\pm} < 2. \tag{4.5}$$

$\mathbf{ENT^+}$

In figures 4.11, 4.12, and 4.13 we present the results for ENT^+. These results violate the threshold for every possible combination of two modes and for every quotient of coupling parameters g_2/g_1, thus certifying the presence of entanglement.
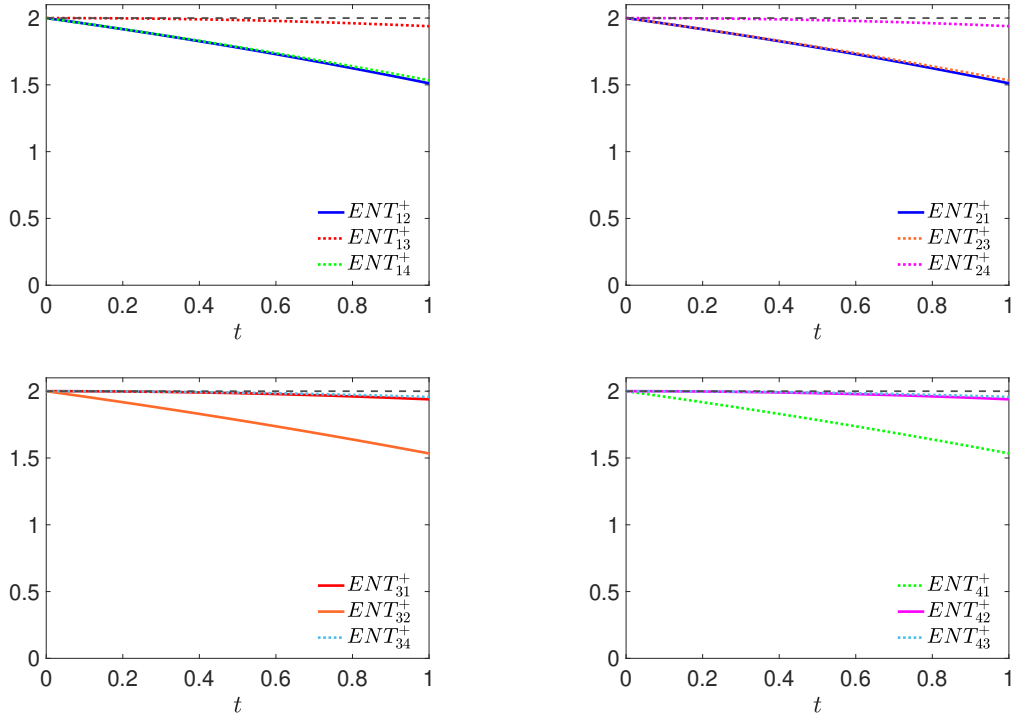
FIGURE 4.11: Results for ENT$^+$ for different pairings of modes using the following parameters: $g_2/g_1 = 1$, $nsu = 10^7$.
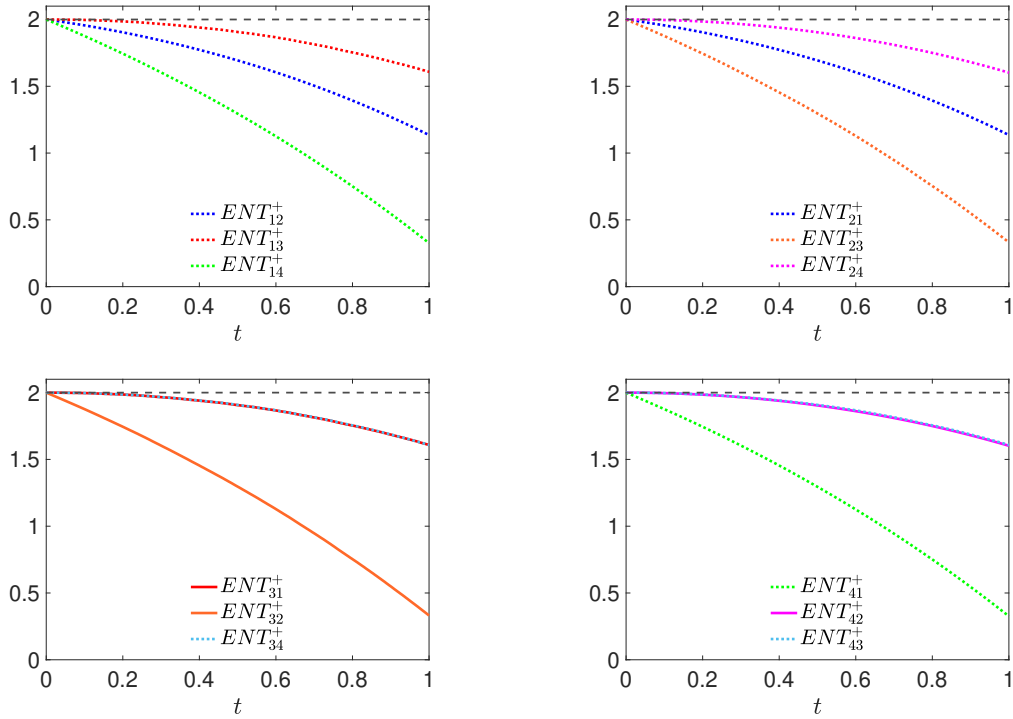

FIGURE 4.12: Results for ENT$^+$ for different pairings of modes using the following parameters: $g_2/g_1 = 3$, $nsu = 10^7$.
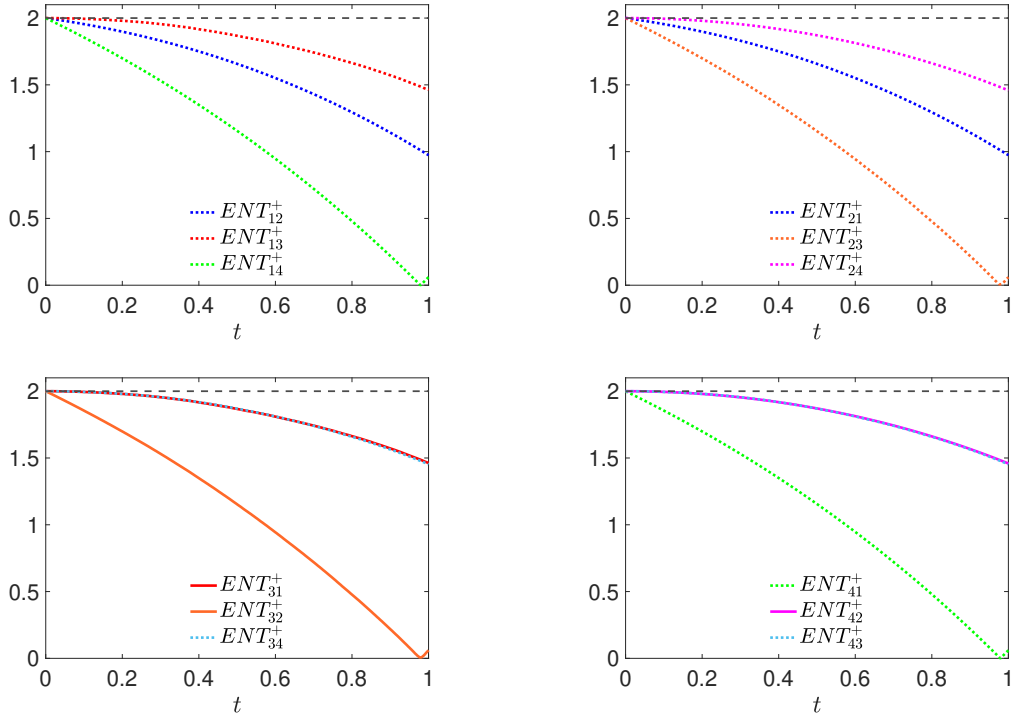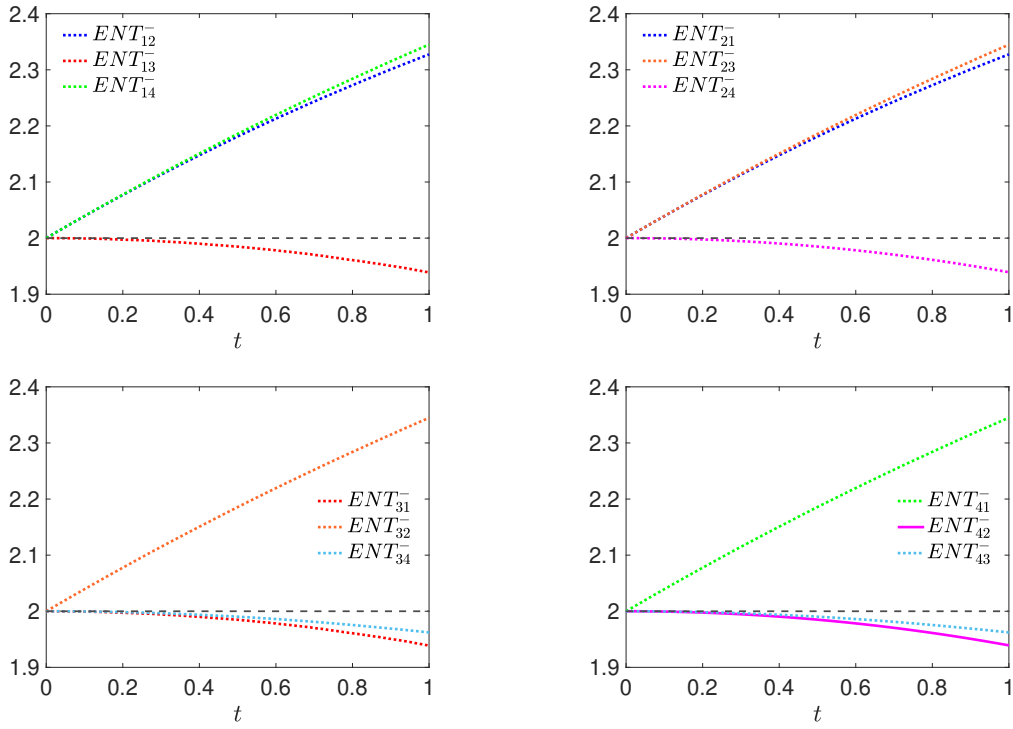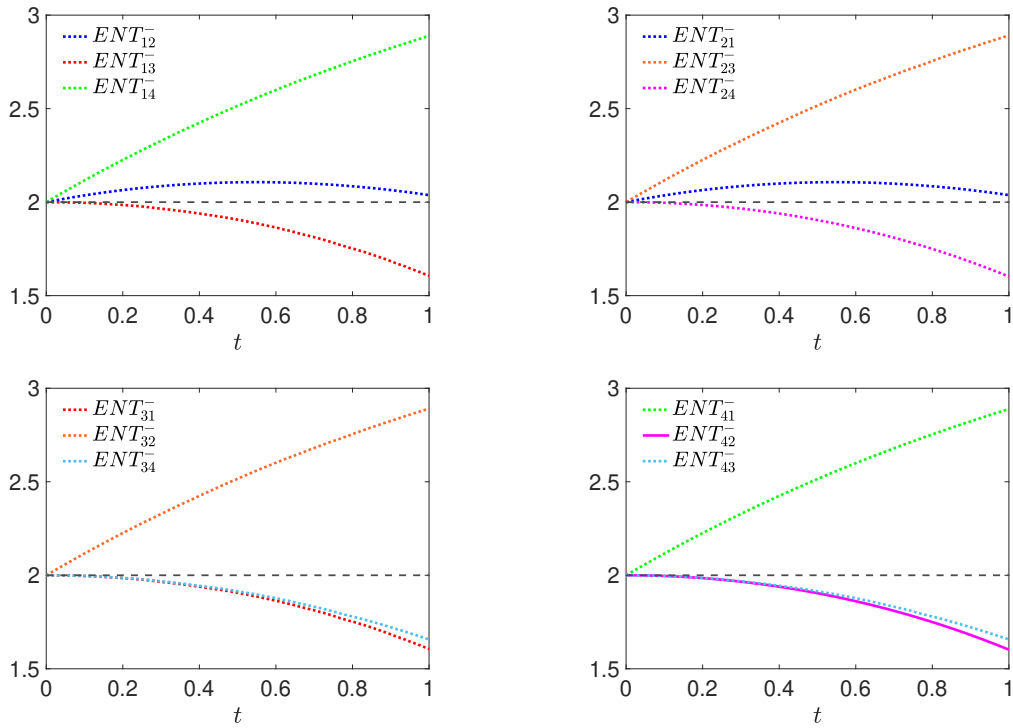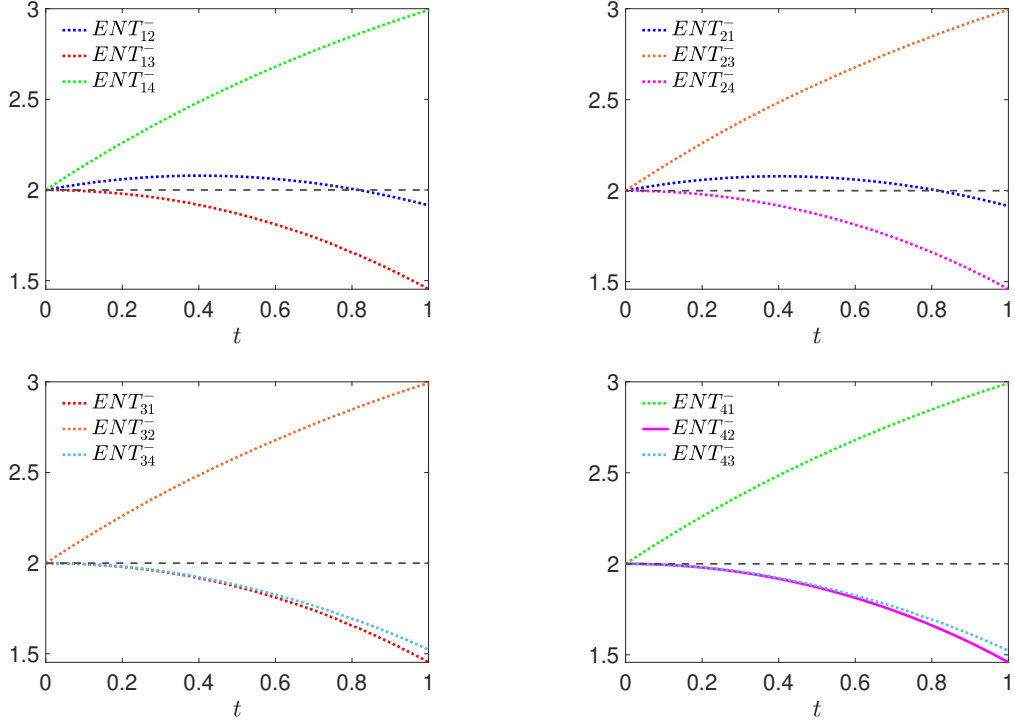
FIGURE 4.13: Results for ENT$^+$ for different pairings of modes using the following parameters: $g_2/g_1 = 3.5$, $nsu = 10^7$.

ENT$^-$

Results for ENT$^-$ are shown in figures 4.14, 4.15, and 4.16. Unlike the witness ENT$^+$, this witness does not violate the threshold for every quotient of the coupling parameters, or for every combination of modes. There is always at least one combination of modes in which entanglement is not certified. However it is important to note that every criterion discussed in this work is a sufficient but not necessary condition to find entanglement, thus the violation of ENT$^+$ already certifies the presence of this quantum correlation when considering a specific pair of modes.

FIGURE 4.14: Results for ENT$^-$ for different pairings of modes using the following parameters: $g_2/g_1 = 1$, $nsu = 10^7$.

FIGURE 4.15: Results for ENT$^-$ for different pairings of modes using the following parameters: $g_2/g_1 = 3$, $nsu = 10^7$.

FIGURE 4.16: Results for ENT$^-$ for different pairings of modes using the following parameters: $g_2/g_1 = 3.5$, $nsu = 10^7$.

4.6.3   Criterion for 4-partite entanglement

Following the criterion by Teh et al. that was mentioned in subsection 2.9.3, we consider a particular case of the general criterion by defining the quantities $\hat{U}$ and $\hat{V}$ as:

$$
\begin{aligned}
\hat{U} &= \hat{X}_1 - \frac{1}{\sqrt{3}}\left(\hat{X}_2 + \hat{X}_3 + \hat{X}_4\right) \\
\hat{V} &= \hat{P}_1 + \frac{1}{\sqrt{3}}\left(\hat{P}_2 + \hat{P}_3 + \hat{P}_4\right)
\end{aligned}
\tag{4.6}
$$

We proceed to calculate the variances for these quantities. These variances will be used, together with the thresholds of the different possible bipartitions, to certify the presence of entanglement for every case. These thresholds were calculated in subsection 2.9.3. The sum of the variances of $\hat{U}$ and $\hat{V}$ is presented in figure 4.18 comparing two different quotients for the coupling parameters.
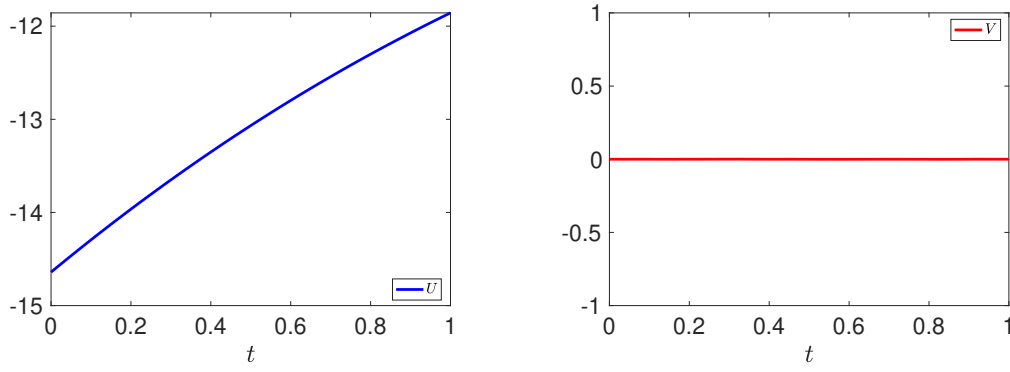
FIGURE 4.17: Expectation values for operators $\hat{U}$ and $\hat{V}$ considering parameters $g_2/g_1 = 3$, $nsu = 10^6$.

In the following figures we present the sum of the variances, along with the thresholds for entanglement for different bipartitions. This entanglement criterion was discussed in section 2.9.3, as well as the threshold for each bipartition. Entanglement is certified for each bipartition if the sum of the variances of $\hat{U}$ and $\hat{V}$ falls below its respective threshold. The results shown in figure 4.18 include each of the thresholds for the different bipartitions. As time increases, entanglement is certified in more of these different bipartitions. Results in figure 4.19 only exhibit the simplified threshold for genuine multipartite entanglement. We present two cases with distinct values for the quotient between the coupling parameters. The case for which both coupling parameters have the same value, $g_2/g_1 = 1$, does not exhibit entanglement, except for the bipartition $234 - 1$, as it is shown in figure 4.20.

(A) Sum of the variances using coupling parameters quotient $g_2/g_1 = 3$

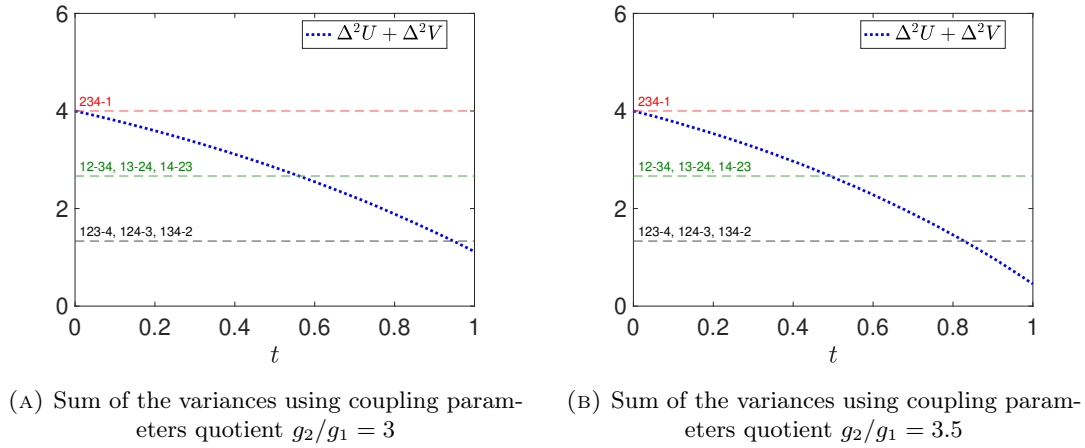(B) Sum of the variances using coupling parameters quotient $g_2/g_1 = 3.5$

FIGURE 4.18: Comparison of the 4-partite entanglement criterion for different bipartitions using a distinct coupling parameters quotient.
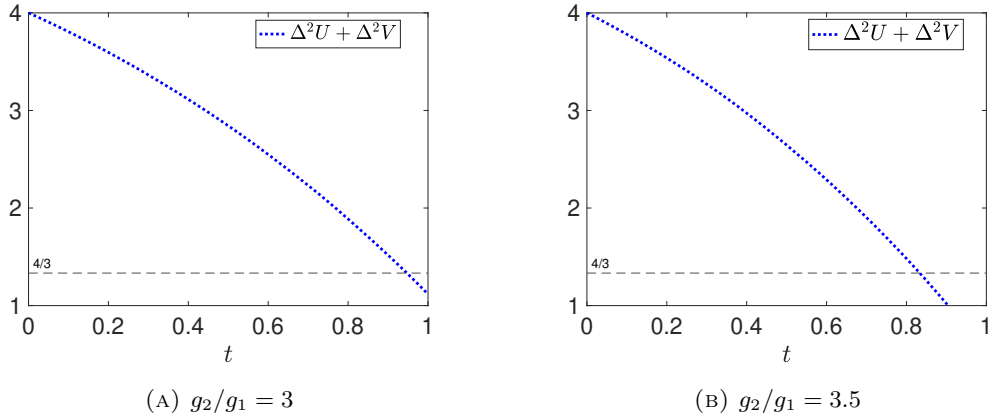
FIGURE 4.19: Comparison of the 4-partite entanglement criterion using only one inequality with a distinct coupling parameters quotient.
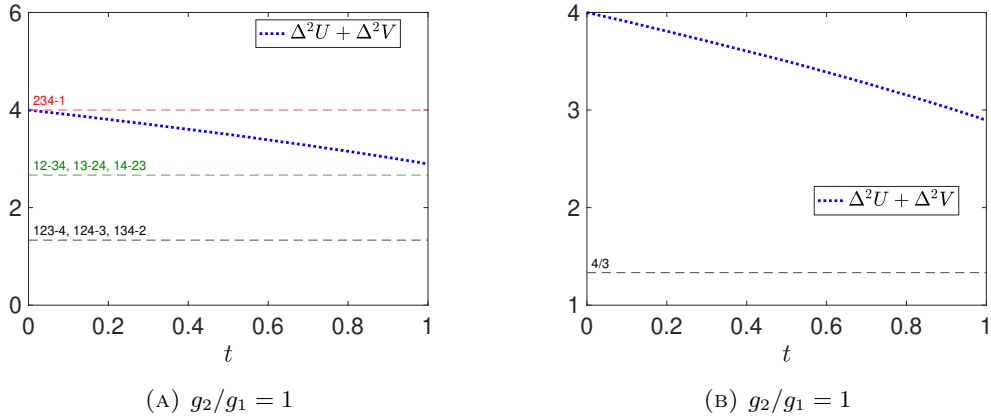

FIGURE 4.20: Entanglement criterion for $g_2/g_1 = 1$. The only bipartition for which entanglement was found is $234 - 1$.

4.7 Steering witnesses

In this section we present the results for the different steering witnesses, as well as a discussion on whether the quantum correlation was certified or not. As it was the case for the previous section, first we consider two witnesses that test for steering between two parties and we use it for all the different pairings and later we present the multipartite case.

4.7.1 EPR

This criterion, presented by Margaret Reid [52], is used to determine steering between two parties, and uses inferred variances. It is asymmetric, thus, for a given pair of subsystems it is necessary to test before and after permuting the modes. As it was discussed previously in section 2.10.1, the quantity $\text{EPR}_{i|j}$ is defined as:

$$\text{EPR}_{i|j} = V_{\inf}(\hat{X}_i)V_{\inf}(\hat{P}_j), \tag{4.7}$$

where V_{inf} denotes the inferred variance. Mathematically, these variances are:

$$V_{\text{inf}}(\hat{X}_i) = \Delta^2(\hat{X}_i) - \frac{\left[\Delta^2(\hat{X}_i, \hat{X}_j)\right]^2}{\Delta^2(\hat{X}_j)}, \tag{4.8}$$

$$V_{\text{inf}}(\hat{P}_i) = \Delta^2(\hat{P}_i) - \frac{\left[\Delta^2(\hat{P}_i, \hat{P}_j)\right]^2}{\Delta^2(\hat{P}_j)}, \tag{4.9}$$

Steering is certified if the following inequality is satisfied $EPR_{i|j} < 1$. Results for the possible mode pairings are shown in figures 4.21, 4.22 and 4.23.
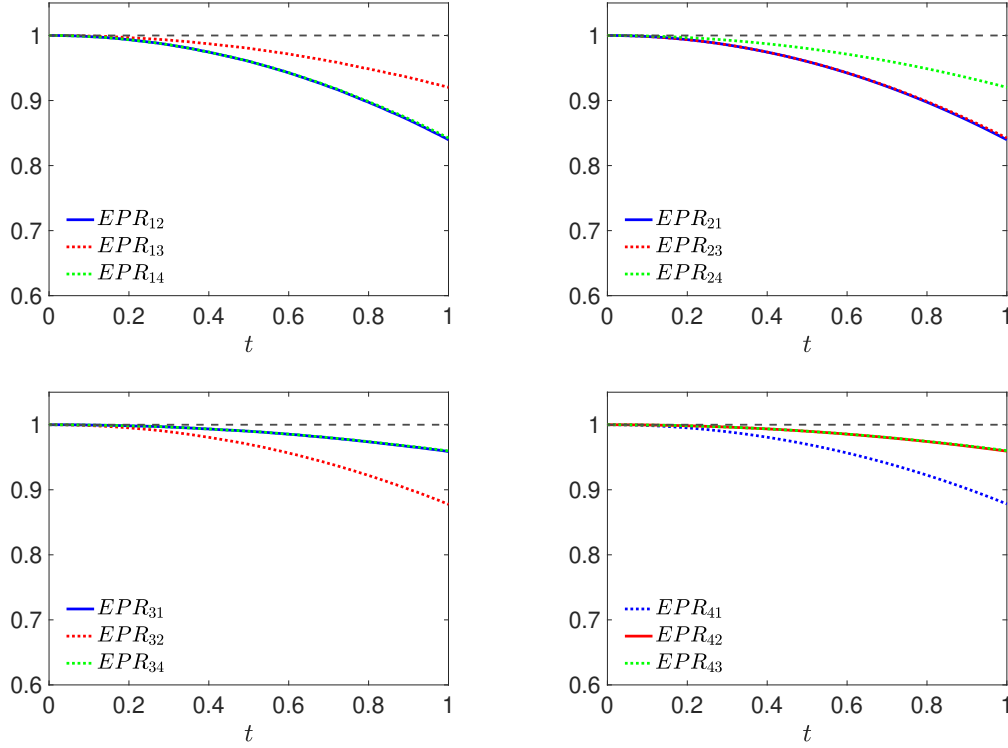

FIGURE 4.21: EPR Steering witness results for different pairings of modes the following parameters, $g_2/g_1 = 1$, $nsu = 10^7$.
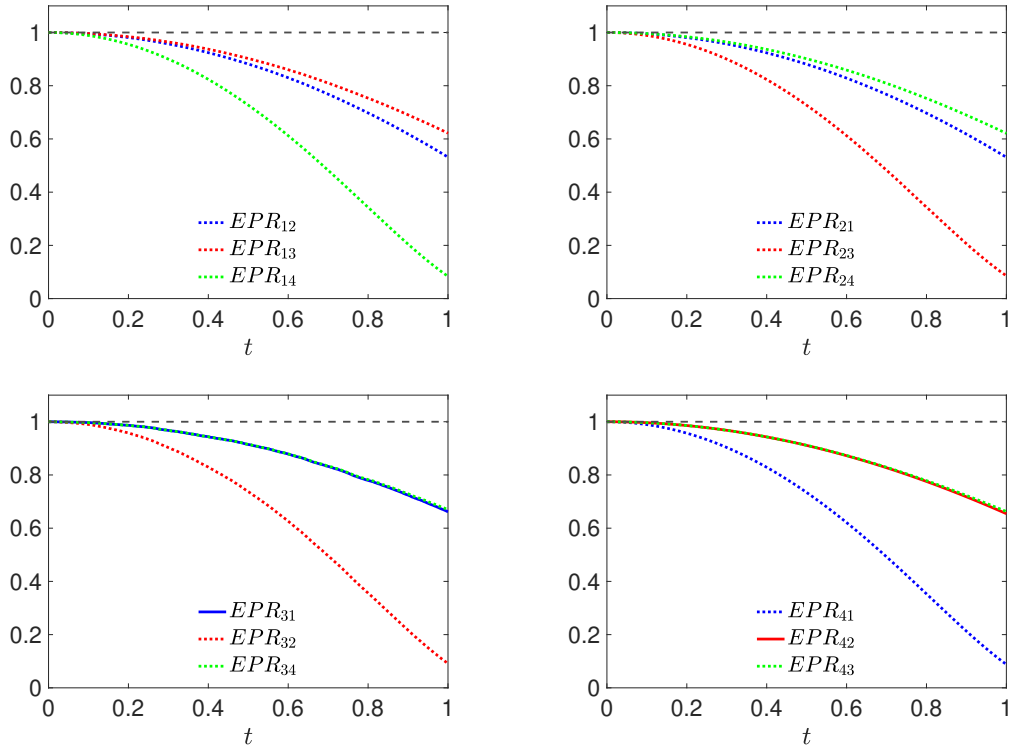
FIGURE 4.22: EPR Steering witness results for different pairings of
modes for the following parameters, $g_2/g_1 = 3$, $nsu = 10^7$.
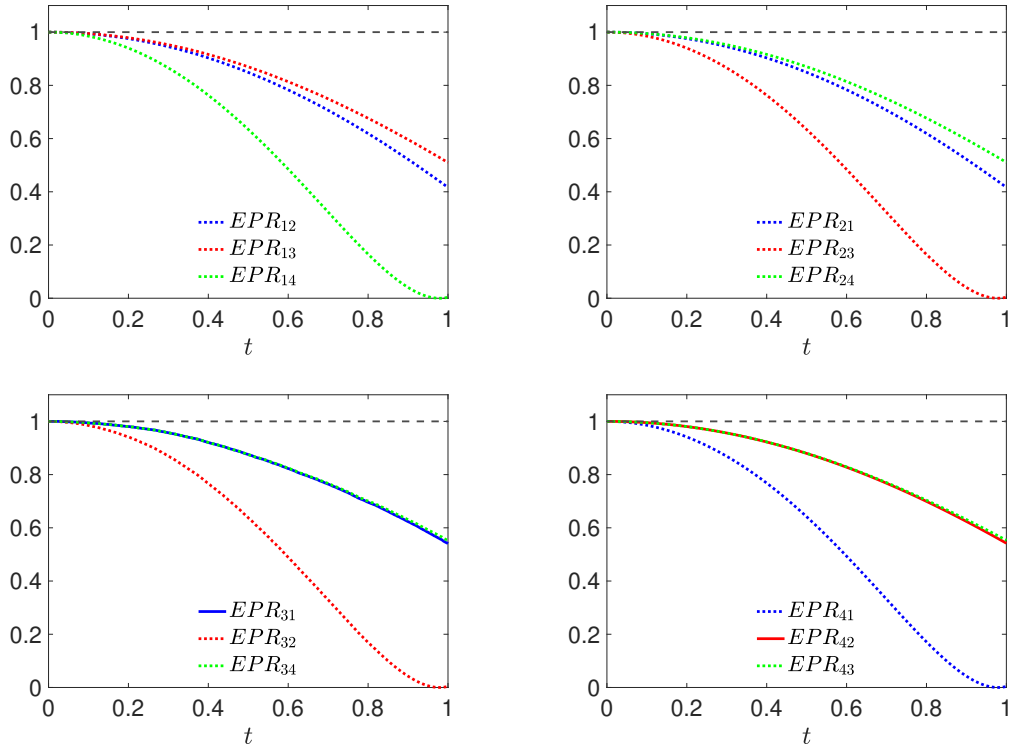

FIGURE 4.23: EPR Steering witness results for different pairings of
modes for the following parameters, $g_2/g_1 = 3.5$, $nsu = 10^7$.

Results obtained for all possible mode pairings are below the threshold, thus certifying that steering is present for the 4 modes. The more conspicuous difference found by increasing the value for g_2/g_1 is that while this quantity increases, the value for the witness decreases until it eventually reaches zero and stays there. This can be interpreted as steering remaining as time goes by.

4.7.2 S Steering criterion

Proposed by Reid et. al. [53], this criterion also tests for steering but does not use inferred variances, instead, it utilizes standard deviations. It certifies steering if the following inequality is satisfied:

$$S = \Delta(\hat{X} - g_x\hat{X})\Delta(\hat{P} + g_p\hat{P}) < 1 \qquad (4.10)$$

where g_x and g_p are arbitrary real coefficients that are optimized so that they minimize S, as it was already mentioned. We are considering the symmetric case in which $g_x = g_p = k$, because it reduces the computational complexity of the optimization for these parameters. Results are shown in figure 4.26.
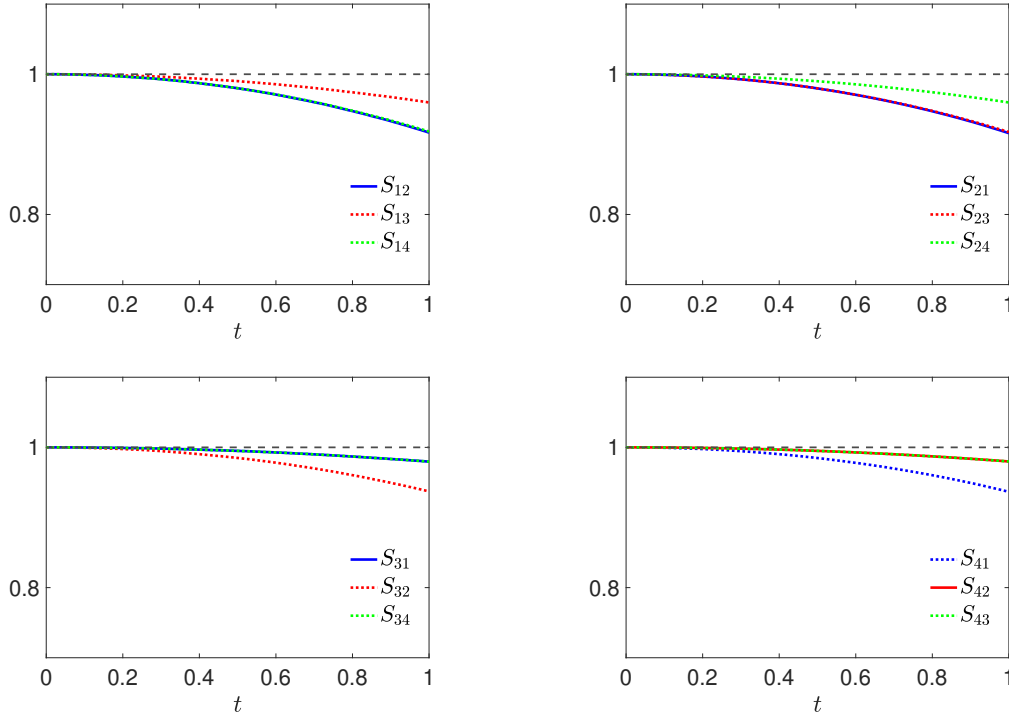

FIGURE 4.24: Results for the steering parameter S, using the following parameters: $g_2/g_1 = 1$, optimized k, $nsu = 10^7$.
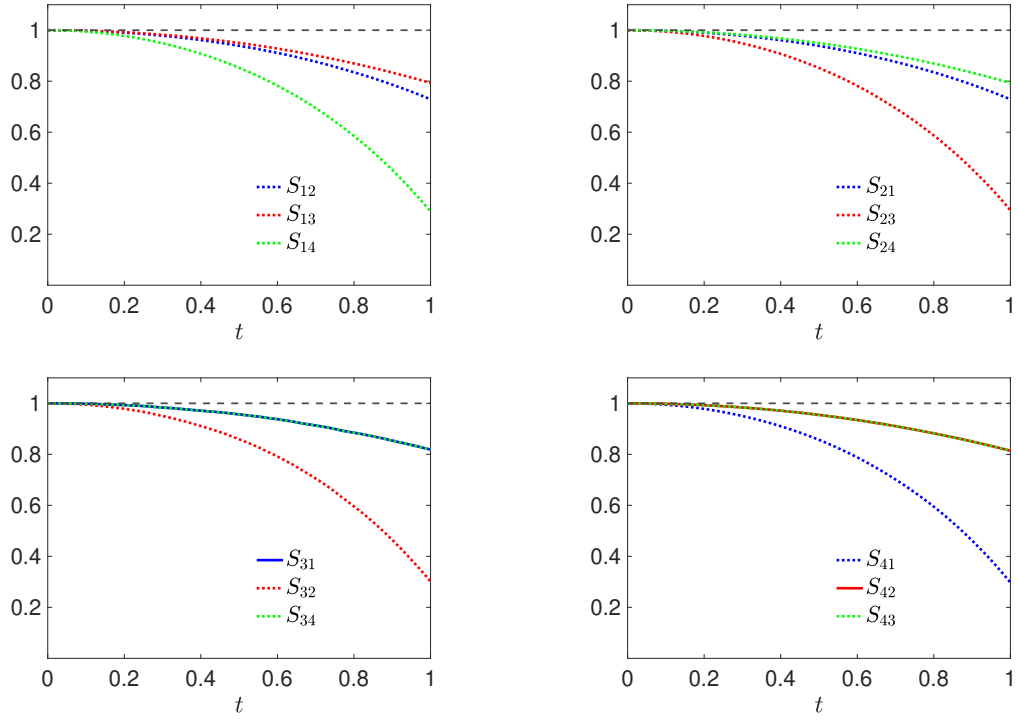
FIGURE 4.25: Results for the steering parameter S, using the following parameters: $g_2/g_1 = 3$, optimized k, $nsu = 10^7$.
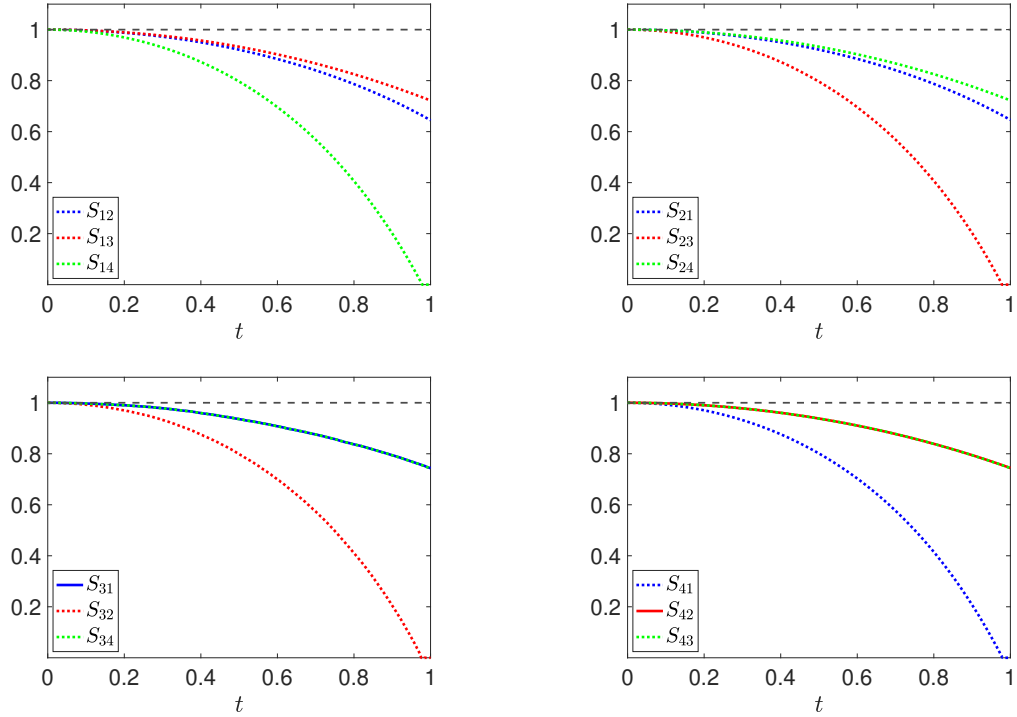

FIGURE 4.26: Results for the steering parameter S, using the following parameters: $g_2/g_1 = 3.5$, optimized k, $nsu = 10^7$.

Results show that for every case, steering is certified. Nevertheless, when increasing the quotient between the two coupling parameters, that is g_2/g_1, the product of

the standard deviations fall down below the threshold faster. It was important for us to analyze the cases in which this product reaches zero faster, since we wanted to find out if there was a revival in which the S witness starts to increment again after reaching a minimum value. Furthermore, we wanted to make sure that S does not become negative since standard deviations are always non-negative values.

4.7.3 Genuine multipartite steering criterion

This following criterion was discussed in subsection 2.10.3 and, as the former, also depends on the product of standard deviations of witnesses u and v, which were defined by the authors as:

$$
\begin{aligned}
u &= h_1 x_1 + h_2 x_2 + h_3 x_3 + h_4 x_4, \\
v &= g_1 p_1 + g_2 p_2 + g_3 p_3 + g_4 p_4,
\end{aligned}
\tag{4.11}
$$

If we consider the particular bipartition $1 - 234$, then the violation of the following inequality certifies steering of subsystem 1 by subsystem 234.

$$
\Delta u \Delta v \geq |g_1 h_1|,
\tag{4.12}
$$

Otherwise, if the following inequality is violated, subsystem 234 can be steered by subsystem 1:

$$
\Delta u \Delta v \geq |g_2 h_2 + g_3 h_3 + g_4 h_4|.
\tag{4.13}
$$

Two-way steering is certified when both of these inequalities are violated, or what is equivalent, when the minimum of the two numbers on the right hand side is subdued. Same procedure can be applied for the seven possible bipartitions of the 4 modes. The different thresholds for the possible bipartitions were calculated and reported in subsection 2.10.3. Results for this criterion are shown in figure 4.27.

(A) $g_2/g_1 = 3$

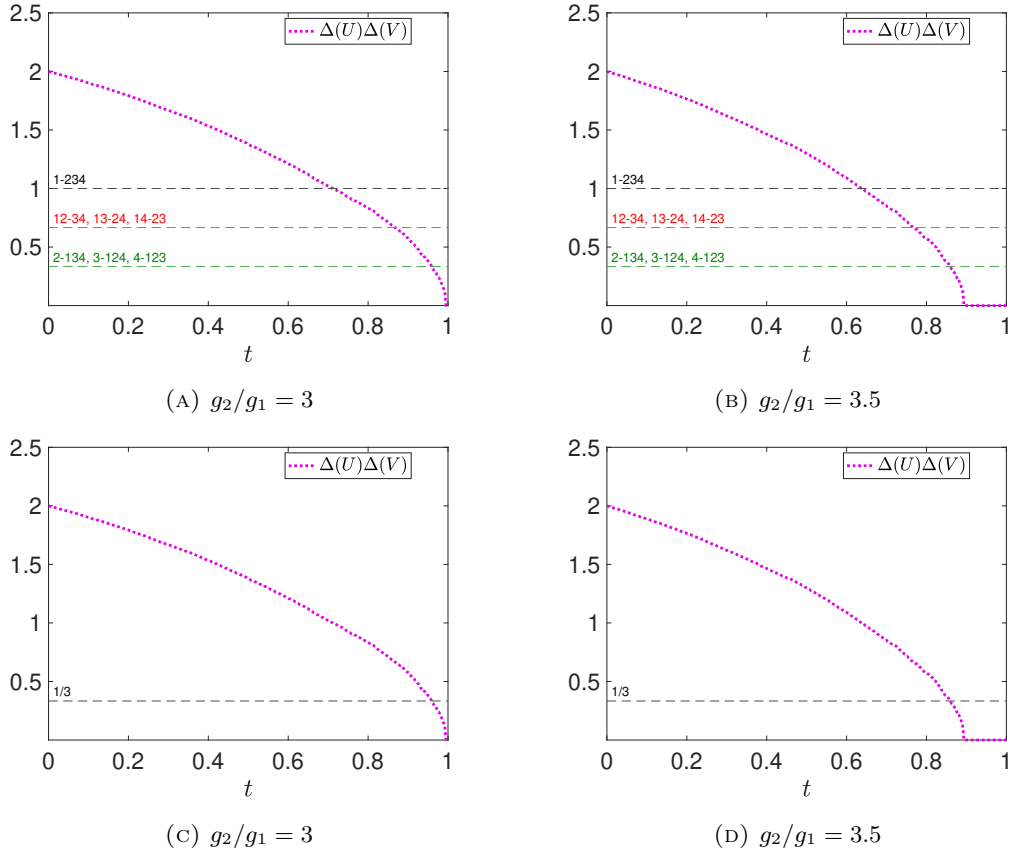(B) $g_2/g_1 = 3.5$

(C) $g_2/g_1 = 3$

(D) $g_2/g_1 = 3.5$

FIGURE 4.27: Genuine steering witnesses. (A) and (B) show the thresholds for every possible bipartition, using the quotient between the coupling parameters $g_2/g_1 = 3$ and $g_2/g_1 = 3.5$, respectively. (C) and (D) are the cases with only one inequality using the quotient between the coupling parameters $g_2/g_1 = 3$ and $g_2/g_1 = 3.5$, respectively.

Results shown in figure 4.27 for this criterion certify that steering is present for every possible bipartition of the four modes. In other words, genuine 4-partite steering is present in the system. As the quotient g_2/g_1 increases, the thresholds are violated quicker. However, in the case in which $g_2 = g_1$, steering was not certified. Results for this case are shown in figure 4.28.
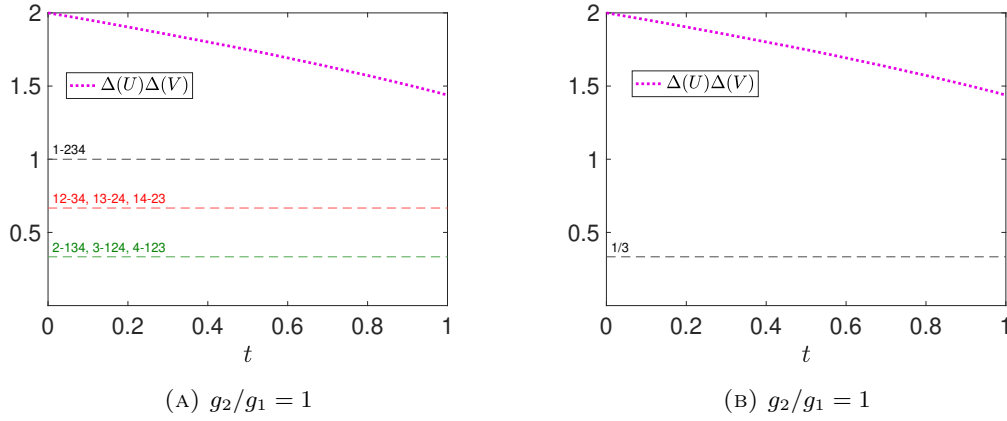
(A) $g_2/g_1 = 1$

(B) $g_2/g_1 = 1$

FIGURE 4.28: Genuine steering criterion for $g_2/g_1 = 1$. (A) shows the threshold for every bipartition and (B) shows the simplified threshold. Steering was not certified for this case.

4.8 Coupling parameters regime

Now that has been certified that quantum correlations are present in the system under specific conditions, namely a range of values for the quotient between the coupling parameters, it is possible to look for this regime by comparing results for different values of g_1 and g_2.

Results for this section show two witnesses, $ENT_{1i}, i = 2, 3$ for entanglement and $EPR_{3j}, j = 1, 4$ for steering. Values are taken for time $t = 0.9049$ but for different combinations of values of g_1 and g_2. We consider here values from 0.1 up to 1.0 by steps of 0.1 for the coupling parameters. The regime for these parameters in which the correlations are certified is then discussed.

4.8.1 Entanglement

(A) Entanglement between modes 1 and 2.

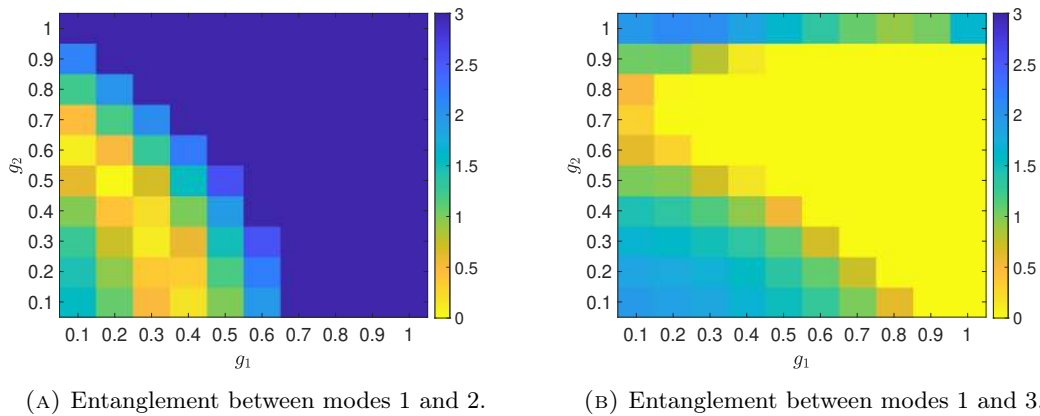(B) Entanglement between modes 1 and 3.

FIGURE 4.29: ENT_{1i}^+ entanglement criterion for different combinations of parameters g_1 and g_2. (A) shows the correlation between modes 1 and 2. (B) shows the case for modes 1 and 3. These particular pairings were chosen because they contrast considerably from each other. Entanglement is certified when $ENT_{ij}^+ \leq 2$.

Results of figure 4.29 show that entanglement is not present when both of the coupling parameters have the same value of 0.1. This is consistent with the results shown in section 4.6.2. However, once either of these quantities increase, entanglement is certified. For ENT^+_{12} there is another regime for larger values of g_1 and g_2 in which entanglement ceases to exist. The reason for which we chose these parameters is that the entanglement criterion ENT^+ certified entanglement for every pairing of the modes, unlike the other entanglement witnesses $D_{i,j}$ and ENT^-. Furthermore, when comparing results using this witness for a given pair of modes, the resulting grids were equal, regardless of the permutation of said modes. This is consistent with our knowledge of entanglement as a symmetric correlation.
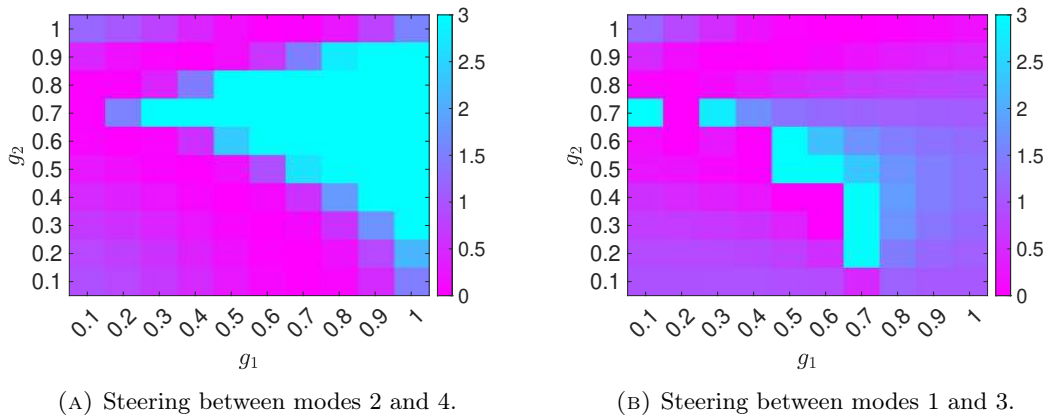
4.8.2 Steering

(A) Steering between modes 2 and 4. (B) Steering between modes 1 and 3.

FIGURE 4.30: EPR steering criterion for different combinations of parameters g_1 and g_2. (A) shows the correlation between modes 1 and 3. (B) shows the case for modes 3 and 4. These pairings were chosen because they contrast considerably to each other. Steering is certified whenever $\text{EPR}_{ij} \leq 1$.

The results shown in figure 4.30 do not certify steering when $g_1 = g_2 = 0.1$, but as the quotient g_2/g_1 increases its value, steering is certified. This is consistent with the results shown in section 4.7.1. Thus, in the entanglement case, the value of each of the coupling parameters is important, while for the steering correlation, it is the quotient between the two of them that allows us to find the quantum correlation. It is also worth mentioning that, while we can find steering for most of the values of g_1, as the parameter g_2 increases in both of these grids, we can no longer certify steering, but after increasing the parameter some more, we can certify it again. This type of behaviour is known as *death and revival*. Unlike the entanglement case, results from the same pairing of modes were not equal. This again shows consistency with steering being an asymmetric correlation.

Chapter 5

Conclusions

The main objective of this work was to certify the presence of two non-local quantum correlations, nameley, entanglement and steering, in a given non-linear system. We were interested in this system because it produces the correlations in two continuous variables and it does so for multiple parties. The methodologies used for this work consisted in a phase space method, called the positive-P representation, and the Heisenberg evolution equations. Using the former, a set of stochastic differential equations was obtained and was solved numerically. Meanwhile, the Heisenberg evolution equations yielded a set of coupled differential equations that was solved analytically using software. The solutions were consistent between the two procedures and described the dynamical behaviour of the annihilation and creation operators for four modes of light. By employing these solutions, observable quantities were calculated. Two in particular are of special relevance; these are called the *quadratures*, $\hat{X}$ and $\hat{P}$, and they serve, respectively, as analogous to position and momentum for modes of light. The quadratures were later used for defining quantities known as *witnesses* that are capable of certifying the presence of the quantum correlations known as *entanglement* and *steering*.

After testing thoroughly using several distinct witnesses, the results obtained certify the presence of these two quantum correlations between the four modes of light under specific conditions. Namely, both correlations are present when the quotient between two quantities called *coupling parameters*, which are denoted by g_1 and g_2, is greater or equal than 3. These coupling parameters are related to the complex amplitude of the two pump beams involved in the system. Furthermore, it was also shown that, as time passes, both entanglement and steering become present for more bipartitions of the four modes until eventually they develop into genuine multipartite entanglement and steering. This means that every mode of light is correlated with each other. The case for full multipartite entanglement and steering was not studied in this work.

Our results presented in section 4.8 show parts of the regime for the coupling parameters in which quantum correlations are certified. The work could be extended towards describing this regime more generally for a larger range of parameters g_1 and g_2.

Future work could be directed towards finding whether monogamy relations are present for multipartite steering and entanglement for the specific case of four modes. As far as we are concerned, there is no criteria for monogamy relations regarding four parties. Therefore, working towards monogamy relations for this specific case is an interesting line of research.

Bibliography

[1] Albert Einstein, Boris Podolsky, and Nathan. Rosen. "Can Quantum-Mechanical Description of Physical Reality Be Considered Complete?" In: *Phys. Rev.* 47 (10 May 1935), pp. 777–780.

[2] Stuart Freedman and John Clauser. "Experimental Test of Local Hidden-Variable Theories". In: *Phys. Rev. Lett.* 28 (14 Apr. 1972), pp. 938–941.

[3] Alain Aspect, Philippe Grangier, and Gérard Roger. "Experimental Tests of Realistic Local Theories via Bell's Theorem". In: *Phys. Rev. Lett.* 47 (7 Aug. 1981), pp. 460–463.

[4] Alain Aspect, Philippe Grangier, and Gérard Roger. "Experimental Realization of Einstein-Podolsky-Rosen-Bohm Gedankenexperiment: A New Violation of Bell's Inequalities". In: *Phys. Rev. Lett.* 49 (2 July 1982), pp. 91–94.

[5] Alain Aspect, Jean Dalibard, and Gérard Roger. "Experimental Test of Bell's Inequalities Using Time-Varying Analyzers". In: *Phys. Rev. Lett.* 49 (25 Dec. 1982), pp. 1804–1807.

[6] Marissa Giustina et al. "Significant-Loophole-Free Test of Bell's Theorem with Entangled Photons". In: *Phys. Rev. Lett.* 115 (25 Dec. 2015), p. 250401.

[7] Lynden K. Shalm et al. "Strong Loophole-Free Test of Local Realism". In: *Phys. Rev. Lett.* 115 (25 Dec. 2015), p. 250402.

[8] Bas Hensen et al. "Loophole-free Bell inequality violation using electron spins separated by 1.3 kilometres". In: *Nature* 526.7575 (2015), pp. 682–686.

[9] Anton Zeilinger. "Experiment and the foundations of quantum physics". In: *Rev. Mod. Phys.* 71 (2 Mar. 1999), S288–S297.

[10] John Clauser and Abner Shimony. "Bell's theorem. Experimental tests and implications". In: *Rep. Prog. Phys.* 41.12 (1978), p. 1881.

[11] AAPPS Bulletin. *News and views (1&2) 2022 Nobel Prize in Physics; 53rd AAPPS Council Meeting; 2022 Nishina Memorial Award; 2023 JPS Award.* 2023.

[12] Dagmar Bruß. "Characterizing entanglement". In: *J. Math. Phys.* 43.9 (2002), pp. 4237–4251.

[13] Juan Yin et al. "Entanglement-based secure quantum cryptography over 1,120 kilometres". In: *Nature* 582.7813 (2020), pp. 501–505.

[14] Artur Ekert. "Quantum cryptography based on Bell's theorem". In: *Phys. Rev. Lett.* 67 (6 Aug. 1991), pp. 661–663.

[15] Dik Bouwmeester et al. "Experimental quantum teleportation". In: *Nature* 390.6660 (1997), pp. 575–579.

[16] Charles Bennett et al. "Teleporting an unknown quantum state via dual classical and Einstein-Podolsky-Rosen channels". In: *Phys. Rev. Lett.* 70 (13 Mar. 1993), pp. 1895–1899.

[17] Akira Furusawa and Nobuyuki Takei. "Quantum teleportation for continuous variables and related quantum information processing". In: *Physics reports* 443.3 (2007), pp. 97–119.

[18] Richard Jozsa and Noah Linden. "On the role of entanglement in quantum-computational speed-up". In: *Proc. R. Soc. Lond. Ser. A: Mathematical, Physical and Engineering Sciences* 459.2036 (2003), pp. 2011–2032.

[19] Ryszard Horodecki et al. "Quantum entanglement". In: *Rev. Mod. Phys.* 81 (2 June 2009), pp. 865–942.

[20] David Bohm. "Quantum Theory Prentice-Hall". In: *Englewood Cliffs, NJ* (1951).

[21] Roope Uola et al. "Quantum steering". In: *Rev. Mod. Phys.* 92 (1 Mar. 2020), p. 015001.

[22] Howard M. Wiseman, Steve J. Jones, and Andrew C. Doherty. "Steering, Entanglement, Nonlocality, and the Einstein-Podolsky-Rosen Paradox". In: *Phys. Rev. Lett.* 98 (14 Apr. 2007), p. 140402.

[23] Erwin Schrödinger. "Discussion of probability relations between separated systems". In: *Math. Proc. Cambridge Philos. Soc.* 31.4 (1935), pp. 555–563.

[24] Erwin Schrödinger. "Probability relations between separated systems". In: *Math. Proc. Cambridge Philos. Soc.* 32.3 (1936), pp. 446–452.

[25] John S. Bell. *Speakable and unspeakable in quantum mechanics: Collected papers on quantum philosophy.* Cambridge university press, 2004.

[26] Nicolas Gisin. "Bell's inequality holds for all non-product states". In: *Physics Letters A* 154.5-6 (1991), pp. 201–202.

[27] Valerio Scarani. *Bell nonlocality.* Oxford University Press, 2019.

[28] Nicolas Brunner et al. "Bell nonlocality". In: *Rev. Mod. Phys.* 86 (2 Apr. 2014), pp. 419–478.

[29] Jeremy L O'brien. "Optical quantum computing". In: *Science* 318.5856 (2007), pp. 1567–1570.

[30] Matthew J Donald, Michał Horodecki, and Oliver Rudolph. "The uniqueness theorem for entanglement measures". In: *Journal of Mathematical Physics* 43.9 (2002), pp. 4252–4272.

[31] Michael Walter, David Gross, and Jens Eisert. "Multipartite entanglement". In: *Quantum Information: From Foundations to Quantum Technology Applications* (2016), pp. 293–330.

[32] Antonio Acín, Nicolas Gisin, and Lluis Masanes. "From Bell's Theorem to Secure Quantum Key Distribution". In: *Phys. Rev. Lett.* 97 (12 Sept. 2006), p. 120405.

[33] Vittorio Giovannetti, Seth Lloyd, and Lorenzo Maccone. "Quantum-enhanced measurements: beating the standard quantum limit". In: *Science* 306.5700 (2004), pp. 1330–1336.

[34] Miles J Padgett. "Orbital angular momentum 25 years on". In: *Optics express* 25.10 (2017), pp. 11265–11274.

[35] Yi-Han Luo et al. "Quantum Teleportation in High Dimensions". In: *Phys. Rev. Lett.* 123 (7 Aug. 2019), p. 070505.

[36] Xiao-Min Hu et al. "Experimental High-Dimensional Quantum Teleportation". In: *Phys. Rev. Lett.* 125 (23 Dec. 2020), p. 230501.

[37] Nicolas J. Cerf et al. "Security of Quantum Key Distribution Using d-Level Systems". In: *Phys. Rev. Lett.* 88 (12 Mar. 2002), p. 127902.

[38] Daniele Cozzolino et al. "High-Dimensional Quantum Communication: Benefits, Progress, and Future Challenges". In: *Advanced Quantum Technologies* 2.12 (2019), p. 1900038.

[39] Murray K. Olsen. "Continuous-variable Einstein-Podolsky-Rosen paradox with traveling-wave second-harmonic generation". In: *Phys. Rev. A* 70 (3 Sept. 2004), p. 035801.

[40] Murray K. Olsen. "Third-harmonic entanglement and Einstein-Podolsky-Rosen steering over a frequency range of more than an octave". In: *Phys. Rev. A* 97 (3 Mar. 2018), p. 033820.

[41] Edgar A. Rojas González et al. "Continuous-Variable Triple-Photon States Quantum Entanglement". In: *Phys. Rev. Lett.* 120 (4 Jan. 2018), p. 043601.

[42] Alessandra Gatti, Enrico Brambilla, and Ottavia Jedrkiewicz. "Engineering multipartite coupling in doubly pumped parametric down-conversion processes". In: *Phys. Rev. A* 103 (4 Apr. 2021), p. 043720.

[43] Alessandra Gatti. "Multipartite spatial entanglement generated by concurrent nonlinear processes". In: *Phys. Rev. A* 104 (5 Nov. 2021), p. 052430.

[44] Peter D. Drummond and Crispin W. Gardiner. "Generalised P-representations in quantum optics". In: *Journal of Physics A: Mathematical and General* 13.7 (1980), p. 2353.

[45] Alexander Streltsov. *Quantum correlations beyond entanglement.* Springer, 2015.

[46] Lynden Shalm et al. "Three-photon energy–time entanglement". In: *Nature Physics* 9.1 (2012), pp. 19–22.

[47] Run Y. Teh and Margaret D. Reid. "Criteria for genuine N-partite continuous-variable entanglement and Einstein-Podolsky-Rosen steering". In: *Phys. Rev. A* 90 (6 Dec. 2014), p. 062337.

[48] C. S. Wu and I. Shaknov. "The Angular Correlation of Scattered Annihilation Radiation". In: *Phys. Rev.* 77 (1 Jan. 1950), pp. 136–136.

[49] Anton Zeilinger. "Quantum entanglement: a fundamental concept finding its applications". In: *Physica Scripta* 1998.T76 (1998), p. 203.

[50] Charles H. Bennett and Stephen J. Wiesner. "Communication via one- and two-particle operators on Einstein-Podolsky-Rosen states". In: *Phys. Rev. Lett.* 69 (20 Nov. 1992), pp. 2881–2884.

[51] Charles Bennett et al. "Teleporting an unknown quantum state via dual classical and Einstein-Podolsky-Rosen channels". In: *Phys. Rev. Lett.* 70 (13 Mar. 1993), pp. 1895–1899.

[52] Margaret D. Reid. "Demonstration of the Einstein-Podolsky-Rosen paradox using nondegenerate parametric amplification". In: *Phys. Rev. A* 40 (2 July 1989), pp. 913–923.

[53] Margaret D. Reid et al. "Colloquium: The Einstein-Podolsky-Rosen paradox: From concepts to applications". In: *Rev. Mod. Phys.* 81 (4 Dec. 2009), pp. 1727–1751.

[54] Qiong Y. He and Margaret D. Reid. "Genuine Multipartite Einstein-Podolsky-Rosen Steering". In: *Phys. Rev. Lett.* 111 (25 Dec. 2013), p. 250403.

[55] Steve Jones, Howard Wiseman, and Andrew Doherty. "Entanglement, Einstein-Podolsky-Rosen correlations, Bell nonlocality, and steering". In: *Phys. Rev. A* 76 (5 Nov. 2007), p. 052116.

[56] Daniel Cavalcanti and Paul Skrzypczyk. "Quantum steering: a review with focus on semidefinite programming". In: *Reports on Progress in Physics* 80.2 (2016), p. 024001.

[57] Vitus Händchen et al. "Observation of one-way Einstein–Podolsky–Rosen steering". In: *Nature Photonics* 6.9 (2012), pp. 596–599.

[58] Z. Y. Ou et al. "Realization of the Einstein-Podolsky-Rosen paradox for continuous variables". In: *Phys. Rev. Lett.* 68 (25 June 1992), pp. 3663–3666.

[59] Lars Lydersen et al. "Hacking commercial quantum cryptography systems by tailored bright illumination". In: *Nature photonics* 4.10 (2010), pp. 686–689.

[60] Ilja Gerhardt et al. "Full-field implementation of a perfect eavesdropper on a quantum cryptography system". In: *Nature communications* 2.1 (2011), p. 349.

[61] Cyril Branciard et al. "One-sided device-independent quantum key distribution: Security, feasibility, and the connection with steering". In: *Phys. Rev. A* 85 (1 Jan. 2012), p. 010301.

[62] Claude E. Shannon. "Communication theory of secrecy systems". In: *The Bell System Technical Journal* 28.4 (1949), pp. 656–715.

[63] Otfried Gühne and Géza Tóth. "Entanglement detection". In: *Physics Reports* 474.1-6 (2009), pp. 1–75.

[64] Anthony Mark Fox. *Quantum optics: an introduction*. Vol. 15. Oxford university press, 2006.

[65] David J. Griffiths and Darrell F. Schroeter. *Introduction to quantum mechanics*. Cambridge university press, 2018.

[66] Gerardo Adesso and Fabrizio Illuminati. "Entanglement in continuous-variable systems: recent advances and current perspectives". In: *Journal of Physics A: Mathematical and Theoretical* 40.28 (2007), p. 7821.

[67] Christian Weedbrook et al. "Gaussian quantum information". In: *Rev. Mod. Phys.* 84 (2 May 2012), pp. 621–669.

[68] Hans A. Bachor and Timothy C Ralph. *A guide to experiments in quantum optics*. John Wiley & Sons, 2019.

[69] Roy J. Glauber. "Coherent and Incoherent States of the Radiation Field". In: *Phys. Rev.* 131 (6 Sept. 1963), pp. 2766–2788.

[70] Gerardo Adesso, Sammy Ragy, and Antony R Lee. "Continuous variable quantum information: Gaussian states and beyond". In: *Open Systems & Information Dynamics* 21 (2014), p. 1440001.

[71] Christopher Gerry and Peter Knight. *Introductory quantum optics*. Cambridge university press, 2005.

[72] Crispin Gardiner and Peter Zoller. *Quantum noise: a handbook of Markovian and non-Markovian quantum stochastic methods with applications to quantum optics*. Springer Science & Business Media, 2004.

[73] Laura Rosales-Zárate et al. "Decoherence of Einstein–Podolsky–Rosen steering". In: *J. Opt. Soc. Am. B* 32.4 (2015), A82–A91.

[74] Margaret D. Reid, Qiong Y. He, and Peter D. Drummond. "Entanglement and nonlocality in multi-particle systems". In: *Frontiers of Physics* 7 (2012), pp. 72–85.

[75] Roy J. Glauber. "The Quantum Theory of Optical Coherence". In: *Phys. Rev.* 130 (6 June 1963), pp. 2529–2539.

[76] Raúl Toral and Pere Colet. *Stochastic numerical methods: an introduction for students and scientists*. John Wiley & Sons, 2014.

[77] Michael J. Werner and Peter D. Drummond. "Robust algorithms for solving stochastic partial differential equations". In: *Journal of computational physics* 132.2 (1997), pp. 312–326.

[78] Laura Rosales-Zárate et al. "Probabilistic quantum phase-space simulation of Bell violations and their dynamical evolution". In: *Phys. Rev. A* 90 (2 Aug. 2014), p. 022109.

[79] Peter D. Drummond and M. G. Raymer. "Quantum theory of propagation of nonclassical radiation in a near-resonant medium". In: *Phys. Rev. A* 44 (3 Aug. 1991), pp. 2072–2085.

[80] Reeta Vyas and Surendra Singh. "Exact Quantum Distribution for Parametric Oscillators". In: *Phys. Rev. Lett.* 74 (12 Mar. 1995), pp. 2208–2211.

[81] Peter D. Drummond et al. "Simulating complex networks in phase space: Gaussian boson sampling". In: *Phys. Rev. A* 105 (1 Jan. 2022), p. 012427.

[82] Hannes Risken. *Fokker-Planck equation*. Springer, 1996.

[83] Crispin W Gardiner et al. *Handbook of stochastic methods*. Vol. 3. Springer Berlin, 1985.

[84] Avner Friedman. *Stochastic differential equations and applications*. Courier Corporation, 2012.

[85] Charles H. Henry and Rudolf F. Kazarinov. "Quantum noise in photonics". In: *Rev. Mod. Phys.* 68 (3 July 1996), pp. 801–853.

[86] Bernt Øksendal. *Stochastic differential equations*. Springer, 2003.

[87] Simon Kiesewetter, Ria R. Joseph, and Peter D. Drummond. *The Stochastic Toolbox User's Guide – xSPDE3: extensible software for stochastic ordinary and partial differential equations*. 2023.

[88] Sixia Yu et al. "All Entangled Pure States Violate a Single Bell's Inequality". In: *Phys. Rev. Lett.* 109 (12 Sept. 2012), p. 120402.

[89] Asher Peres. "Separability Criterion for Density Matrices". In: *Phys. Rev. Lett.* 77 (8 Aug. 1996), pp. 1413–1415.

[90] Paweł Horodecki et al. "Operational criterion and constructive checks for the separability of low-rank density matrices". In: *Phys. Rev. A* 62 (3 Aug. 2000), p. 032310.

[91] Lu-Ming Duan et al. "Inseparability Criterion for Continuous Variable Systems". In: *Phys. Rev. Lett.* 84 (12 Mar. 2000), pp. 2722–2725.

[92] Vittorio Giovannetti et al. "Characterizing the entanglement of bipartite quantum systems". In: *Phys. Rev. A* 67 (2 Feb. 2003), p. 022320.

[93] Peter van Loock and Akira Furusawa. "Detecting genuine multipartite continuous-variable entanglement". In: *Phys. Rev. A* 67 (5 May 2003), p. 052315.

[94] Margaret D. Reid and Peter D. Drummond. "Quantum Correlations of Phase in Nondegenerate Parametric Oscillation". In: *Phys. Rev. Lett.* 60 (26 June 1988), pp. 2731–2733.

[95] Run Y. Teh et al. "Full multipartite steering inseparability, genuine multipartite steering, and monogamy for continuous-variable systems". In: *Phys. Rev. A* 105 (1 Jan. 2022), p. 012202.

[96] Himadri Shekhar Dhar et al. "Monogamy of quantum correlations-a review". In: *Lectures on General Quantum Correlations and their Applications* (2017), pp. 23–64.

[97] Valerie Coffman, Joydip Kundu, and William K. Wootters. "Distributed entanglement". In: *Phys. Rev. A* 61 (5 Apr. 2000), p. 052306.

[98] William K. Wootters. "Entanglement of Formation of an Arbitrary State of Two Qubits". In: *Phys. Rev. Lett.* 80 (10 Mar. 1998), pp. 2245–2248.

[99] Xianfei Qi, Ting Gao, and Fengli Yan. "Measuring coherence with entanglement concurrence". In: *Journal of Physics A: Mathematical and Theoretical* 50.28 (2017), p. 285301.

[100] Pranaw Rungta and Carlton M. Caves. "Concurrence-based entanglement measures for isotropic states". In: *Phys. Rev. A* 67 (1 Jan. 2003), p. 012307.

[101] Florian Mintert. "Concurrence via entanglement witnesses". In: *Phys. Rev. A* 75 (5 May 2007), p. 052302.

[102] Tobias J. Osborne and Frank Verstraete. "General Monogamy Inequality for Bipartite Qubit Entanglement". In: *Phys. Rev. Lett.* 96 (22 June 2006), p. 220503.

[103] Yu Luo et al. "General monogamy of Tsallis q-entropy entanglement in multiqubit systems". In: *Phys. Rev. A* 93 (6 June 2016), p. 062340.

[104] Gerardo Adesso, Alessio Serafini, and Fabrizio Illuminati. "Multipartite entanglement in three-mode Gaussian states of continuous-variable systems: Quantification, sharing structure, and decoherence". In: *Phys. Rev. A* 73 (3 Mar. 2006), p. 032345.

[105] Laura Rosales-Zárate et al. "Monogamy inequalities for certifiers of continuous-variable Einstein-Podolsky-Rosen entanglement without the assumption of Gaussianity". In: *Phys. Rev. A* 96 (2 Aug. 2017), p. 022313.

[106] Sze M. Tan. "Confirming entanglement in continuous variable quantum teleportation". In: *Phys. Rev. A* 60 (4 Oct. 1999), pp. 2752–2758.

[107] Margaret D. Reid. "Monogamy inequalities for the Einstein-Podolsky-Rosen paradox and quantum steering". In: *Phys. Rev. A* 88 (6 Dec. 2013), p. 062108.

[108] Sisira Suresh et al. "Review on theoretical aspect of nonlinear optics". In: *Rev. Adv. Mater. Sci* 30.2 (2012), pp. 175–183.

[109] Christophe Couteau. "Spontaneous parametric down-conversion". In: *Contemporary Physics* 59.3 (2018), pp. 291–304.

[110] Atsushi Yabushita and Takayoshi Kobayashi. "Spectroscopy by frequency-entangled photon pairs". In: *Phys. Rev. A* 69 (1 Jan. 2004), p. 013806.

[111] Stefanie Barz et al. "Heralded generation of entangled photon pairs". In: *Nature photonics* 4.8 (2010), pp. 553–556.

[112] S. Castelletto, I. P. Degiovanni, and M. L. Rastello. "Quantum and classical noise in practical quantum-cryptography systems based on polarization-entangled photons". In: *Phys. Rev. A* 67 (2 Feb. 2003), p. 022305.

[113] Han Zhang et al. "Preparation and storage of frequency-uncorrelated entangled photons from cavity-enhanced spontaneous parametric downconversion". In: *Nature Photonics* 5.10 (2011), pp. 628–632.

[114] Paul G. Kwiat et al. "New High-Intensity Source of Polarization-Entangled Photon Pairs". In: *Phys. Rev. Lett.* 75 (24 Dec. 1995), pp. 4337–4341.

[115] Paul G. Kwiat et al. "Proposal for a loophole-free Bell inequality experiment". In: *Phys. Rev. A* 49 (5 May 1994), pp. 3209–3220.

[116] Alipasha Vaziri, Gregor Weihs, and Anton Zeilinger. "Experimental Two-Photon, Three-Dimensional Entanglement for Quantum Communication". In: *Phys. Rev. Lett.* 89 (24 Nov. 2002), p. 240401.

[117] Andrés Agustí et al. "Tripartite Genuine Non-Gaussian Entanglement in Three-Mode Spontaneous Parametric Down-Conversion". In: *Phys. Rev. Lett.* 125 (2 July 2020), p. 020502.

[118] Ottavia Jedrkiewicz et al. "Hot-spots and gain enhancement in a doubly pumped parametric down-conversion process". In: *Optics Express* 28.24 (2020), pp. 36245–36259.

[119] Alexander J.H. van der Torren et al. "Spatially entangled 4-photons states from a periodically poled KTP crystal". In: *Quantum Information and Measurement*. Optica Publishing Group. 2012, QT4B–4.

[120] Jason Schaake, Warren Grice, and Travis. Humble. "Four-photon polarization-entangled states with minimal spectral and spatial entanglement". In: *Quantum Electronics and Laser Science Conference*. Optica Publishing Group. 2012, QF3F–1.

[121] Ottavia Jedrkiewicz et al. "Golden ratio gain enhancement in coherently coupled parametric processes". In: *Scientific Reports* 8.1 (2018), p. 11616.

[122] Jun John Sakurai and Eugene D. Commins. *Modern quantum mechanics*. 1995.